SUSTAINABILITY ASSESSMENT OF ADDITIVE MANUFACTURING IN THE PRESENCE OF UNCERTAINTIES

A Thesis Submitted in Partial Fulfillment of the Requirements for the Degree of

DOCTOR OF PHILOSOPHY

by

Faladrum Sharma

(Roll No. 166103105)

Department of Mechanical Engineering

Indian Institute of Technology Guwahati

Guwahati 781039

INDIA

January 2022

Department of Mechanical Engineering,
Indian Institute of Technology Guwahati,
Guwahati-781039, INDIA

CERTIFICATE

It is certified that the work contained in the thesis entitled "**Sustainability Assessment of Additive Manufacturing in the Presence of Uncertainties**" is submitted by Mr. Faladrum Sharma to the Indian Institute of Technology Guwahati for the award of the degree of Doctor of Philosophy. The work has been carried out under my supervision in the Department of Mechanical Engineering, Indian Institute of Technology Guwahati. This work has not been submitted elsewhere for the award of any other degree or diploma.

Dr. Uday Shanker Dixit
Professor
Department of Mechanical Engineering,
Indian Institute of Technology Guwahati,
Guwahati-781039, INDIA

Date: January 24, 2022

DECLARATION

I declare that,

a. The work contained in this thesis is original and has been done by me under the guidance of my supervisor.
b. The work has not been submitted to any other institute for any degree or diploma.
c. I have followed the guidelines provided by the institute in preparing the thesis.
d. I have confirmed the norms and guidelines given in the ethical code of conduct of the institute.
e. Whenever I used materials (data, theoretical analysis, figure and text) from other sources, I have given due credit to them by citing them in the text of the thesis and giving their detail in references.

Faladrum Sharma

Dedicated to Almighty GOD, My Late Grandmother Mrs. Snehalata Devi, My Teachers and My Parents

Acknowledgement

I am privileged to take this opportunity to express my respect towards all who have supported me during the tenure of my PhD programme at IIT Guwahati. The first person I would like to express my sincere gratefulness is my supervisor **Prof. Uday Shanker Dixit**. I feel fortunate for getting the opportunity to work under him as a research scholar. His endless support, encouraging interactions and constructive criticism was a great driving force for me to carry out this research work.

I express my sincere gratitude to my doctoral committee members **Prof. S. Senthilvelan**, **Dr. Manas Das** and **Prof. Subhash Thota** for their encouragement and suggestions throughout the study. I express my sincere thanks to the former and present heads of the Department of Mechanical Engineering, Prof. A.K. Das, Prof. S.K. Dwivedy, Prof. S. Senthilvelan and Prof. KSR Krishna Murthy**.** I would also like to thank the staff members of the Department office and Central Workshop for their support and cooperation. A special thanks to Mr. Gwmchar Baro for helping me in carrying out experiments. Also, the financial support provided by the Ministry of Human Resource and Development (MHRD), India is greatly acknowledged.

I express my sincere thanks to my friends Dr. Besufekad Negash Fetene, Dr. W.G. Jiru, Dr. Polash Pratim Dutta, Dr. Rajkumar Shufen, Dr. Vikash Kumar, Dr. Amit Raj, Mr. Sujoy Tikader, Mr. Nitish Bhardwaj, Mr. Nilkamal Mahanta, Mr. Kaustabh Chatterjee, Mr. Bappa Das, Mr. G. Safiur Rahiman, Mr. Bhanu Prakash Bonthala, Mr. Snehal Shende and Mr. Biswajeet Barman. Special thanks to all my Umiam hostel mates who made my stay enjoyable and memorable.

I am always indebted to my parents for generously encouraging me and providing moral support during every footstep of my life. My father Mr. Balindra Nath Sharma, my mother Mrs. Pranita Sharma and my sister Miss Susismita Sharma deserve my wholehearted thanks. I will be grateful to them for sharing every responsibility in my family during my PhD. Finally, I would like to express my special thanks to all those who have helped me in various ways directly and indirectly during the tenure of my Ph.D. work. I shall always be grateful to the entire fraternity of IIT Guwahati for their encouragement and wishes.

Faladrum Sharma

IIT Guwahati

Abstract

Additive manufacturing (AM) has gained enormous attention in the present digital era of sustainable manufacturing. It is popularly known as 3D printing and is one of the foundations of the fourth industrial revolution, i.e., Industry 4.0. This technology has promising applications in several fields, viz., medical, aerospace, construction, automobiles and electronics. Despite the unique advantages offered by AM, there is a hesitation in purchasing a 3D printer and including it in the manufacturing route. Although it is adopted by some industries, its rate of adoption is not high as predicted in the past. One of the main reasons is the concern of sustainability. AM needs to be cost-effective as well as sustainable to compete with traditionally established manufacturing technologies.

The focus of the thesis is to explore the sustainability of AM in the presence of uncertainties. Cost analysis is carried out to assess its competitiveness with other manufacturing processes. For this, first, a cost estimation model is proposed. The cost estimation model is developed based on several elements, i.e., material, operator, slicing and overhead cost. One of the most important steps in cost analysis is to determine the build time. Hence, as a part of cost estimation, build time estimation models of two popular AM processes, viz., selective laser sintering (SLS) and fused deposition modelling (FDM) are developed. The analytical models are developed based on machine kinematics and geometrical parameters. For SLS, the model is validated with data available in the existing literature. For FDM, the model is validated by conducting in-house experiments.

In practice, the parameters are often uncertain and vary with management policies. Hence, to take into account uncertainties, the deterministic cost model is converted into a fuzzy set-based cost model. For this, the uncertain quantities are treated as fuzzy variables and suitable arithmetic operations are performed. For simplicity, only linear triangular fuzzy members are used in this work for uncertain parameters. The low (l) and the high (h) estimates are assigned a membership grade of 0.5, whereas the most likely (m) estimate is assigned a membership grade of 1. The cost model is illustrated with examples. The cost of different parts fabricated by SLS and FDM are evaluated. First, the deterministic model is used to obtain the cost. The most dominating part in the cost estimation is the machine depreciation. It is a part of overhead cost. Later, based on fuzzy set-based theory, the fuzzy cost estimates are obtained. The fuzzy cost of the parts is obtained in the form of a triplet. The working conditions of a typical Indian factory is considered. Based on the information

available in different internet sources and literature, cost parameters are quantified. The cost is obtained in Indian dollars. However, all the cost related elements are reported in dollar as it is considered a universal currency.

In the next part of cost analysis, SLS, a typical AM process is compared with injection moulding (IM) based on cost competitiveness considering the demand scenario. A cost model for IM is developed based on the information available in literature. The cost of IM is obtained by the algebraic summation of material, mould and processing cost. For SLS, the cost remains almost constant irrespective of the number of quantities albeit with some fluctuations. The design time associated with the designer and the slicing cost gets reduced with the number of quantities of the part. The processing cost per quantity (when the part is fabricated inside the machine chamber) is dependent on the build time per quantity. On the other hand, for IM, the cost per quantity decreases with an increase in the number of quantities. The mould cost, the most dominating cost component and the processing cost are divided among the units of the product. Based on the results obtained, it is seen that for some situations, some estimates of a process are lower and some are higher in comparison to the other process. For this, the concept of fuzzy reliability is used. The reliability estimates at different values of fuzzy cost are obtained. Based on the reliability estimates, a favourable manufacturing process is chosen.

The next part of the work delivers guidelines to an organization for assessing the utilization of AM. For this, a parameter, called utilization factor (U_f) is proposed based on total production time and available time. Based on U_f, the proper use of 3D printing is evaluated. U_f is incorporated in the cost model to understand its impact on the production cost. Typical cases of under, proper and over utilization of a 3D printer are discussed. The effect of U_f on the production cost for fabricating the same product and two different products are discussed. To compare two manufacturing processes, the unit cost and total production time for injection moulding (IM) and 3D printing are evaluated. Membership grades for suitability are provided based on cost and time. Assigning membership grades is subjective and may vary from organization to organization. The ability of AM to produce a product digitally reduces the requirement of human labour. This may give rise to unemployment amongst the labourers. To address such societal issues, a quantitative method to evaluate the labour penalty cost due to the reduction in employment is presented.

For environmental sustainability, approach for the estimation of energy consumption is discussed. Every AM process follows a similar pattern of layer by layer manufacturing, but the working principle varies for different processes. Hence, energy

consumption also varies. The energy consumption models of SLS and FDM are described based on their working principle. The importance of different energy-consuming elements is described. The energy consumed for a single as well as multiple parts are evaluated. The results revealed that the mass and volume of a fabricated part give some indication about the energy consumption, but it also depends on part complexity. The energy consumption of the parts is used to estimate the energy cost and the amount of CO_2 emission. The energy cost is estimated based on the values of energy consumption and electricity rate. For simplicity, it is taken as the cost of electricity. The amount of CO_2 emission in kg is estimated on an annual basis.

Overall, the work content of this thesis contributes to the sustainability evaluation of additive manufacturing processes. As the first pillar of sustainability, cost analysis of AM is carried out in the presence of uncertainties. Necessary guidelines are provided for industries willing to adopt AM. In the context of environmental aspect, energy consumption models are proposed where the role of energy consuming elements of AM based machines is described. Some aspects of social sustainability of AM and its impact on the society is discussed.

Contents

List of Figures

List of Tables

Nomenclature

Roman letters

A_b	Area of mould base cavity
A_f	Cross-sectional area of the filament
a_l	Acceleration of the laser beam
a_n	Acceleration/retardation of the nozzle in FDM
a_r	Acceleration/deceleration of the roller
c	Correction factor
C^*	Cost at which possibility index is evaluated
c_d	Completion date of the product
C_I	Confidence interval
C_{IM}	Cost of an injection moulded part
C_L	Left (lower) limit of cost
$c_{material}$	Material cost per unit mass
$C_{material}$	Material cost
C_{mb}	Mould base cost
C_{mm}	Mould manufacturing cost
C_{mould}	Mould cost
$c_{operator}$	Operator cost per hour
$C_{operator}$	Operator cost
$c_{overhead}$	Overhead cost per hour
$C_{overhead}$	Overhead cost
c_p	Specific heat of the powder
c_{pb}	Specific heat of the baseplate
c_{pm}	Specific heat of melted polymer
$C_{processing}$	Processing cost
c_{ps}	Specific heat of solid polymer
C_R	Right (upper) limit of cost
$c_{slicing}$	Slicing cost per hour
$C_{slicing}$	Slicing cost
C_{total}	Total cost

C_u	Unit cost, i.e., cost per quantity
d_d	Due date of the product
d_h	Scan spacing
d_l	Laser beam diameter
d_n	Diameter of the nozzle in FDM
d_{powder}	Diameter of the powder
d_{roller}	Diameter of the roller
E_d	Energy density of a laser
$E_{extrusion}$	Energy required in extrusion
E_{heater}	Total energy consumed by the heater system
E_{ir}	Energy consumed by the infrared heater
$E_{melting}$	Total energy required during melting
E_{misc}	Miscellaneous energy
E_p	Energy consumed by the movable platform
E_{piston}	Total energy consumed by the piston
E_r	Total energy spent by the roller
E_{rh}	Energy consumed by the resistive heater
E_{roller}	Total energy consumed by the roller
F_i	Amount of time spent on i^{th} job
F_r	Resistive force provided by the powder to the roller
G	Acceleration due to gravity
h	High estimate of a parameter
$H(T)$	Temperature-dependent term for viscosity
h_b	Height of the bounding box
h_p	Thickness of cavity and core plates
h_{ps}	Height travelled by the piston
h_z	Height of the part
I_d	Percentage of infill density
I_r	Moment of inertia of the roller about its centre
K	Power law fit parameter
$\overline{\overline{l}}$	Grand mean
l	Low estimate of a paramete

l_1 and l_3	lengths of the extruder corresponding to zone I and III, respectively
l_b	Length of the bounding box
$\bar{l}_j$	Mean length
l_n	Time required for traversing a distance in FDM
l_r	Distance travelled by the roller
l_s	Percentage loss of the material
l_t	Layer thickness
l_x	Length of the part
m	Most likely estimate of a parameter
m_b	Mass of the base plate
m_e	Mass of the extruded material
m_f	Material constant
m_p	Mass of the powder
m_{ps}	Mass of the piston
m_r	Mass of the roller
N	Power law fit parameter
n_c	Number of cavities in the mould
n_d	Replicates of a sample
n_f	Deciding factors
N_l	Number of layers present in the part
n_p	Number of quantities of a part
n_s	Number of samples
N_s	Total number of scans
$P(x)$	Probability of each quantity
p_i	Perimeter of rectangular EFGH
P_I	Possibility index
P_{ir}	Power rating of the infrared heater
P_l	Power rating of the laser
p_o	Perimeter of rectangular ABCD
p_y	Production yield in injection moulding
q_f	Heat of fusion
Q_m	Heat required during melting of the filament

Q_r	Heat input
R_e	Reliability
r_o	Ratio of overhead cost to other cost
r_p	Ratio of the volume of the actual part to that of the bounding box
r_r	Radius of the cylindrical roller
r_u	Ratio of actual cost to the cost with U_f=1
s	Distance BE in layer
S_b	Surface area of the bottom of a part
s_f	Strategy factor
s_m	Standard deviation of the means
S_t	Surface area of the top of a part
T	Temperature at the end of the extruder
t	Time taken to travel the overall empty distance BE in a layer
T_0	reference temperature at which the power-law fit parameters are determined
t_{3D}	Time for 3D printing for a product
t_a	Time required to travel the distance BC in a layer
t_{al}	Lower estimate of available time
t_{am}	Most likely estimate of available time
t_{ap}	Time for adding powder by the roller
t_{au}	Upper estimate of available time
t_{build}	Total build time
t_c	Cooling time
t_{cm}	Time for conventional manufacturing
t_{cycle}	Cycle time in injection moulding
t_d	Tardiness, i.e., the time difference between completion date and due date
t_{design}	Time required to convert the CAD model to proper STL file format
t_{eo}	Time required in ending operations
T_f	Final temperature
t_f	Injection time or fill time
T_i	Initial temperature
t_i	Time taken for stage i

t_{ideal}	Ideal time to traverse
t_{ii}	Time taken for stage ii
t_{iii}	Time taken for stage iii
t_{iv}	Time taken for stage iv
t_l	Time for traversing a distance in FDM process
T_m	Melting temperature of the material
t_{mp}	Time required for machine preparation
t_{pp}	Time required for post-processing
t_r	Total time to travel at rapid velocity
t_{r1}	Time taken to cover the distance BE in a layer
t_{r2}	Time taken to cover the distance BC or DE in a layer
t_{rs}	Mould resetting time
t_{scan}	Time required to scan
t_{setup}	Setup time of the machine
t_v	Time taken for stage v
U_f	Utilization factor
V_b	Volume of the bounding box
v_f	Velocity of the filament at the entry of the extruder
v_n	Maximum velocity of the nozzle in FDM
V_{net}	Net volume of part to be filled
V_{part}	Volume of the actual part
v_{ps}	Velocity of the piston
v_r	Maximum attainable velocity of the roller
v_{ra}	Rapid velocity of the laser nozzle
v_s	Scan velocity of the laser beam
w_b	Width of the bounding box
w_y	Width of the part
$\bar{x}$	Mean value

Greek letters

ΔP_1	Pressure drop in the extruder
α	Activation energy
β	Reliability index

β_f	Parameter for assisting decision process
β_n	Nozzle angle of the extruder
$\dot{\gamma}$	Shear rate
η	Viscosity of the material
η_{ir}	Efficiency of the infrared heater
η_m	Efficiency of the motor
η_r	Efficiency of the resistive heater
μ	Membership grade
μ_o	Overall membership grade
ρ_m	Density
σ	Standard deviation
Φ	Material constant
ω_r	Maximum attainable angular velocity by the roller

List of abbreviations

ABC	Activity-based costing
ABS	Acrylonitrile butadiene styrene
AHP	Analytic hierarchy process
AM	Additive manufacturing
ANN	Artificial neural network
BJ	Binder jetting
CAD	Computer aided design
CM	Conventional manufacturing
CNC	Computer numerical control
DMD	Direct metal deposition
DOE	Design of experiments
DP	Dimensional performance
EBM	Electron beam melting
FDM	Fused deposition modelling
HTP	Human toxicity potential
IM	Injection moulding
LCA	Life cycle analysis
LOM	Laminated object manufacturing

OEE	Overall equipment effectiveness
PBF	Powder bed fusion
PLA	Polylactic acid
PPE	Personal protective equipment
RP	Rapid prototyping
SFF	Solid Freeform Fabrication
SLA	Stereolithography
SLM	Selective laser melting
SLS	Selective laser sintering
SM	Subtractive manufacturing
STL	Standard tessellation language

Chapter 1
Introduction

1.1 Additive manufacturing

Additive manufacturing (AM) refers to the practice of making a product layer by layer based on a digital model prepared by computer-aided design (CAD) software. AM is one of the foundations of the fourth industrial revolution, i.e., Industry 4.0. This layer-by-layer method of manufacturing was patented by George J. Peacock in 1902 for making laminated horseshoes (Yang et al. 2017). At that time, computers were not available, but Peacock's method can be considered as an initiator to AM. Initially, AM emerged as rapid prototyping (RP) technology in the 1980s. AM emerged as rapid prototyping (RP) technology in the 1980s. The purpose was to build a prototype before the final configuration for commercialization.

This emerging technology is referred by numerous names: automated fabrication, freeform fabrication, digital fabrication, layer manufacturing, rapid manufacturing, rapid tooling, rapid prototyping and 3D printing. Though there is still a debate regarding the acceptance of a universal terminology, the recently adopted ASTM standards use the term additive manufacturing (AM). However, the most commonly used spoken term is 3D printing (Weller et al. 2015). This disruptive technology is inherent in efficient use of raw materials and producing minimum waste unlike conventional manufacturing. Also, it does not require any fixtures or cutting tools. Advances in this technology have resulted in producing implants, aero parts, robots and even a house. AM comprises the following steps:

- A 3D solid model is developed in the computer and converted to STL (standard tessellation language/standard triangle language) file format. The continuous geometry is converted into small triangles.
- The file is then transferred to the AM machine. Some operations are done to ensure proper size, position and orientation of the part.
- The part is built by automated process in the AM machine. However, skilled monitoring is needed to ensure minimum error of the parts.
- The final step includes removal of the part and post-processing. The part is removed from the build platform. Post-processing involves clean-up of the part and proper finishing before final commercialization.

There are several AM processes. These can be classified either based on raw material or the process of layer formation. Based on raw material, the processes are classified into powder-based, liquid-based and solid-based. Based on the layer formation mechanism, AM can be classified into the following processes— vat photopolymerization, material extrusion, powder bed fusion, direct energy deposition, binder and material jetting, and sheet lamination.

1.2 Need for sustainability analysis of additive manufacturing

The origin of sustainability can be traced back to the eighteen century. At that time, the focus was only on environmental protection (Michelsen et al. 2016). This perception has gained huge attention due to increasing environmental concerns. Sustainable development, as reported by Brundtland Commission in 1987, is "to meet the need of the present as well as safeguarding the need of the future generation" (Imperatives 1987). Since then, several concepts were proposed over the years. The World Summit held in 2005 put forward a universally acceptable concept of sustainability as a combination of economic, environmental and societal aspects (Ma et al. 2018). These are considered as three pillars of sustainability. In the context of AM, its birth and development took place by the drive of sustainability. The coaction of AM with sustainability can lead to a new dawn in the coming era of manufacturing. It is claimed that AM will be the most promising campaigner for sustainable development. In spite of several claims made for AM, there is an unwillingness for adopting it.

1.3 Scope and primary objective of the thesis

This thesis attempts to get answers to the following questions:

- Is it worthy to invest in AM for an industry in spite of the presence of conventionally established manufacturing technologies?
- What are the necessary factors that need to be considered before purchasing a 3D printer?
- Based on these factors, how the suitability of a 3D printer can be assessed?

1.4 Organization of the thesis

The content of this thesis is organized as follows:

- The present chapter briefly introduces AM, its relevance to sustainability along the primary objectives and organization of the thesis.

- Chapter 2 provides a literature review on economic, environmental and societal aspects of AM. Important deciding factors for procuring AM in an industry are discussed. Subsequently, inferences from the literature review and detailed objectives are presented.
- Chapter 3 presents cost estimation of AM in uncertain conditions. The importance of different cost elements and activities relevant to AM are discussed. For illustration, two popular AM processes, i.e., selective laser sintering (SLS) and fused deposition modelling (FDM) are considered.
- Chapter 4 presents cost analysis of AM and conventional manufacturing technology. The concept of fuzzy reliability is proposed to compare two uncertain costs and choose a favourable manufacturing process. Also, a variable demand scenario is considered.
- Chapter 5 presents a method for assessing the utility of AM in an organisation. The concept of utilisation factor is introduced and its effect on production planning and associated costs are discussed. Also, a method to evaluate the labour penalty due to reduction in employment is presented.
- Chapter 6 discusses the energy consumption of AM. Analytical models based on the working principle of two popular AM processes, SLS and FDM are presented. The effect on the energy consumption based on the production of single and multiple parts are discussed.
- Chapter 7 presents the Conclusion and the scope of future work. This is followed by references and appendices.

Chapter 2
Literature Survey and Detailed Objectives

2.1 Introduction

In recent years, the sustainability concerns of additive manufacturing (AM) have gained significant attention. A review on all three facets of sustainability, i.e., economic, environmental and societal, pertinent to AM technology, is discussed in this chapter. Section 2.2 presents a review of economic aspects of AM. Several cost estimation models of different AM processes developed over the years are discussed. Section 2.3 presents the energy estimation for different AM processes. Section 2.4 discusses the societal aspects of AM. Section 2.5 presents a review of various factors and motives for procuring AM.

2.2 Economic sustainability of additive manufacturing

The concept of engineering economy is based on a proper time value of money. It acts as a catalyst for increasing profitability. A robust understanding of cost assessment is a key factor for attaining economic sustainability (Ma et al. 2018). Cost assessment is a crucial parameter for demand, worth and functionality of the product to be customized. For this, a necessary requirement is the estimation of build time. Build time influences several elements of production cost. A prudent estimation of build time helps in evaluating the cost of the process as well as comparing its productivity with other manufacturing processes. Hence, it is necessary to have a basic understanding of how different process parameters influence the build time of an AM process. Section 2.2.1 discusses the build time estimation models in AM. Section 2.2.2 discusses the cost estimation models in additive manufacturing.

2.2.1 Build time estimation models of additive manufacturing

Build time is defined as the time required to produce the part in the AM based machine. Sometimes, time consumed in pre-processing operation and post-processing operation is also considered as a part of build time. Several attempts have been made to understand the effect of machine and geometry related parameters on build time of an AM process. Estimation of an AM based technology is process specific and varies according to the working principle. Numerous models, viz., analytical, parametric and soft computing models have been proposed for estimating the build time in AM process. The following subsections discuss different build time estimation models developed in the past.

2.2.1.1 Analytical models

In one of the earliest investigations, Kechagias et al. (1997) attempted to estimate the build time for two different laser-based AM processes, i.e., stereolithography (SLA) and laminated object manufacturing (LOM). At that time, these technologies were at infant stage and the term 'additive manufacturing' (AM) was not coined. These processes were referred to as rapid prototyping (RP). For both the processes, time was estimated as algebraic summation of time taken in layer preparation and layer processing. Layer preparation comprises the time to form a new layer, time required by the platform to move downwards and delay time. Layer processing time comprises the time taken by the laser to scan a layer according to the geometry of the part. Different parts were fabricated to validate the accuracy of the proposed methodology. The deviation between the experimental value and estimated value was estimated. For SLA, the lowest and highest deviation of build time was found to be 0.3% and 14.5%, respectively; whereas for LOM, the lowest and highest deviation was found to be 3.45% and 54.83%, respectively.

In another early attempt, Alexander et al. (1998) proposed a methodology to estimate the build time of two popular AM processes, i.e., fused deposition modelling (FDM) and SLA. These processes were referred to as layered manufacturing. The build time (t_{build}) was given by

$$t_{build} = t_{man} + t_{idle}, \tag{2.1}$$

where t_{man} is the manufacturing time where the part and support are produced in a layer by layer fashion. On the other hand, t_{idle} is the non-production time. This time period involves the movement of the nozzle without depositing material, cleaning of the nozzle, command execution time and movement of the z axis. The time estimated by this method underestimated the true time, as the effect of acceleration, deceleration and the time taken for changing the direction of the nozzle was not considered.

A popular laser-based process that uses polymeric material is selective laser sintering (SLS). It is one of the oldest and popular powder bed fusion AM processes. Specific to SLS, Pham and Wang (2000) investigated the effect of machine parameters such as roller speed, roller travel distance, delay time, laser scan speed and laser scan spacing for estimating the build time. The study considered two SLS machines and four different raw materials for case studies. The maximum error, i.e., the difference between actual and estimated build time was 8%. The authors highlighted that inclusion of the effect of acceleration and deceleration of the roller can make the model more accurate. In another

study confined to SLS, Zhang and Bernard (2013) proposed a method to estimate the build time for a single part, similar multiple parts and mixed parts. The model comprised laser-based parameters such as laser velocity, laser diameter and hatching distance. However, some important parameters specific to SLS process such as roller velocity, roller travel distance, delay time was not considered. Instead, the recoating time, a part of layer preparation time was taken as six seconds. The time required for machine preparation and ending operation was considered as one hour. Two products having different geometrical features and sizes were considered for the case study; these were dissimilar products and the ratio of their volumes was 19:1.

In extrusion-based AM process, i.e, FDM, Thrimurthulu et al. (2004) proposed a methodology to estimate the build time of a part based on fundamental machine and geometrical parameters. They assumed that the deposition of the thermoplastic material is continuous and there is no interruption. Also, the study ignored the non-productive time and the effect of orientation of the part in the printing process. Assuming continuous deposition of the molten material, t_{build} was obtained as

$$t_{build} = \frac{V_p}{a_n v_e}, \tag{2.2}$$

where V_p is the volume of the part to be fabricated, a_n is the cross-sectional area of the nozzle and v_e is the extrusion velocity of the filament. The time estimated by this method will be different from the actual build time, as non-productive time (lowering down of the platform, time between ending and starting between two different paths) was not considered. This gap was addressed in the work of Han et al. (2003). They carried out a build time analysis for FDM process. The algorithm to estimate the build time comprised the procedure to determine the repositioning and cleaning time of the nozzle. The authors proposed adaptive slicing (variable layer thickness) method by dividing the part into different zones; each zone was assigned a different layer thickness. Parts having simple geometry, e.g., a cylinder, comprised only one zone. However, the parts having complex geometrical features like sharp curvatures had multiple zones.

In another study specific to FDM process, Komines et al. (2018) presented analytical as well as empirical build time estimation models, which were validated by experiments. As per the authors, the build time is highly influenced by the acceleration of the nozzle especially for fabricating complex geometrical parts. In the analytical approach, the deposition time was estimated as the time required by the nozzle head to move with

constant velocity and the acceleration time of the nozzle. On the other hand, in the parametric approach, an acceleration coefficient was considered. However, the effect of different geometries on acceleration was not mentioned explicitly. The analytical model produced relatively more accurate results than the parametric model.

2.2.1.2 Parametric models

Specific to SLS, Ruffo et al. (2006b) proposed a parametric model for estimating the build time. They explored the effect of geometrical parameters on the build time of an object. The overall build time was given by algebraic summation of recoating time, scanning time, and heating and cooling time (t_{hc}); t_{hc} was taken as one hour. Case studies were conducted and it was reported that two parts having same height and volume may take different time to build.

The effect of different orientations (rotation about different axes) of a part on the build time was explored by Rathee et al. (2017). They built a cylindrical shaped object by FDM process. They conducted several experimental runs and used response surface methodology, a statistical based technique, to establish parametric models. The layer thickness had the maximum effect on the build time irrespective of any orientation. Build time was the least for orientation having the minimum z height; although it may increase the cross-sectional area of a layer, it also reduces the number of layers in the z direction. However, it was observed by Chacon et al. (2017) that specific to some geometries and process parameters, the orientation having lesser number of layers took relatively more time. High printing speed and feed rate may increase the deposition rate of the material, but repositioning of the nozzle takes additional time due to the effect of acceleration and deceleration.

2.2.1.3 Soft computing models

Some researchers used artificial neural network (ANN), a popular soft computing technique in build time estimation of AM processes. For example, Munguia et al. (2009) proposed an ANN model for the time-estimation in SLS process based on geometrical features of the product. They considered height of the part, volume of the part and bounding box as input parameters (referred to as input neurons). A bounding box is an imaginary cuboidal shaped box that contains every edge of the part. Munguia et al. (2009) took same examples as taken by Ruffo et al. (2006b) and compared the results. The average error in time estimation obtained by ANN model was reduced to 2.08% from 14.98% as obtained by empirical relation of Ruffo et al. (2006b). In another ANN based study, Di Angelo and Di Stefano

(2011) estimated the build time of several AM processes including SLA, SLS, FDM, LOM and three-dimensional printing (3DP). For this, they considered the part's height and volume, layer thickness and repositioning movements. Experiments were conducted only for FDM and 3DP considering six test cases. The average percentage errors for FDM and 3DP were 11.5% and 12%, respectively.

2.2.2 Cost estimation models of additive manufacturing

Proper knowledge of cost estimation is crucial for decision making in academia, research and business. The survival of any manufacturing company is at stake unless it is influenced by a proper cost estimation approach. A customer expects a product at a reasonable cost without any compromise in the quality. Underestimation of cost results in the financial loss of business that hampers its growth. On the other hand, overestimation of cost results in the loss of goodwill of the company and customer relations.

Cost estimation techniques can be broadly divided into two categories— qualitative and quantitative (Niazi et al. 2006). Qualitative technique lies on the wise utilisation of the historical data. The similarity between the old and new parts are identified. It is based on a comparative analysis of a new product with the previously manufactured products to identify the similarities in the new ones. The past data and experience guide to generate reliable cost estimation for the newly developed product. Expert judgement is preferable for adopting this technique. On the other hand, a quantitative technique is based on identifying different cost elements to manufacture the product. Cost is estimated using analytical function comprising necessary cost variables. Every cost variable gives an idea about different resource consumption involved in manufacturing the product. One of the popular cost estimation approaches is activity-based costing (ABC). It falls under the category of quantitative technique (Andrade et al. 1999). This technique is practised amongst several small to large scale industries. It identifies all the activities and the accompanying cost for making an end-usable product. For example, in machine handling, an operator is associated with machine setup and basic maintenance. Here, the cost is associated with the operator also. For running the machine, the cost is associated with depreciation, utilization, running time and number of shifts. ABC approach measures the performance activity-by-activity. If an activity incurs a high cost in the production cycle without adding much value to the final product, the management scrutinizes the activity and tries to improve it.

2.2.2.1 Preliminary investigations

Alexander et al. (1998) estimated the cost for two processes— FDM and SLA. The total cost was taken as the summation of prebuild, build and post-processing costs, i.e.,

$$C_{total} = C_{prebuild} + C_{build} + C_{post-processing}. \quad (2.3)$$

The prebuild cost comprised the cost involved in positioning and scaling the part, slicing the part and computational cost involved for fixing necessary parameters. The build cost comprised the power consumption, machine capital, depreciation, maintenance and the material cost. The post-processing cost included the cost involved in removing the support structures and performing finishing operations. It was emphasised that proper build orientation could lower the build and post-processing cost. This study assumed that the cost of each stage was independent and performed one after the other. Based on orientation, the minimum and maximum cost for FDM was $ 72 and $ 113, respectively, for a specific product. For SLA, minimum and maximum cost was $ 102 and $ 129, respectively. In another early attempt, Xu et al. (2001) evaluated the cost of AM by considering the cost of material, cost of running the machine, cost of data preparation and cost of post-processing. They considered FDM and three laser-based AM viz., SLA, selective laser sintering (SLS) and laminated object manufacturing (LOM). Unlike the study of Alexander et al. (1998) that considered material cost as a part of build cost, this study considered the cost of material separately.

Later, investigations were carried out to compare AM with other manufacturing processes based on cost-competitiveness. For example, Hopkinson and Dickens (2003) compared the costs incurred in AM and injection moulding (IM). For AM, three cost elements were considered— machine cost, labour cost and material cost. The costs of IM, SLA, FDM and SLS for producing typical components were compared. The authors estimated the unit costs of two different parts (one of small size and the other of medium size). They found that for a small-sized part, SLA and FDM were profitable for manufacturing up to 6000 quantities. On the other hand, SLS was economical for manufacturing up to 14000 quantities. For the medium-sized part, SLA and FDM were economical for manufacturing up to 700 quantities. SLS process was not considered for manufacturing the medium-sized part. For low volume of production, IM was found to be an expensive process.

Ruffo et al. (2006a) proposed a new cost model for SLS to estimate the unit cost of the small-sized part earlier considered by Hopkinson and Dickens (2003). The unit costs of

the small-sized part were compared when manufactured by SLS and IM processes. The cost of build (C_{build}) was estimated as

$$C_{build} = C_{direct} + C_{indirect}, \tag{2.4}$$

where C_{direct} is the direct cost associated with the material and $C_{indirect}$ is the time-dependent indirect cost associated with the machine, software, labour, maintenance and overhead. Based on this model, SLS process was found to be favourable for manufacturing up to 9000 quantities as compared to 14000 quantities estimated by Hopkinson and Dickens (2003). Ruffo et al. (2006a) also discussed the effect of orientation of the parts during manufacturing on the cost. They suggested the recycling of powders to reduce the cost of the part.

2.2.2.2 Production of mixed parts in the build chamber

Ruffo and Hague (2007) explored how manufacturing several parts simultaneously in a build chamber can achieve a cost reduction. Two different automotive parts, one of a smaller size and the other of large volume were considered for the case study. The authors focussed on the aspect that a manufacturing company always sets a build chamber with the highest packing ratio to lower the unit cost of a product and achieve economy of scale. Rickenbacher et al. (2013) attempted to estimate the cost of every individual part produced in a build chamber. The AM process chosen was selective laser melting (SLM). The model comprised several different cost elements including the cost to produce an inert gas environment. However, the energy consumption was excluded. The cost of a part was given by

$$C_{total} = C_{prep} + C_{buildjob} + C_{setup} + C_{build} + C_{removal} + C_{substrate} + C_{pp}, \tag{2.5}$$

where C_{total} is the total manufacturing cost, C_{prep} is the cost of preparing geometrical data for orientation and support structures of the part, $C_{buildjob}$ is the cost associated with the part for arranging it in the machine chamber, C_{setup} is the setup cost of the machine, C_{build} is the cost for building the part in the machine, $C_{removal}$ is the cost involved in removing the part from the machine, $C_{substrate}$ is the cost to separate the parts from substrate and C_{pp} is the cost for post-processing that involves removal of the support structures and surface finishing. Three parts having different volumes (14.65 cm^3, 4.9 cm^3, 2.02 cm^3) were considered as a case study. The costs of the largest and the smallest part when manufactured separately in the machine were found to be € 1800 and € 500, respectively. However, if all three parts are manufactured simultaneously, an average cost reduction of 41% was achieved. Hence,

by properly utilizing the build space in the machine, cost per part can be significantly reduced.

To take the advantage of both AM and other manufacturing processes, some researchers have combined AM with other processes. For example, Manogharan et al. (2016) used electron beam melting (EBM) for fabricating the part and a CNC machine for finishing operation. The total cost of the hybrid process (C_{total}) was given by

$$C_{total} = C_{EBM} + \left\{ C_{CNC} \left(t_{setup} + t_{finish} \right) \right\} + C_{tooling} n_{finish}, \tag{2.6}$$

where C_{EBM} is the overall cost of EBM, C_{CNC} is the manufacturing cost per unit time by CNC, t_{setup} is the set-up time, t_{finish} is the finishing time, $C_{tooling}$ is the cost of tooling and n_{finish} is the number of finishing passes. It was observed that reducing the EBM production time by 50% and 90% reduces the unit cost by 40% and 72%, respectively. On the other hand, material cost had a lesser effect on the production cost; 50% reduction in material cost resulted in reduction of unit cost by only 8%. The economic advantage of the hybrid process for expensive and harder to machine materials was analysed by a case study on load bearing assembly.

Yang and Li (2018) formulated a cost model for stereolithography process to evaluate the unit cost of parts in a mixed allocation. The algorithm was developed based on the height, volume and complexity of the part to be produced. It was found from case studies that total cost of the parts produced in mixed production layout was 6.18% less than that produced in non-mixed production layout. Sensitivity analysis showed that initial investment of the machine and material cost were the most influential cost parameters. The authors further emphasised that inclusion of dimensional accuracy of the parts and environmental sustainability will make the model more comprehensive.

Baumers et al. (2019) demonstrated that increasing the processing speed or deposition rate of the raw material reduces the unit cost of the part. They considered two AM processes, i.e., SLA and material jetting. For SLA, increasing the processing speed (in cm^3 per hr) by 98 % reduces the specific cost (in cost per unit volume) by 37 %. For material jetting, increasing the processing speed by 183 % reduces the specific cost by 39 %. It shows that reduction in cost is not proportionate to the increase in processing speed. In a recently conducted studies, Soskic et al. (2019) provided a detailed cost breakdown of multi-jet fusion process. It is a recently emergent process of powder bed fusion AM technology. They considered material, labour, energy as direct cost and equipment, overhead as indirect cost. The authors highlighted that for quotation of 3D printed parts;

managers need information on cost of individual parts rather than cost of the batch of produced parts.

2.2.2.3 Energy consideration in cost estimation

In laser-based AM process, viz., SLM and EBM, researchers considered energy consumption in the cost estimation (Baumers et al. 2012, Baumers et al. 2013, Baumers et al. 2016). The energy consumption along with the material costs were considered as direct cost. The cost of build (C_b) was given by

$$C_b = \dot{C}_i t_b + \left\{ C_{rm} \left(m_p + m_s \right) \right\} + C_e E_b, \tag{2.7}$$

where $\dot{C}_i$ is the total indirect cost per hour, t_b is the build time, C_{rm} and C_e are the unit costs of raw material and energy, respectively, m_p and m_s represent the mass of the build part and support structure, respectively and E_b is the energy consumption for the entire build. The study demonstrated that build cost is dependent on the percentage utilization of the machine chamber. However, this model did not consider post-processing and recycling cost. This gap was addressed by Lindemann et al. (2012). They highlighted that the post-processing cost was a significant parameter after machine and material cost. The post-processing activity included operations like removal of support material, surface finishing and quality control.

Baumers et al. (2016) constructed models for EBM and direct metal laser sintering (DMLS) AM processes. They demonstrated that it is possible to make AM cost-competitive even for mass production scenarios. The authors also emphasised that economies of scale can be achieved by increasing the size of build chamber of the machine, increasing deposition speed of the material and by depositing material on multiple positions simultaneously.

2.2.2.4 Effect of redesign possibility due to AM on production cost

With growing popularity of AM, parts that were previously manufactured by conventional manufacturing (CM) were redesigned and again produced by AM. The intention was to achieve an economic advantage over CM by reducing the number of sub-parts and usage of raw material (Atzeni et al. 2010; Atzeni and Salmi 2012: Laureijs et al. 2017). In one of the studies, Atzeni et al. (2010) made a cost analysis of an IM machine and two SLS machines, one of smaller size and the other of larger size. The part selected for the study was a fluorescent lamp holder. The holder that initially comprised several sub-parts was redesigned to reduce the number of sub-parts. The estimation using a cost model indicated

that the small-sized SLS machine was more economical for producing up to 87000 quantities and the large-sized SLS machine up to 73000 quantities. Sensitivity analysis was carried out for both IM and SLS to determine the dependence of various cost elements on the final production cost. It was found that the mould cost was the only significant parameter for IM, whereas for SLS, the machine cost and the material cost were the significant parameters.

Atzeni and Salmi (2012) further applied the concept of redesign for producing aircraft metallic parts by AM. They considered selective laser melting (SLM) and high pressure die casting (HPDC) machine. They found that SLM was economical for manufacturing up to 42 parts. In another similar study, Laureijs et al. (2017) considered part redesign of engine brackets used in aviation industry. They found that metallic AM is economical than forging process even up to an order of 12,000 quantities. It was further emphasized that better process control and reducing the material cost can further improve the economy of AM.

2.2.2.5 Consideration of complexity in AM cost estimation

It is evident from several research works that a manufacturing process is chosen based on the cost consideration. However, Fera et al. (2018) claimed that complexity issues based on geometry, information and operation should also be a deciding factor for determining the proper manufacturing route. This claim holds true especially for processes like AM that provides numerous freedoms to produce complex-shaped parts. For this, Fera et al. (2018) proposed a complexity index and associated it with AM cost. Although AM cost is hardly affected by the complexity; however, most of the other manufacturing processes, e.g., subtractive manufacturing (SM), require higher cost if complexity increases. It was highlighted that the difference between SM and AM is also related to how jobs are allocated in a production run. AM offers the ability to produce several parts of varying geometries simultaneously. However, SM is able to produce only a single part at a time. Hence, for SM, cost is directly associated with the amount of resources required to produce that part, but in AM, the cost can be divided amongst all the parts produced in the build.

2.2.2.6 Mould production by AM and its effect on production cost

AM is also beneficial to make the replica of a part referred to as pattern. This pattern can then be used to produce several quantities of that part. Ingole et al. (2009) made use of AM to produce different patterns for casting and plastic industries. A model was proposed where the reduction of lead time and cost was addressed. The authors considered the cost

of material consumption, machine operation, operator involvement and pre and post-processing operation. To correlate the cost and its benefits with parts of varying geometries, a complexity index (i) was introduced in terms of the volume of model material (m_b), support material (s_m) and build time (t_b):

$$i = \frac{m_b + s_m}{t_b}. \tag{2.8}$$

Eq. (2.8) implies that i should increase if t_b is less. However, this is arguable as complex parts requiring more time to fabricate should have higher value of i. Hence, the concept of complexity index needs more justification. It was found that the cost involved in machine operation cost was mostly influenced by complexity index. The unit cost of patterns made by AM was less for small scale volume of production. The authors emphasised that although cost estimation assists in making a financial decision, but it does not help to quantify other attributes like quality, customisation, satisfaction and manufacturability. Also, it was claimed that it is not necessary to include part design in the cost model as it is more or less the same for all manufacturing processes. However, this claim was opposed by other researchers.

Achillas et al. (2017) explored the advantages of various AM technologies (polyjet, FDM, SLA and SLS) over injection moulding (IM) by comparing in terms of lead time and production cost. Their methodology aimed to explore if AM could be included in the production portfolio of a company. Achillas et al. (2017) considered four different products in the case study; each product having different demand in the market. Different cost components considered were material cost, machinery cost, labour cost and fixed cost. However, an additional component, i.e., the cost of mould was considered in IM. A utilization factor was included in labour cost component for both IM and AM. It relied on the condition of manual, fully automated and semi-automated operation. It was found that IM was most expensive for producing parts in the range of 1–100 quantities due to the high manufacturing cost of the steel mould. Producing softer mould by polyjet that lasts up to 50 cycles make polyjet process economical for producing quantities in the range of 100–1000. Amongst AM, SLS was the most economical due to the low cost of the raw material.

2.2.2.8 Effect of dimensional performance of a part on production cost

Assessment of part quality with the manufacturing cost has received less attention. Haghighi and Li (2018) attempted to fill this necessary gap. They explored how selecting the proper parameters can maximize the dimensional performance (DP) as well as minimize

the manufacturing cost for FDM process. DP was evaluated by producing a rectangular part in different orientations. The parameters chosen were layer thickness, infill density, inclination and direction. The cost was estimated as per the model of Baumers et al. (2016), i.e., Eq. (2.7). It was found that reducing the layer thickness and infill density improves the dimensional performance of a part. A comparison with the cost reduction and the changes in DP in three axes (x, y and z) was made. The concluding remark made was that for obtaining better DP, high manufacturing cost is not a necessity.

2.2.2.8 Consideration of part failure, rejection rate in cost estimation

An important consideration, i.e., build failure was included by Baumers et al. (2017) in the cost analysis in the manufacturing of an air blower by direct metal laser sintering (DMLS). The authors investigated the steps that are to be repeated if failure occurs in the middle of the manufacturing operation. A constant probability of build failure (p_c = 0.025%) during the deposition of each layer was assumed. However, the relation between the probability of failure and part geometry was not considered. Considering build failure, the total cost (C_{total}) was given by

$$C_{total} = \frac{v\,C_{build}}{\left(1 - p_c\right)^n} + \dot{C}_{labour}\, t_{pp}, \tag{2.9}$$

where v is the volume fraction of the part (ratio of the volume of the part to the volume of entire build), C_{build} is the total build cost, p_c is the probability of build failure per layer, n is the number of layers, $\dot{C}_{labour}$ is the labour cost rate comprising indirect, material and energy costs and t_{pp} is the time required for post-processing. The component chosen was an air blower used in packaging industry. The cost model achieved a savings of 37.5% in AM processing route as compared to a conventional route.

Fera et al. (2017) proposed a cost allocation scheme for the production scenario in which parts of different geometries are built simultaneously. They emphasized that down time of the machines, rejection rate and quality losses should also be considered in cost models. For this, the authors considered the impact of overall equipment effectiveness (OEE). It is a measure of how efficiently a manufacturing operation is utilized. OEE was proposed in terms of theoretical production time ($t_{theoritical}$) and real production time (t_{real}):

$$t_{real} = \frac{t_{theoritical}}{\text{OEE}}. \tag{2.10}$$

However, the formulation for evaluating OEE was not provided. Some simplifications in the cost model were made, e.g., at a particular height, cost is allocated uniformly to all the

parts present at that level of height and not in proportion to their area. Overall, this model is quite suitable for cost estimation when a build consists of a number of similar or dissimilar parts.

2.3 Environmental assessment of additive manufacturing

During the process of converting a raw material to the final product, energy is consumed at every stage. The proper assessment of the energy requirement of a manufacturing process and reducing it is a significant strategy for achieving environmental sustainability. Environmental sustainability aims to minimize the use of natural resources, energy consumption and carbon footprint.

A widely adopted tool by the researchers to access environmental impact of a manufacturing process is by conducting life cycle analysis (LCA). LCA is a widely adopted method for assessing environmental sustainability. It is a systematic analysis to assess the environmental impacts of a product or process during its entire life cycle (Westkämper 2000). It involves thorough evaluation of environmental impacts from the production, through raw material extraction, processing, manufacturing, distribution and use, to the disposal phase of a product. LCA offers valuable insights on how different factors can make a system or process more environmentally efficient. The environmental impact is quantified by a numerical value, named as Eco-indicator. It represents the environmental impact of the process based on the findings from the life cycle assessment. The higher the value of the indicator, the greater is the impact of the product on the environment. The value of the Eco-indicator helps in decision-making processes by providing insights into areas of improvement for the corresponding product.

Based on LCA of AM, Luo et al. (1999) carried one of the earliest studies to evaluate the environmental impact. They referred AM as Solid Freeform Fabrication (SFF). At that time, the technology was in an early phase of development. The authors considered three typical SFF processes: stereolithography (SLA), selective laser sintering (SLS) and fused deposition modelling (FDM). Multiple equipment was considered for each of the processes. The analysis was based on the database of Environment and Resource Management Data (ERMD). Luo et al. (1999) estimated the energy consumption rate (in kWhr per kg) and quantified the overall environmental effect for processing unit amount of raw material for each of the AM processes. The final environmental scores for SLA, SLS and FDM processes varied in the range of 23.03–36.58, 23.80–37.25 and 24.25–208.55.

2.3.1 Energy estimation of additive manufacturing

Mongol et al. (2006) investigated the effect of different machine parameters on the electricity consumption of three different AM processes, i.e., thermojet, FDM and SLS. They considered a typical geometrical part in their analysis. The parameters in the study comprised orientation, position, height, layer thickness, quantity of support material and manufacturing time. The authors presented the influence of parameters in a qualitative manner by classifying into three levels (small, moderate and big). It was observed that minimizing the height of the part results in minimum electricity consumption for thermojet and SLS process. However, for FDM process, reducing the volume of the support structure results in minimum electricity consumption.

Morrow et al. (2007) carried out a comparative analysis of AM and conventional manufacturing (end milling) in terms of energy consumption for tool manufacture. They considered a laser based direct metal deposition (DMD) AM process in their study. The authors considered the manufacturing of a mould insert plate, mirror fixture, and remanufacturing of a stamping die. The aim was to explore how energy consumption was influenced by solid-to-cavity volume ratio (r). It is the ratio of the mass of the product to the mass of the fully solid product enclosed in a bounding box. It was found that the manufacturing of the insert plate ($r > 7$) by AM process consumed 3 GJ more energy as compared to end milling. However, for mirror fixture ($r = 0.33$), the AM process consumed less energy and is more environmentally friendly as compared to end milling.

Sreenivasan et al. (2010) studied the involvement of different components of an AM machine in energy consumption. They conducted experiments on a selective laser sintering (SLS) machine and recorded the power consumption by a current measuring instrument. They suggested to replace the heating system of the machine, that consumes the maximum energy, with a better thermal control system. They also suggested to use an efficient laser system for reducing the energy consumption.

Baumers et al. (2011) classified the energy consumption of laser sintering AM machines based on the geometry and height of the part, time required to build the part and the energy consumed during the warm-up and cool-down of the machine chamber. They considered two AM machines having different build volumes and heating elements. One comprised infrared and resistive heating elements while the other comprised only resistive heaters. Two prosthetic parts were built on each two AM machines in a single build. The energy consumed by the machine having only resistive heaters consumed 56.75 kWhr whereas the other machine consumed 66.02 kWhr.

Paul and Anand (2012) discussed the dependence of energy consumption on part geometry, layer thickness, orientation of the part and total area of sintering in an SLS process. However, their study was limited only to laser energy consumption based on the virtual manufacturing of a cube, a cylinder and a functional part comprising flat and curved surfaces. It was found that for a particular layer thickness, laser energy consumption of cube and the cylinder increases with orientation angle up to a certain limit, and then again decreases. However, such pattern was not observed for the functional part. The laser energy consumption was minimum (0.6 kJ) for the cylinder at a layer thickness of 0.1 mm, whereas the maximum energy consumption (21.69 kJ) was for the functional part at a layer thickness of 0.03 mm. An optimisation model was proposed to compute the minimum laser energy based on part orientation and slice thickness.

Ullah et al. (2013) compared SLA and a subtractive process, viz., wood-sawing technique in context of emission of carbon dioxide gas (involved in model building material and model making process) and consumption of natural resources. They proposed a sustainability index (S_I) as

$$S_I = \{C_M V_M + E_P f_E\} V_M R_M, \tag{2.11}$$

where C_M is the CO_2 footprint per unit volume of material production, V_M is the amount of fresh material per model, E_P is the energy consumption per model, f_E is the conversion factor for determining amount of CO_2 and R_M is the measure of resource depletion per unit volume. A lower value of S_I indicates a more sustainable process. In context of consumption of natural resources, SLA is better than the subtractive manufacturing process. On the other hand, subtractive process is better than SLA from the viewpoint of carbon dioxide emission. A critical volume of the raw material (8 cm^3 for SLA and 220 cm^3 for subtractive process) was evaluated where both the processes have same environmental impact. The authors emphasised that the use of better photosensitive resins will make SLA more sustainable.

With respect to energy consumption, researchers also carried out comparative studies with other manufacturing technologies to assess the environmental sustainability of AM. Telenko and Seepersad (2012) made a comparative study of SLS and injection moulding (IM) based on energy requirements. The part considered for this study was a paintball gun handle made of nylon polyamide. Fabrication of such parts require legal permission in some countries. The total energy consumption by SLS was considered as the energy required in the processing of feedstock and the energy consumption during the

building process. The authors emphasized that full utilization of the machine chamber, reducing the powder loss and reducing the scanning time of layers can make SLS process more energy-efficient. Considering full utilization, a total of 150 quantities could be produced. It was observed that choosing the proper orientation of the part can vary the energy consumption by 60% in SLS. Also, SLS consumes more energy if mould fabrication in injection moulding (IM) is not considered. For such cases, SLS consumed more than three times the energy required in IM for producing the same quantities of the part. The model did not consider transportation, storage and recycling of the part.

Le Bourhis et al. (2013) assessed the environmental impact of a metallic AM machinery based on material, fluid and electricity consumption. Electricity consumption was further categorized as energy consumed by the laser, cooling system and motors. For case study, the authors considered the manufacturing of a cuboidal shaped wall of dimensions 100 × 12 × 50 mm^3 by two different approaches. They demonstrated how choosing a proper approach can have a lower environmental impact than the other. The environmental impacts were expressed in mPts; a higher score means higher detrimental effect. The score of one approach was 547 mPts and the other was 567 mPts.

By considering four stages of a product, viz., pre-manufacturing, manufacturing, usage and post-usage, Hapuwatte et al. (2016) evaluated the product sustainability index (P_{SI}) for conventional manufacturing and AM by assigning equal weightage to economic, environmental and societal aspects of sustainability. P_{SI} was given by

$$P_{SI} = \frac{1}{3}\left(E_n + E_c + S\right), \tag{2.12}$$

where E_n, E_c and S are the sub-index score for economic impact, environmental impact and social impact, respectively. A high value indicates a more sustainable process. The economic aspects comprised initial investment of the machine and overhead costs, while the environmental aspects comprised material usage, energy consumption and emission. Lastly, the societal aspects comprised product quality, safety, durability and functionality. Two cases were considered; a flat design object and a complex model comprising 3D features. The environmental sub-index of AM is higher for both simple and the complex object. Overall, P_{SI} of AM is higher for complex object whereas for the simple object, P_{SI} of CM is higher.

Priarone and Ingarao (2017) assessed a subtractive process and a combination of both AM and subtractive process. The comparison and the selection of an appropriate process was based on minimum energy consumption and CO_2 emission. The production of

parts made of stainless steel and titanium alloys were considered. The total energy (E_{total}) requirement was evaluated as

$$E_{total} = E_{mat} + E_{mfg} + E_{trn} + E_{use}, \tag{2.13}$$

where E_{mat}, E_{mfg}, E_{trn} and E_{use} are the energy demand for material production, manufacturing, transportation and use phase. The authors stated that apart from considering energy and CO_2 emission, economic aspect is also a criterion for selecting the most appropriate manufacturing process.

Watson and Taminger (2018) proposed a model to determine if conventional manufacturing (CM) or AM is energy efficient for producing a metallic part. The model considered different manufacturing stages viz., production of feedstock material, transportation and recycling. Separate energy consumption models were presented for both AM and CM. The decisive variable in the model was based on a ratio α. A critical value of α was evaluated by setting the mathematical expression of energy consumption for AM and CM as equal. For α less than the critical value, AM was preferable, else CM was preferable. However, it was highlighted that if energy consumed in non-productive operations are considered, the critical value of α cannot be evaluated. Hence, the scope of the proposed methodology is limited.

Faludi et al. (2015) employed LCA methodology to compare environmental impacts of three types of machinery— CNC, FDM and inkjet machine. Several factors such as raw material, electrical energy, disposal costs, waste generated, transportation and disposal costs were considered. Individual ecological impacts were determined considering varying machine utilization. Parts made of Acrylonitrile Butadiene Styrene (ABS), a popular thermoplastic polymeric material was considered as a case study. FDM machine was found to be the most sustainable at the maximum utilization of the machine, irrespective of the density of the model material. It was emphasized that using a single machine for producing the maximum number of products should be the strategy for reducing environmental impact.

Tang et al. (2016) stated that environmental assessment of AM based on LCA is limited due to lack of life-cycle data. They also highlighted that LCA does not consider the design stage of manufacturing process. This may be justified for CM, but not for AM as the design freedom it provides can have a huge impact on the environment. For this, an attempt was made to consider the design aspect in LCA. The authors developed a

framework for optimizing design features to make an aerospace engine bracket by binder jetting AM and CNC milling process. An environmental impact index (E_i) was proposed:

$$E_i = f\left(p_{design}, p_{machine}, p_{material}, p_{operation}\right), \tag{2.14}$$

where p_{design}, $p_{machine}$, $p_{material}$ and $p_{operation}$ are the design, machine, material and operation dependent parameters, respectively. To optimize the design, functional surface (FS) and functional volume (FV) were generated. FS is a surface that is required for carrying out a specific function by a product. For example, a bearing may need one FS for supporting it to ground and another FS for supporting the journal in it. FV is a geometry volume that connects the surfaces. The binder jetting AM process was found to be more sustainable requiring less energy and emitting less carbon dioxide gas. The methodology developed can be beneficial for industrialists for selecting the most suitable AM process to create minimum environmental impact.

Liu et al. (2018) compared the environmental performance of direct energy deposition (DED) with milling process. They considered manufacturing a gear as a case study. Due to the space constraint of DED machine, the size of the gear was taken as 1.26 cm^3. To assess the environmental impact, they considered several factors such global warming potential, ozone depletion potential, acidification potential and abiotic depletion potential. It was found that the energy consumed (in Whr) by DED and milling process was 803 and 127, respectively. It was reported that low powder efficiency of DED process is responsible for more material consumption.

In a recently conducted study, Kwon et al. (2020) evaluated three AM process, viz., binder jetting, powder bed fusion (PBF) and material extrusion. Also, they considered two PBF based AM machines, one having smaller bed size and the other of larger bed size. The effect of part orientation and production volume on the environment was explored. Building 200 parts were considered as high-volume production. It was found that PBF based machine of smaller and bigger bed size were most environmentally friendly for low volume and high-volume production, respectively. On the other hand, binder jetting was found to be least environmentally. In another study, Ma et al. (2021) conducted LCA of an FDM produced part to assess its environmental impact. As a case study, a cube of size 27 cm^3 produced by PLA raw material under different conditions was considered. The effect of different parameters, i.e., layer height, infill density, printing speed and printing temperature were investigated on the energy consumption. The manufacturing of the cube comprised several steps including PLA granulate and filament production, transportation

of granulate and filament, pre-processing, main production phase and post-processing. The maximum and the minimum energy consumption (in Whr) were 18 and 267, respectively.

Yoon et al. (2017) compared the energy consumption of injection moulding (IM), milling process and AM. Each process was modelled in terms of energy consumption and individual components. An object of volume 4.5 cm^3 having slots and holes was selected as a case study. ABS raw material was selected for producing the objects. The electrical energy consumption for each experiment was measured by a power measuring instrument. The energy consumed (in Whr) for producing one part by IM, milling process and AM was 832.4, 40.8 and 717.1, respectively. IM consumed maximum energy for one part, but for producing multiple parts, IM consumes less energy. Conducting a break-even analysis of this case study is a relevant future work.

Huang et al. (2016) demonstrated how adopting AM can reduce energy consumption and greenhouse gas emissions pertinent to aircraft components. Comparative analyses were conducted in the case study considering different materials, viz, steel as well as alloys of titanium, nickel and aluminium. It was found that producing a part by AM instead of CM can reduce the weight of an aircraft bracket up to 65%. Also, energy savings per aircraft and its associated greenhouse gas emission reduction can be up to 11170 GJ and 900 metric ton, respectively. The authors predicted that by the year 2050, proper adoption of AM can save up to 2.8 billion GJ energy.

Li et al. (2017) analysed the environmental impact of different AM processes, viz, FDM, SLA and polyjet. The impact was quantified on the basis of material preparation, building process (energy consumed), use phase and disposal. Polyjet process was found to have the most adverse impact (125.1 mPt) and FDM was the most environmentally friendly having an impact score of 12.23 mPts. Amongst all the processes, FDM provides the flexibility to produce parts with less usage of raw material, i.e, low infill density.

Xu et al. (2015) developed a mathematical model of energy consumption in a binder jetting (BJ) AM process. The model was proposed considering shape of the part, orientation, layer thickness and other process parameters. Based on the working principle of BJ process, an approach to estimate the time required in spreading a new layer and printing is provided. The proposed method was validated by manufacturing a cylinder of height and radius 4 mm and 1.5 mm, respectively. Based on the different set of parameters, the minimum and the maximum amounts of energy obtained from the proposed model were 1558.76 kJ and 4226.57 kJ, respectively. This model provided more than 95% accuracy with the experimental results. However, the energy during sintering and curing were

neglected. The authors emphasized that these should be included for a robust assessment of energy consumption in BJ process.

Kellens et al. (2014) presented parametric models to quantify the environmental footprint based on energy and resource consumption. The models were developed considering build height and volume of the parts to be produced. Power analyser was used to measure the power consumption for different components of the machine. The environmental impact was assessed based on the energy consumed during printing, compressed air consumption to produce inert atmosphere inside the chamber and leftover powder after printing. Although polyamide powders have negligible environmental and health effect, even then the authors suggested to use ventilation system to extract the dust particles during the removal of the product from the chamber.

Peng (2016) analysed the energy consumption of FDM process. The energy consumed was categorised as primary energy and secondary energy. Primary energy represents the energy consumed during heating and melting the thermoplastic material. The secondary or the indirect energy represents the energy consumed during product design, printing settings, warming up of the build platform and geometrical parameters.

Yang et al. (2017) proposed a mathematical model for the energy consumption of vat photopolymerisation based AM process, i.e., stereolithography (SLA). The overall energy consumption ($E_{overall}$) was obtained as

$$E_{overall} = E_{curing} + E_{platform} + E_{cooling}, \tag{2.15}$$

where E_{curing} is the energy consumed during the curing process by UV light source, $E_{platform}$ is the energy consumed by the build platform and $E_{cooling}$ is the energy consumed by the cooling system. Experiments were conducted to validate the model and design of experiments (DOE) was implemented based on controllable parameters, viz., layer thickness, curing time and orientation. Using optimal set of parameters, the energy consumption was reduced to 127.7 kJ compared to the default conditions where energy consumed was 278.7 kJ. The authors also stated that industries equipped with SLA based AM machines can reduce CO_2 emission from 415 pounds to 191.5 pounds for monthly production of 3000 parts.

2.4 Societal aspects of additive manufacturing

Social sustainability is the third pillar of sustainability. It has received relatively less attention as compared to economic and environmental aspects of sustainability. Societal aspects are related to well-being and safety of human beings. Hornick and Roland (2013)

highlighted that with the development of AM, the need for training and developing new technical skills in educational field has risen. Students who are familiar with this technology can test their creativity and make innovative products. Trained individuals can also deploy low-cost 3D printers in small businesses (Matos and Jacinto 2019).

AM has proved to be instrumental in providing efficient as well as quality health care. For example, after the outbreak of Corona Virus disease (COVID-19) in December 2019, there was an urgent need of personal protective equipment (PPE) in the form of facemask and face shields. During this urgent need, a FDM based 3D printer was able to manufacture 112 ready-to-use face shields (Armijo et al. 2020). Bio-medical products such as orthosis, limbs and implants can be effectively fabricated as per patients' requirement (Huang et al. 2013). Also, in the process of drug delivery, AM can produce ready-to-use tablets oral tablets in high quantity (Shahrubudin et al. 2020). Despite some benefits offered by AM, some detrimental effects of AM are also reported. Huang et al. (2013) investigated the ill effects of material handling during AM process. They highlighted that the effects of materials like epoxy resins used in SLA, polyamides and ABS used in SLS have not been explored much. For example, a liquid resin named "TuxedoTMG3-HCM" undergoes alteration and mutation that can cause serious health related issues. In another study, Bours et al. (2017) developed an approach to assess the risk of exposure to raw material used in 3D printing. They considered two materials for comparison. One was liquid resin used in SLA and the other is polylactic acid (PLA) used in FDM. Three levels, viz., level 0, level 1 and level 2 were considered to assess the sustainability. Level 0 and 2 describe the worst- and best-case scenarios, respectively. In the evaluation of the post-processing stage, the material waste was addressed by E_{factor}:

$$E_{factor} = \frac{m_m}{m_p} - 1, \tag{2.16}$$

where m_m is the total mass of the material to make the part and m_p is the final mass of the printed part. Based on the comparison of the two materials in different life cycle stages, PLA was categorised as level 2 while the resin was categorised as level 1.

Ma et al. (2018) explored the ill effects of PLA material used in FDM process on the human health. For this, they evaluated a quantity referred as human toxicity potential (HTP) during the manufacturing a gear. HTP was evaluated for several stages during manufacturing, viz., design, printing phase, service and end of life. HTP is zero for the activity that does not have any ill effects to human health, e.g., design stage. *HTP* was evaluated as

$$HTP = w_a t_a + w_w t_w + w_s t_s, \tag{2.17}$$

where t_a, t_w and t_s are the toxicity potentials with respect air, water and soil, respectively, t_a, t_b and t_s are the weights for emissions to air, water and soil, respectively. It was found the HTP score for printing, service and end of life was 1.84, 5.82 and 15.65, respectively. Overall, the HTP score was obtained as 23.31.

Matos et al. (2019) explored how AM influence social well-being, quality of living, working condition and economic well-being. For this, they conducted interviews in four Portuguese organisations that use AM technology. Several opinion-based questions were asked and mixed responses were obtained. The viewpoint of the interviewees was analysed as positive, negative, null and mixed. Interviewees said that AM can have a positive impact on the quality of life. It enables the production of customized products and medical products such as prosthetics. Also, it encourages the concept of "do it yourself" (DIY). This enables several educational activities and also improves the learning process. However, the opinion on economic well-being and working conditions is adverse. AM may promote jobs but its digital nature can also increase unemployment. It requires comparatively less skill to operate as compared to CNC lathe or mill (Faludi et al. 2015). Hence, the workers have to settle with the salary of low skilled jobs.

Another major social concern with the growing popularity of AM is authorisation and legal issues. The increasing application of AM has raised several issues on the interpretation of intellectual property rights (IPR) system (Hornick and Roland 2013). IPR is a legal right that aims to protect the creations and inventions resulting from intellectual efforts in the field of technology, design, artistry and literary works. Some concerns of IPRs specific to AM comprise copyright, patent and trademark (Ballardini 2019). The digital feature of this technology permits everyone to re-design an existing model, produce the product and even sell the product along with its associated CAD model. Steenhuis and Pretorius (2017) reported that the ability of AM to produce the model digitally also raises questions on patent infringement. Production of guns and weapons that are illegal as per government directives can be easily created in the CAD format. The circulation of such files and their availability on the internet also poses threats to the defence of a country. Hence, some restrictions must be imposed on the legality of CAD files to avoid misuse of AM.

2.5 Necessary aspects for procuring Additive Manufacturing

An approach to identify the decisive factors for procuring any technology is by conducting a survey analysis. One of the earliest studies on identifying the factors for procuring a 3D printer in a manufacturing industry was carried out by Chin (1998). As mentioned earlier, at that time, the scientific term 'Additive Manufacturing' was not coined and it was known as Rapid Prototyping (RP). Chin (1998) conducted a survey via telephonic interview and personal visits to identify the factors that are necessary to implement AM. Interviews were conducted with experts of Hong Kong manufacturing industries. To take a decision, four necessary factors were identified— managerial, financial, technological and organizational. Authors used analytic hierarchy process (AHP) in his survey. AHP, a popular decision-making technique was implemented to prioritize and rank the factors. The study revealed that the financial aspect, i.e., high initial cost of the machine, is a major concern in procuring RP.

Mellor et al. (2014) conducted a qualitative survey in the form of interview in an industry that had already procured AM machinery. The interviewees were project engineers, upper management personal, technology vendors as well as maintenance personal. The purpose of their study was to identify the factors responsible for deploying AM as a manufacturing process. A framework for AM implementation was developed considering AM strategy, AM technology, organizational change, system of production and AM supply chain. However, the survey was conducted only in a single industry that is a supplier of powder bed fusion based AM process, i.e., SLS and SLM.

Yeh and Chen (2018) highlighted that 3D printing technology is not being adopted at the speed as it was expected. The authors acknowledged four factors, i.e, technology, organization, environment and cost (TOEC), for assessing the adoption of 3D printing. The environmental dimension refers to the market competition, market trend, trading partners and government support. Questionnaire was prepared to conduct a survey in Taiwan amongst industry experts of production, Research and Development (R&D), and marketing department. Fuzzy analytical hierarchy programme (AHP) was implemented to rank different factors. It was found that some opinions varied according to the department. For example, production department believes that technology is more important than organization, but the opinion of R&D and marketing department in this regard was contrasting. However, cost factor was identified as the most influencing factor by all three departments. In another similar study, Sonar et al. (2021) employed AHP to identify and rank several factors to explore the adoption of AM. Survey was conducted in the form of

interviews with managerial level experts. The industries located in western part of India were classified as small, medium and large-sized and have already procured AM technologies. Managerial level experts were the participants. Survey analysis revealed that top level management commitment was the most important in the prioritization of the factors. The financial factor (cost) was ranked 4th unlike the finding of Yeh and Chen (2018).

The intention to use AM technologies vary for different users. Schniederjans (2017) explored the reasons for adopting AM by different users in industries. For this, she conducted a survey. It was found that 67% of the operators had used it for developing prototype and product design, 16% for experimentation purpose, 10% for producing end-usable products and the remaining 7% for demonstrating products to customers. Apart from this, author also emphasized that management must carry out a proper cost-benefit analysis before adopting AM. In a similar study, Niaki et al. (2019) carried out a survey in different companies to identify different motives for procuring AM. A questionnaire was prepared that comprised questions the reasons for using AM in industry. The questionnaire was sent to 807 companies across 22 countries. However, out of these only 88 companies took part in the survey. After obtaining the response, the second round of questionnaire was sent to experts of different sectors to prioritize the reasons for adopting AM. It was found that the motives vary in different sectors. For example, the main reason for the medical sector to procure AM was its ability to produce customised parts. However, for automotive and aerospace sector, the main reason to adopt AM was its ability to produce complex parts. According to authors, the dominating sustainability factor in AM was the economic aspect instead of environmental and social aspects.

Several industries show tremendous interest in AM, but they are not willing to adopt it as a manufacturing route. Yi et al. (2019) explored the reasons for this. They conducted a survey in a German-based manufacturing industry to identify the barriers to deployment of AM. Those were identified insufficient knowledge regarding AM technology, high investment cost, organization transformation and unpredictable benefits. Also, there is an apprehension about intellectual property protection and privacy protection with AM. It was emphasized that the cost estimation in AM is an effective tool that guides decision-making.

2.5.1 Decision support system for procuring 3D Printing

Researchers have also proposed several decision support models to select a proper AM based machinery as per requirement of the user. For example, Masood and Soo (2002)

proposed a rule based expert system to select the best 3D printer as per the users' requirement. A survey in the form of questionnaires was prepared for the user as well the vendors. The questions asked were related to system features, selection criteria, applications, price and machine performance. The response rate of the vendors and users were 70% and 13%, respectively. A computer program was developed based on several selection criteria, viz., cost of the 3D printer, dimensional accuracy along the *x*-*y* and *z* direction, finishing of the part, range of layer thickness, available raw material and the speed of printing a part. Based on the questions and requirement of the user, the program recommends the desired 3D printer along with its specifications and other valuable information.

Byun and Lee (2005) proposed a scheme to select a suitable 3D printer based on TOPSIS, a popular multi-attribute decision making (MADM). Data obtained from the questionnaire were sent to different users such as industries, government institutes and service bureau. Based on these data, the selection criteria were accessed. Six different 3D printers were considered. Apart from cost and build time as the selection criteria, mechanical properties such as surface roughness, accuracy, tensile strength and elongation were also chosen. The mechanical properties were expressed as a single crisp value, whereas the cost and build time was expressed as a fuzzy number. Different weights were assigned to each selection criteria and based on this, a ranking order was developed.

Roberson et al. (2013) proposed a decision-making model for selecting the best printer amongst five desktop 3D printers. Three AM processes, viz., FDM, SLA and LOM were considered. The cost of 3D printers was in the range of $ 1499–$ 20900. A part was printed on each machine and the ranking system was proposed based on material cost, build time, cost of the printer and dimensional accuracy. A scaling factor was employed to compare the differences between single and multiple parts. The scaling factor (s_f) for build time was given by

$$s_f = \frac{t_n}{t_1 n}, \tag{2.18}$$

where n is the number of parts, t_1 is the build time for one part and t_n is the build time of n parts. Similar approach was also used for estimating the scaling factor for material usage. If s_f is less than one, the respective 3D printer is more efficient for producing multiple parts than printing a single part. Else, the printer is suitable for printing only a single part. Based on the ranking system, FDM was ranked the highest.

Recently, Raigar et al. (2020) proposed a decision-making technique comprising the best worst and proximity indexed method. Apart from all the selection criteria considered by Byun and Lee (2005), heat deflection temperature was also chosen a criterion for comparing the AM processes. It is the temperature at which a polymer starts deforming at a particular load. A spur gear was fabricated by four different processes, viz., SLA, FDM, SLS and material jetting (MJ). It was desired to have the high dimensional accuracy and hence was assigned the highest weightage. Based on this, MJ and SLA were ranked the highest and lowest, respectively.

2.5 Major gaps in literature

A review of literature gave a lot of information on the sustainability concerns of AM. Some research gaps, limitations and possibilities for further exploration are summarized as follows:

- Although several models on build time, cost and energy estimation are available in literature, the issue of uncertainty is not addressed. In the previous works, the output is obtained as a single value. In practice, the parameters are uncertain and vary with production places and management policies. Hence, the output varies accordingly.
- It is evident from several research findings that full utilization of the machine yields the lowest unit cost. However, this increases the production time and tardiness. Hence, the supply of a product to the market is delayed. Appropriate delivery time is equally important for economic growth of an industry. However, this concern has received less attention.
- Comparative analysis of AM with other manufacturing processes based on cost estimation is carried out only by break even analysis. Aspect like demand of a product varies with buyers' requirement. Such uncertainties also affect the production cost. Hence, this aspect is also to be included in the decision-making process.
- One of the notable characteristics of AM is its ability to fabricate objects automatically. Hence, there is less demand for workforce. This raises a concern of job security amongst some workers and labourers. The effect of AM on labour work structure, employment and job security of the workers has not been investigated.

2.6 Objectives of the present thesis

Based on the literature survey and the research gaps, the following aspects are explored:

1. Cost analysis of additive manufacturing

Cost analysis of a manufacturing process requires information on different cost elements. For every AM process, cost elements are more or less the same, but some elements may vary based on the working principle. In this thesis, two popular AM processes, i.e., SLS and FDM are considered. For a prudent cost analysis of AM, its comparison with other competitive manufacturing processes is also a necessity. To accomplish this objective, the following two sub-objectives are adopted:

- **Cost estimation of additive manufacturing in the presence of uncertainties**

A cost model of AM is proposed. The model is developed by considering different activities and cost parameters relevant to AM processes. Build time, an important component for cost estimation is proposed analytically for both SLS and FDM. For validation, in-house experiments have been conducted. To consider the uncertainties in cost estimation, the concept of fuzzy sets is introduced. The methodology is demonstrated by examples.

- **Cost comparison of additive manufacturing with traditional manufacturing in the presence of uncertainties**

This objective presents an approach to compare the cost of an AM process, i.e., SLS with a traditional manufacturing process, i.e., injection moulding (IM). The cost estimation procedure for IM is presented. A method to estimate the reliability of the uncertain costs and the expected cost of manufacturing is proposed. Further based on the concept of reliability, the procedure to choose a favourable manufacturing process for a variable demand scenario is presented.

2. Utility assessment of additive manufacturing in an organisation

The second objective proposes a guideline for adopting AM technology in an organisation. For this, the concept of utilisation factor (U_f) and its effect on associated costs is presented. Based on U_f, a decision process on the utilization of AM is proposed. Additionally, a fuzzy set based technique to choose a favourable manufacturing based on deciding factors is demonstrated. A method to evaluate the labour penalty cost due to the reduction in employment is proposed. The overall procedure is illustrated by suitable examples.

3. Energy Consumption of Additive Manufacturing

This objective deals with the energy consumption of AM. Analytical models based on the working principle of two popular AM processes, i.e., SLS and FDM are presented. The role of different energy consuming elements and their necessity is highlighted. The effect of

producing a single as well as multiple parts on the energy consumption is discussed. Also, based on annual production of parts, energy usage and its associated cost, and the amount of carbon dioxide emission is evaluated. The procedure is demonstrated by examples.

The flow chart of this thesis is presented in Figure 2.1.

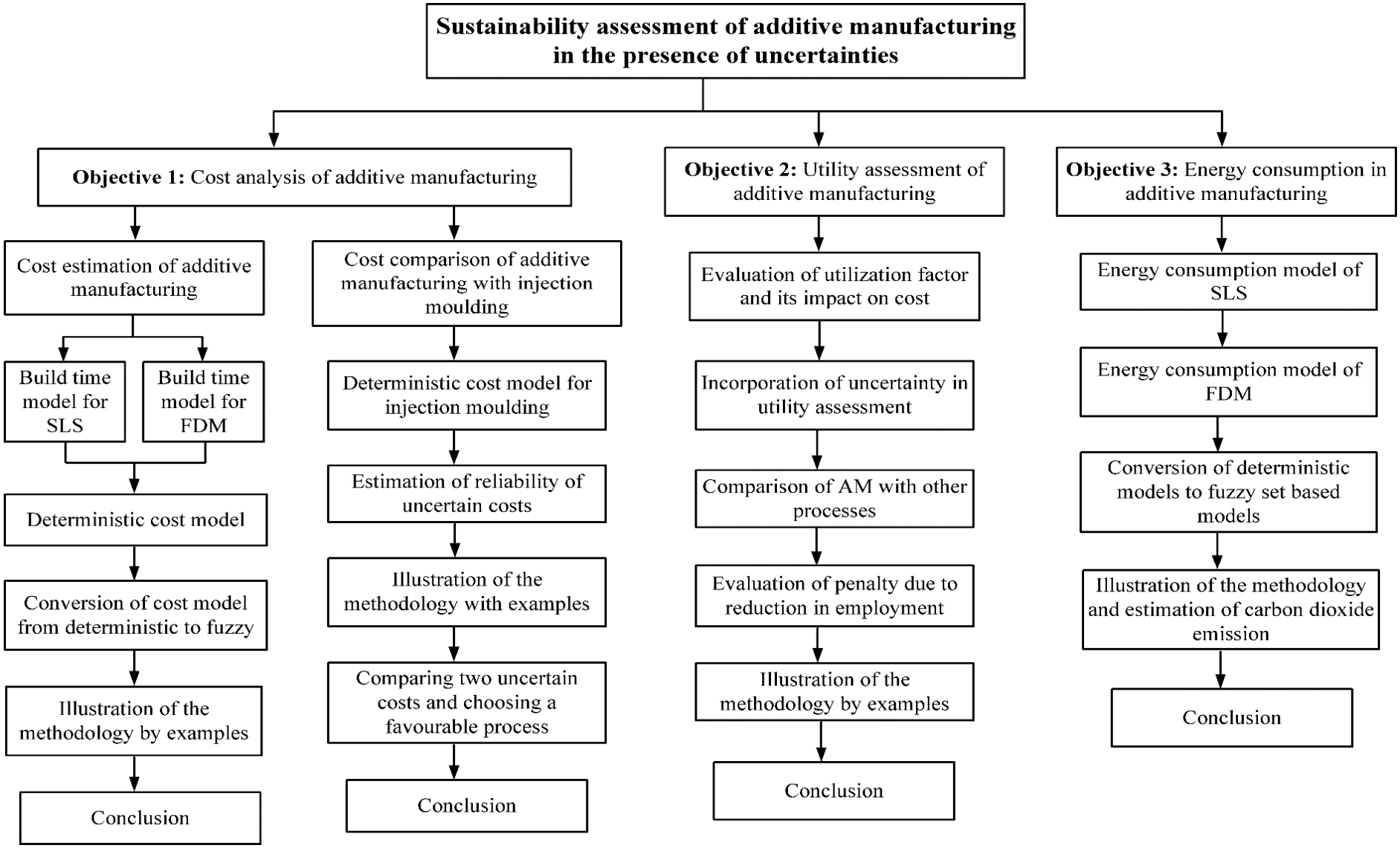

Figure 2.1 Flow chart of the present thesis

Chapter 3
Cost Estimation of Additive Manufacturing

3.1 Introduction

Every organization aims to make profit from the products that it manufactures. To ensure profitability, an organization attempts to estimate the production cost early through a proper cost estimation approach. Cost estimation helps in identifying business potential, preparing production budgets, accessing the sustainability of the process and performing a break-even analysis. To estimate the cost of a product, it is necessary to find the costs involved in various manufacturing operations. This chapter presents an approach for the cost estimation of AM process. For this purpose, two common AM processes, i.e., selective laser sintering (SLS) and fused deposition modelling (FDM) are considered. Although all AM processes follow a common procedure of layer by layer manufacturing, the operating principle differs for every AM process. Hence, it is appropriate to introduce and briefly describe the two processes, i.e., SLS and FDM before describing the procedure for cost estimation. Section 3.2 describes the deterministic model for cost estimation for AM process. Section 3.3 introduces the concept of fuzzy set theory for handling uncertainties. The methodology presented in this chapter is illustrated by examples in Section 3.4. Section 3.5 concludes the chapter.

3.1.1 Selective laser sintering (SLS)

SLS falls under the category of powder bed fusion process, one of the first commercialized AM processes. A schematic of SLS is illustrated in Figure 3.1. It involves the fusion of raw material in the form of polymeric, metallic or ceramic powder. The entire building process takes place inside a closed chamber often referred to as build chamber. A rotating roller spreads the powder and forms a layer in the build area of the chamber. Figure 3.1 shows a roller indicated by the filled circle at one location and an unfilled circle with dotted lines at other location. The heater system is composed of an infrared heater for heating the closed chamber and a resistive heater for maintaining the powder at an elevated temperature but below the melting point throughout the building process. The well-directed laser beam, generally of a CO_2 laser, sinters the powder particles according to the geometry of the part. After the laser sinters the particles of a layer, the movable piston lowers the powder bed vertically according to the layer thickness set by the operator. After this, the powder bed is

again filled up with powder by the roller for sintering by the laser beam. The heap of powder is placed in front of the roller by the power supply system that is controlled by another movable piston. This process repeats until the entire part is built. After the building of the part is completed, it is removed from the build chamber and necessary post-processing activities are performed.

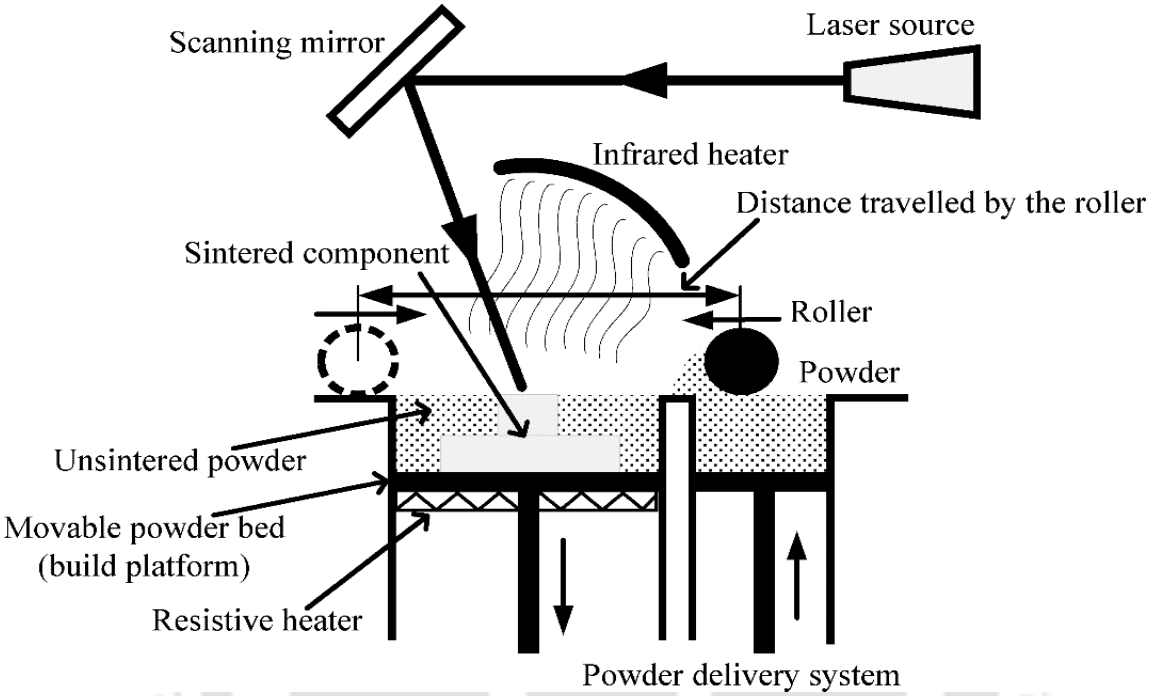

Figure 3.1 An illustration of SLS

3.1.2 Fused deposition modelling (FDM)

Extrusion technology in the form of fused deposition modelling (FDM) or fused filament fabrication (FFF) is a popular and user-friendly AM process (Masood 1996). However, the former term FDM, a trademark of the company Stratasys is more widely referred. It uses raw material in the form of thermoplastic filament material that is fed from the spool to the nozzle. The commonly used filaments are acrylonitrile butadiene styrene (ABS) and polylactic acid (PLA). The filament gets heated to a temperature just above the melting point (1–2 °C greater than the melting point). The semi-liquid material is then extruded from the nozzle and bonds to the previously built layer in the build bed as shown in Figure 3.2. The layer thickness is mainly dependent on the material extrusion rate and speed of the head. After a layer is formed, the platform is lowered down as per the prescribed layer thickness. The deposition of material in a layer-by-layer fashion in the platform continues until the entire part is built. The build platform moves in *z* direction, while the extrusion

nozzle moves in *xy* plane. For producing complicated geometries, FDM equipment with two nozzles, one for the part material and the other for support material, is used. After the entire part is produced, the part that gets stuck to the build bed is removed by a scraper tool. Finally, post-processing operations are done to ensure proper finishing of the part.

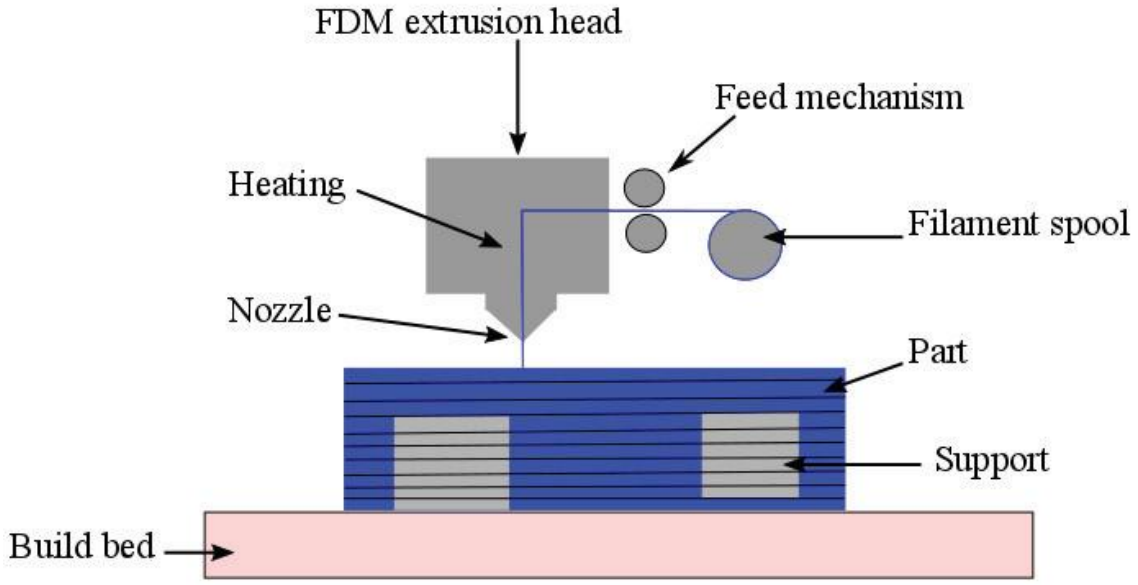

Figure 3.2 An illustration of FDM (Qattawi et al. 2017) (Under a Creative Commons License)

3.2 Deterministic model for cost estimation

Cost estimation methodologies for any manufacturing process, in general, and AM in particular, have several common features. However, some specific details will differ. In this chapter, the methodology for cost estimation of AM process is illustrated. Cost estimation for any additive manufacturing process is largely dependent on the build time.

Cost estimation requires consideration of numerous elements. Table 3.1 lists specific elements of cost that are relevant to AM technology. For developing a comprehensive cost model, several steps are followed in a systematic pattern. First step is the listing of various activities, e.g., pre-processing (designing the computer-aided design (CAD) model, converting to standard tessellation language (STL) format with file transfer and setting up the machine), processing and post-processing (part removal and cleaning). One of the important steps in pre-processing is the design of the printer head. This is also referred to as tool path strategy. Several approaches, viz., raster, spiral, zigzag, continuous and contour strategies have been developed for AM processes. For each strategy, the G code is accordingly generated by the slicing software. The same product can be produced via more than one strategy. However, every strategy has some advantages as well as

disadvantages. For example, the raster tool path strategy is easy to implement but it produces a product with poor dimensional accuracy. On the other hand, the spiral tool path strategy produces a product with relatively good dimensional accuracy but its implementation requires complex algorithms. To obtain the benefits of various tool path strategies, some researchers have also proposed hybrid tool path strategies (Ding et al. 2014). Every product has different geometrical features, hence, accordingly the best possible strategy should be chosen for producing a particular product. In general, low-cost 3D printers do not have the availability of producing a product with different tool path strategies. However, such facilities are available in high-cost 3D printers.

The next step is the estimation of time required for executing each task. In this step, the most crucial is the correct estimation of build time. The main component of the build time is the time to build the part layer by layer in the machine chamber. The heating of the platform in the machine and cooling down after the build process are also considered as a part of the build time. The build time directly influences the majority of the cost elements. Identification of cost elements is a difficult task and there are some differences in the approaches adopted by various researchers (Hopkinson et al. 2003; Ruffo et al. 2006a; Ruffo and Hague 2007; Baumers et al. 2016). In the last step, the cost calculation is carried out by using appropriate algebraic equations.

Table 3.1 Different elements for cost

Cost element	**Sub-elements**
Material cost	Main product, support and post-processing costs
Operator cost	Machine set-up, operating and post-processing costs
Slicing cost	Software and designer costs
Overhead cost	Depreciation, annual maintenance, electricity, factory rent costs

The build time is dependent on the type of AM technology, type of machine, build-orientation, slicing strategy, process parameters and the geometrical complexities of the part. The accurate estimation of build time is time consuming and highly difficult task. It is prudent to develop a reasonably approximate model of build time that requires the minimum possible information. Sections 3.2.1 and 3.2.2 describe the procedure for an approximate build time estimation for two common AM processes, i.e., SLS and FDM, respectively. Section 3.2.3 presents the cost model considering necessary cost elements.

3.2.1 Build time estimation model for selective laser sintering

Specific to SLS, build time can be mainly divided into two parts— time for adding powder by the roller and the time required for scanning. Apart from these, heating and cooling time are also considered (Ruffo et al. 2006b). Powder addition by the roller involves forming a layer of prescribed thickness by depositing powder. The layer of powder is formed in the entire horizontal area (*xy* plane) of the machine bed.

Pham and Wang (2000) provided an approximate formula to predict the time for adding powder by the roller. However, the formula ignored time for attaining the maximum velocity by the roller as well as time required for bringing the roller to the rest. Due to this, time for adding the powder was underestimated. Hence, Pham and Wang (2000) estimated this time empirically. In this study, acceleration and deceleration time are considered. The underlying kinematic behaviour of the roller is illustrated in Figure 3.3. OB represents the time period in which the roller starts from zero velocity to attain the maximum velocity. In the time period BC, the roller travels with constant velocity. Finally, the roller decelerates and comes to rest in the time period CD. The total distance travelled by the roller (l_r) is given by

$$l_r = \frac{1}{2} v_r \frac{v_r}{a_r} + v_r \left(t_{ap} - 2\frac{v_r}{a_r} \right) + \frac{1}{2} v_r \frac{v_r}{a_r}, \tag{3.1}$$

where v_r is the maximum attainable velocity of the roller, a_r is the acceleration and deceleration of the roller during starting and stopping, respectively and t_{ap} is the time for adding powder by the roller. Solving Eq. (3.1), t_{ap} is obtained as

$$t_{ap} = \frac{l_r}{v_r} + \frac{v_r}{a_r}. \tag{3.2}$$

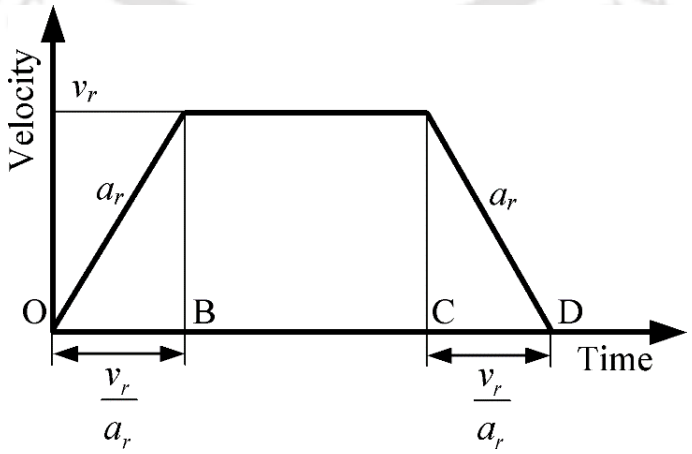

Figure 3.3 A typical time-velocity diagram of the roller

Considering time delay between two successive layers (t_d), t_{ap} is given by

$$t_{ap} = \left(\frac{l_r}{v_r} + \frac{v_r}{a_r} \right) + t_d . \tag{3.3}$$

Time delay that includes lowering down of the platform and roller return time, is a difficult-to-estimate element. The time delay between two layers may depend on the type of powder and judgement of the operator. Eq. (3.3) is applicable for only one layer of powder. For the complete part, t_{ap} is given by

$$t_{ap} = \left\{ \left(\frac{l_r}{v_r} + \frac{v_r}{a_r} \right) + t_d \right\} \frac{h_z}{l_t}, \tag{3.4}$$

where h_z is the height of the part and l_t is the layer thickness. It is assumed that the layer thickness is fixed throughout the height of the part.

The other part of build time is the scanning time. It takes place by the action of a laser beam. It is the process where the part is built layer by layer. Unlike the time estimation for powder addition by the roller, the scanning time is a complex phenomenon and varies for different geometrical features contained in a part. The kinematics involved in scanning is similar to that in powder addition (coating) by the roller. Considering a part to be a rectangular prism, the total number of scans required for scanning one layer (N_s) is given by

$$N_s = \frac{w_y}{d_h + d_l} + 1, \tag{3.5}$$

where w_y is the width of the part, d_h is the scan spacing and d_l is the laser beam diameter. Time required to scan a complete layer (t_{scan}) is given by

$$t_{scan} = \frac{l_x}{v_s} \left(\frac{w_y}{d_h + d_l} + 1 \right) + \frac{v_s}{a_l}, \tag{3.6}$$

where l_x is the length of the part, v_s is the maximum scan velocity of the laser beam and a_l is the acceleration of the laser beam. Representation of necessary parameters involved in scanning process is illustrated in Figure 3.4. Eq. (3.6) gives the time for scanning only one layer of the part. Laser delay time being very small is neglected. For the complete part, the time required to scan (t_{scan}) is given by

$$t_{scan} = \frac{h_z}{l_t} \left\{ \frac{l_x}{v_s} \left(\frac{w_y}{d_h + d_l} + 1 \right) + \frac{v_s}{a_l} \right\}. \tag{3.7}$$

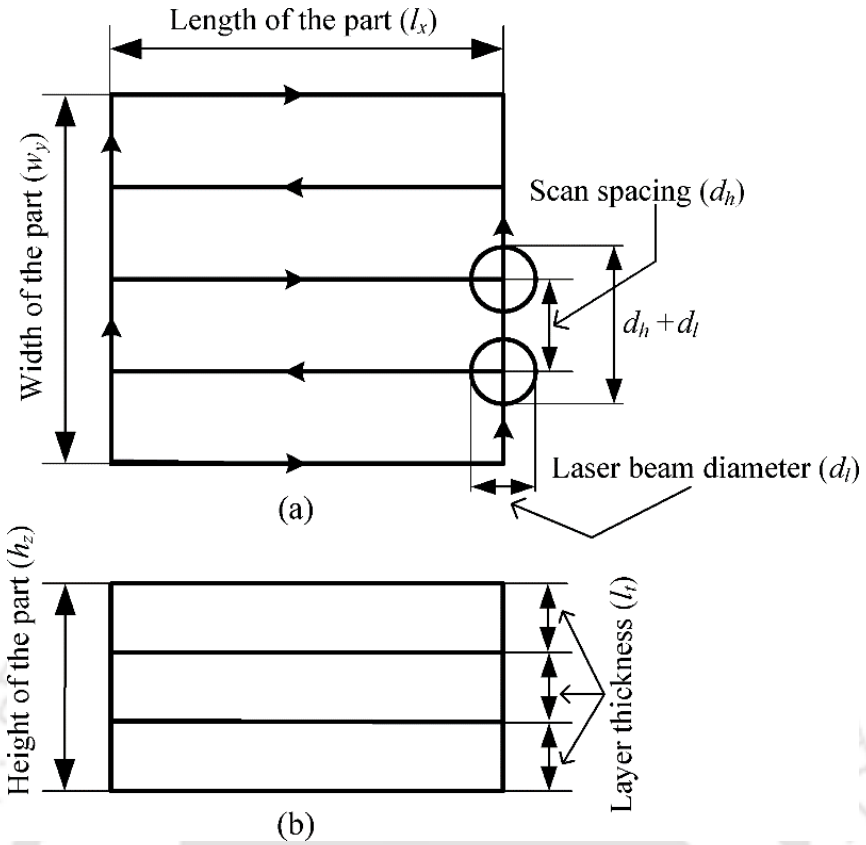

Figure 3.4 A schematic of scanning process: (a) top view of the part illustrating laser beam diameter and scan spacing, (b) front view illustrating layer thickness of the part

Eq. (3.7) is applicable if the part is a rectangular prism. If a part comprises some complex geometrical features, Eq. (3.7) requires modification. For such cases, an approach to estimate t_{scan} was proposed by Ruffo et al. (2006b). They presented an empirical model for build time estimation in SLS process. In their study, they considered a box of cuboidal shape that contained the entire volume of the part. Similar approach is followed in this work. The cuboidal shaped box is termed as a bounding box that refers to the volume of the smallest cuboid that covers every edge of the part to be formed. The ratio of the volume of the actual part (V_{part}) to that of the volume of the bounding box (V_b) is denoted by r_p:

$$r_p = \frac{V_{part}}{V_b}. \tag{3.8}$$

Larger value of r_p indicates that there is less empty space in the bounding box. Incorporating r_p in Eq. (3.7), t_{scan} is obtained as

$$t_{scan} = r_p \frac{h_z}{l_t}\left\{\frac{l_x}{v_s}\left(\frac{w_y}{d_h + d_l} + 1\right) + \frac{v_s}{a_l}\right\}. \tag{3.9}$$

Figures 3.5 and 3.6 illustrate two typical layers where only the dotted filled portion is to be sintered by laser scanning. The laser beam starts from point O and stops at point G. The kinematic behaviour of the laser scan is shown in the time period O to G. Figure 3.5 shows a layer having a small empty space BE. From point B to point E, the laser travels at rapid velocity. At rapid velocity, scanning does not take place. Also, the nozzle cannot attain its maximum rapid velocity due to a small empty space. The distance BE (s) is given by

$$s = v_s t_{r1} + 2 \times \frac{1}{2} \frac{t_{r1}}{2} \left(a_l \frac{t_{r1}}{2} \right), \tag{3.10}$$

where t_{r1} is the time taken to cover the distance BE. Solving Eq. (3.10), t_{r1} is obtained as

$$t_{r1} = \frac{2\left(\sqrt{v_s^2 + a_l s} - v_s\right)}{a_l}. \tag{3.11}$$

Overall, the total time to travel at rapid velocity (t_r) to cover the entire part is given by

$$t_r = \left\{ \frac{2\left(\sqrt{v_s^2 + \left(1 - r_p\right) a_l l_x} - v_s\right)}{a_l} \right\} \left(\frac{w_y}{d_h + d_l} + 1 \right) \frac{h_z}{l_t} + \frac{w_y}{v_s}. \tag{3.12}$$

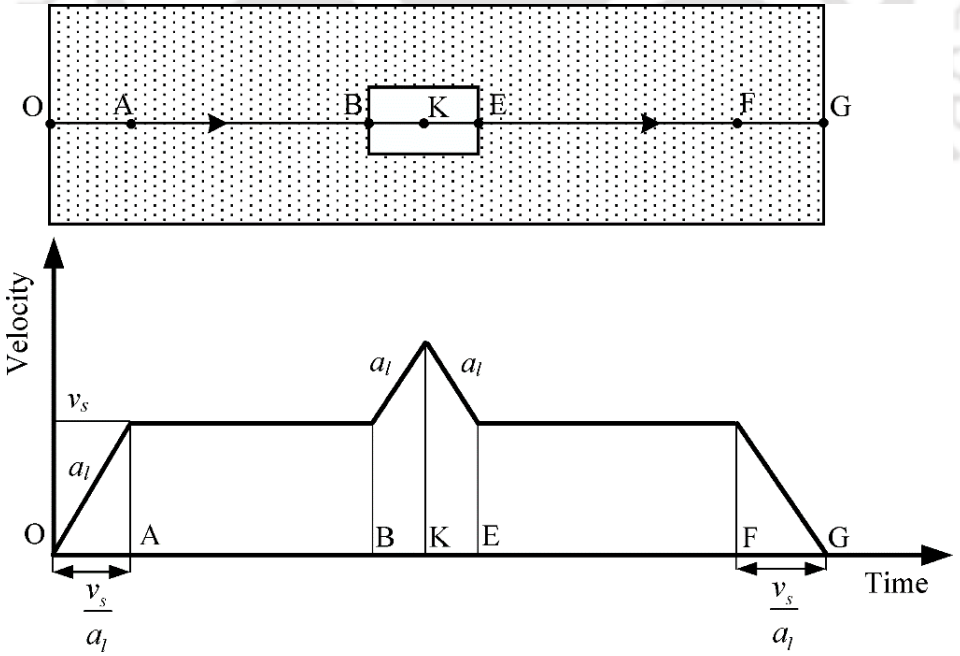

Figure 3.5 A typical layer undergoing sintering process with a small empty space and corresponding time-velocity diagram

In Figure 3.6, the distance BE represented by s is the empty space that is to be travelled at rapid velocity. Since the empty space is large, the laser beam attains its

maximum velocity unlike in Figure 3.5. The distance CD is travelled at maximum rapid velocity by the laser nozzle. Let the time taken to travel the overall empty distance BE be represented by t and the time required to travel the distance BC be represented by t_a. The distance BE (s) is given by

$$s = 2\times\frac{1}{2}\left(v_{ra}-v_s\right)t_a+\left(v_{ra}-v_s\right)\left(t-2t_a\right)+v_s t, \tag{3.13}$$

where v_{ra} is the rapid velocity of the laser nozzle. Solving Eq. (3.13), t is obtained as

$$t=\frac{s}{v_{ra}}+\frac{\left(v_{ra}-v_s\right)t_a}{v_{ra}}. \tag{3.14}$$

Let the time required to cover the distance BC or DE (Figure 3.6) be represented by

$$\frac{t_{r2}}{2}=\frac{v_{ra}-v_s}{a_l}. \tag{3.15}$$

Eq. (3.15) gives the value of time when the laser nozzle has attained its maximum rapid velocity. This is also the maximum value of time to attain the maximum velocity of the laser nozzle. Hence, by replacing t_a in Eq. (3.14) by $t_{r2}/2$ from Eq. (3.15), Eq. (3.14) yields

$$t=\frac{s}{v_{ra}}+\frac{\left(v_{ra}-v_s\right)^2}{v_r a_l}. \tag{3.16}$$

Overall, the total time (t_r) to travel at rapid velocity (the entire part) is given by

$$t_r=\left\{\frac{\left(1-r_p\right)l_x}{v_{ra}}+\frac{\left(v_{ra}-v_s\right)^2}{v_{ra}a_l}\right\}\frac{h_z}{l_t}\left(\frac{w_y}{d_h+d_l}+1\right)+\frac{w_y}{v_s}. \tag{3.17}$$

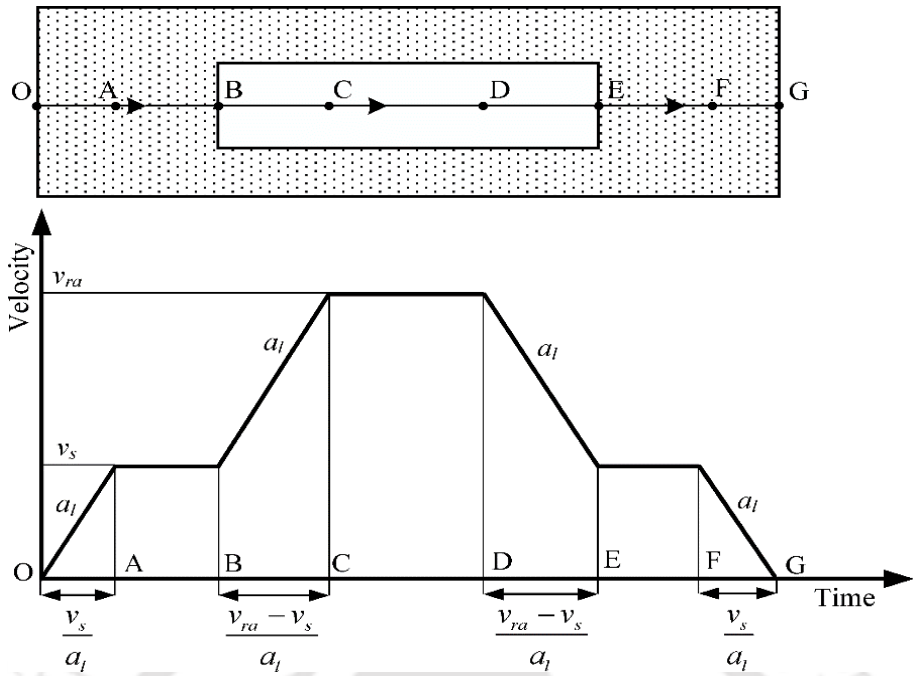

Figure 3.6 A typical layer undergoing sintering process with a large empty space and corresponding time-velocity diagram

In order to determine if an empty space is larger or not, the values of t_{r1} and t_{r2} are determined from Eqs (3.11) and (3.15), respectively. If t_{r1} is smaller than t_{r2}, Eq. (3.12) is applicable; else Eq. (3.17) is applicable. In situations where both small and large empty spaces are present, the time to travel at rapid velocity is given by the weighted combination of the times given by Eq. (3.12) and Eq. (3.17). Overall, the total build time (t_{build}) is given by an algebraic summation:

$$t_{build} = t_{mp} + t_{ap} + t_{scan} + t_r + t_{eo}, \tag{3.18}$$

where t_{mp} is the time required for machine preparation that involves machine set-up, warming up of the closed chamber and other preliminary operations. t_{eo} is the time required in ending operations such as cooling down of the machine chamber and repositioning of the laser beam and powder bed. Eq. (3.18) is applicable only when a single part is built inside the machine chamber. If multiple quantities (say n_p) of the same part are built in the machine chamber, the build time for an individual part is given by

$$t_{build} = \frac{t_{mp} + t_{ap} + t_{eo}}{n_p} + t_{scan} + t_r. \tag{3.19}$$

In this case, the time for adding powder by the roller (t_{ap}) and fixed time components, i.e., the time for machine preparation (t_{mp}) and time for ending operation (t_{eo}) are divided equally amongst all the parts in the machine chamber.

3.2.2 Build time estimation model for fused deposition modelling

The methodology for build time estimation in FDM is developed by considering the building of a hollow rectangular prism. It is then generalized for building any part by using certain factors. Figure 3.7 depicts the top view of the prism with outer boundary ABCD and inner boundary EFGH. It is assumed that the track width of deposition is the same as the nozzle diameter.

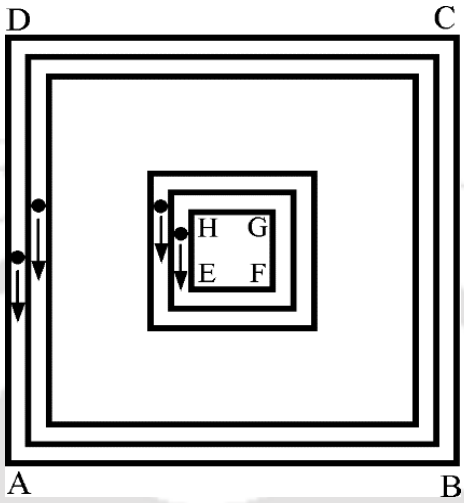

Figure 3.7 A pictorial view representing generation of boundaries in a rectangular layer

The building of the rectangular part is carried out in the following stages:

Stage i: Building of outer surface bounded by rectangular ABCD

During this stage, the nozzle of diameter d_n traverses the outer periphery and deposits the material to make solid layers. If the perimeter of rectangular ABCD is p_o, the nozzle will cover a distance of $(p_o–2d_n)$ in tracing the outer surface. However, usually, the thickness of the wall is enhanced by traversing the nozzle again. In the second time, nozzle will cover a distance of $(p_o–4d_n)$.

Stage ii: Building of inner surface bounded by rectangular EFGH

During this stage, the nozzle of diameter d_n traverses the inner periphery and deposits the material to make solid layers. If the perimeter of rectangular EFGH is p_i, the nozzle will cover a distance of (p_i+2d_n) in tracing the inner surface. During the second trace for enhancing the inner wall thickness, nozzle will cover a distance of (p_i+4d_n).

Stage iii: Building of the bottom surface

During this stage, nozzle will scan the area between inner and outer walls to make the solid bottom surface.

Stage iv: Filling the volume with prescribed infill density: During this stage, the nozzle moves in a zigzag path to build a structure with a prescribed infill density. Infill density

can vary from 0 (no material) to 100% (totally solid structure). Lower the infill density, lesser is the time and material requirement. Figure 3.8 shows a schematic of a fully solid layer and a partially filled layer.

Stage v: Building of the top surface

This stage is similar to stage iii and makes a solid top surface.

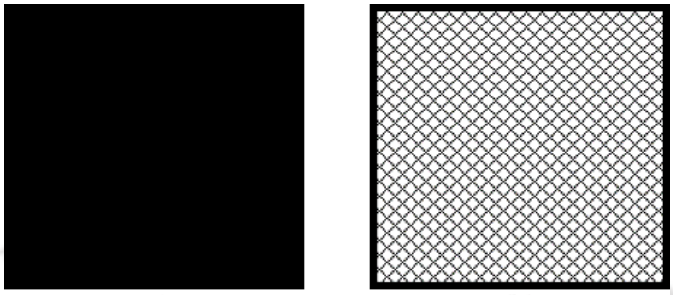

Figure 3.8 Representation of (a) solid layer (100% infill density) and (b) partially filled layer

The motion of the nozzle comprises acceleration, uniform velocity and retardation. The maximum velocity of the nozzle is considered as v_n and uniform acceleration as well as retardation as a_n. Depending on the distance covered by the nozzle, two scenarios of motion may occur as shown in Figure 3.9. It is to be noted that Figure 3.9(a) is similar to Figure 3.3. The nozzle is able to attain the maximum velocity when the traverse distance is large. Hence, similar to Eq. (3.2), time (t_l) for traversing a distance l_n by the nozzle is given by

$$t_l = \frac{l_n}{v_n} + \frac{v_n}{a_n}. \tag{3.20}$$

However, condition for the applicability of Eq. (3.20) is

$$l_n \geq \frac{v_n^2}{2a_n}. \tag{3.21}$$

When the traverse distance is not large, i.e., inequality in Eq. (3.21) is not satisfied, the maximum velocity is not attained as shown in Figure 3.9(b). For this case, the time for traversing a distance l_n is given by

$$t_l = 2\sqrt{\frac{l_n}{a_n}}. \tag{3.22}$$

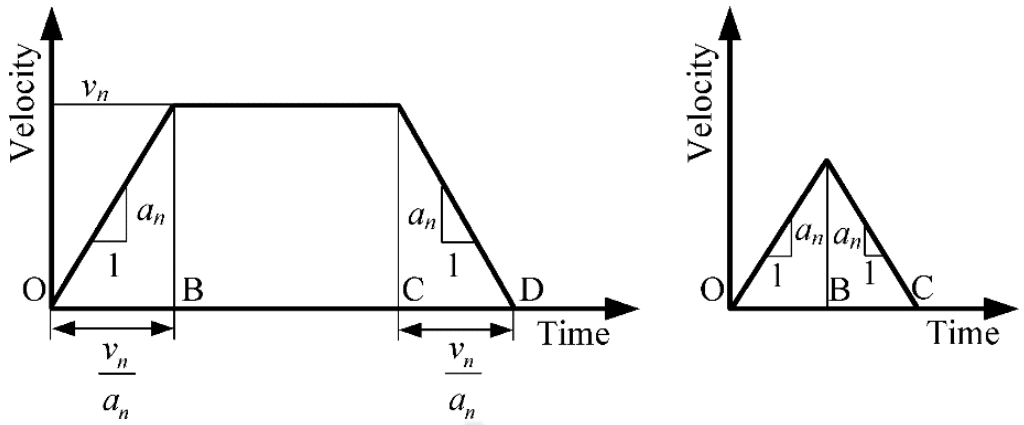

Figure 3.9 Time-velocity diagram of nozzle for covering (a) a large and (b) a small distance

Now time estimation for the aforesaid five stages is as follows:

Stage i: For building the outer wall of thickness equal to twice the nozzle diameter, the distance covered by the nozzle is ($2p_o$–$6d_n$). Considering it as a large distance satisfying the inequality of Eq. (3.21), the time for making one layer in this stage is

$$t_{layer\_i} = \left\{ \frac{(2p_o - 6d_n)}{v_n} + \frac{v_n}{a_n} \right\}. \tag{3.23}$$

If the height of the part is h_z and the layer thickness is l_t, then the time for this stage is

$$t_i = \left\{ \frac{(2p_o - 6d_n)}{v_n} + \frac{v_n}{a_n} \right\} \frac{h_z}{l_t}. \tag{3.24}$$

Stage ii: The time for this stage is obtained, similarly, as

$$t_{ii} = \left\{ \frac{(2p_i + 6d_n)}{v_n} + \frac{v_n}{a_n} \right\} \frac{h_z}{l_t}. \tag{3.25}$$

Stage iii: The solid bottom surface is obtained by scanning the nozzle over the entire surface S_b between inner and outer walls. Thus, the time during this stage is

$$t_{iii} = \frac{S_b}{v_n d_n}. \tag{3.26}$$

Stage iv: In this stage, the volume has to be filled with prescribed infill density. As the volume deposition rate is $v_n d_n l_t$, the ideal time required in this stage is

$$t_{iv\_ideal} = \frac{V_{net} I_d}{100 v_n d_n l_t}, \tag{3.27}$$

where V_{net} is the net volume to be filled and I_d is the percentage infill density. V_{net} is obtained in the following way. Let the volume of an imaginary bounding box (rectangular prism) of length l_b, width w_b and height h_b be V_b. The ratio of the part volume V_{part} to V_b is given by

$$r_p = \frac{V_{part}}{V_b}. \tag{3.28}$$

Then, the net volume (V_{net}) is given by

$$V_{net} = r_p \left(l_b - 2d_n\right)\left(w_b - 2d_n\right)\left(h_b - 2l_t\right). \tag{3.29}$$

This value of V_{net} can be substituted in Eq. (3.27) to get a time estimation. However, due to non-uniform motion, the actual time will be more than this ideal estimate. It is very tedious to carry out the proper motion analysis, particularly at the planning stage. A simplified approach is to assume that the nozzle undergoes a number of cycles by starting from rest, reaching the peak velocity and after some time retarding to again come at rest. Consider that in a cycle, it covers a traverse distance l_n. In that case, the actual time of traverse can be estimated from Eq. (3.20) or Eq. (3.22). On the other hand, the ideal time to traverse this length is

$$t_{ideal} = \frac{l_n}{v_n}. \tag{3.30}$$

Hence, a correction factor c can be obtained by dividing the actual time by the ideal time. Thus,

$$c = \begin{cases} 1 + \dfrac{v_n^2}{a_n l_n} & \text{for } l_n \geq \dfrac{v_n^2}{2a_n}, \\ 2v_n\sqrt{\dfrac{1}{a_n l_n}} & \text{otherwise.} \end{cases} \tag{3.31}$$

Finally, the estimated time for Stage iv is obtained as

$$t_{iv} = c\, t_{iv\_ideal}. \tag{3.32}$$

Accuracy of estimation is highly dependent on choosing a typical representative value of l_n. Another important kinematic parameter in FDM is jerk. Jerk resembles the velocity jump that occurs instantaneously when the nozzle initiates acceleration or the retardation phase (Comminel el al. 2018). Actually, the jerk should be expressed in m/s^3, but it is expressed by machine manufacturers in m/s, considering velocity change in very small interval (almost instantaneously). It also determines how fast the nozzle changes its direction while depositing molten material. As per Messimer et al. (2019), jerk setting greater than 20 mm/s increases the vibration in the machine resulting in the dimensional error of the printed part. The corners of a produced part appear to be slightly elevated and rounded. On the other hand, jerk setting lower than 1 mm/s prevents the nozzle to move very slowly resulting in

irregularities with the melt pool of the extruded molten material from the nozzle. In this work, for simplicity, the effect of jerk in build time estimation is not considered.

Stage v: This stage is similar to Stage iii. If the top surface area is S_t, then the time during this stage is

$$t_v = \frac{S_t}{v_n d_n}. \tag{3.33}$$

Now, the total build time (t_{build}) is estimated by combining the time estimates of all the five stages, i.e,

$$t_{build} = t_i + t_{ii} + t_{iii} + t_{iv} + t_v. \tag{3.34}$$

3.2.2.1 Determination of lower and upper limits of time estimate

Accurate estimation of the correction factor (c) described in Section 3.2.2 is a difficult task. This factor depends on the representative average length (l_n) travelled by the nozzle in different paths in the xy plane. For a part, l_n is estimated as the mean of the shortest and the largest distance travelled by the nozzle during material deposition. Figure 3.10 illustrates two layers to be scanned by the laser beam. The arrow shows the direction of travel by the laser beam. For both cases, l_n is $(a+d)/2$.

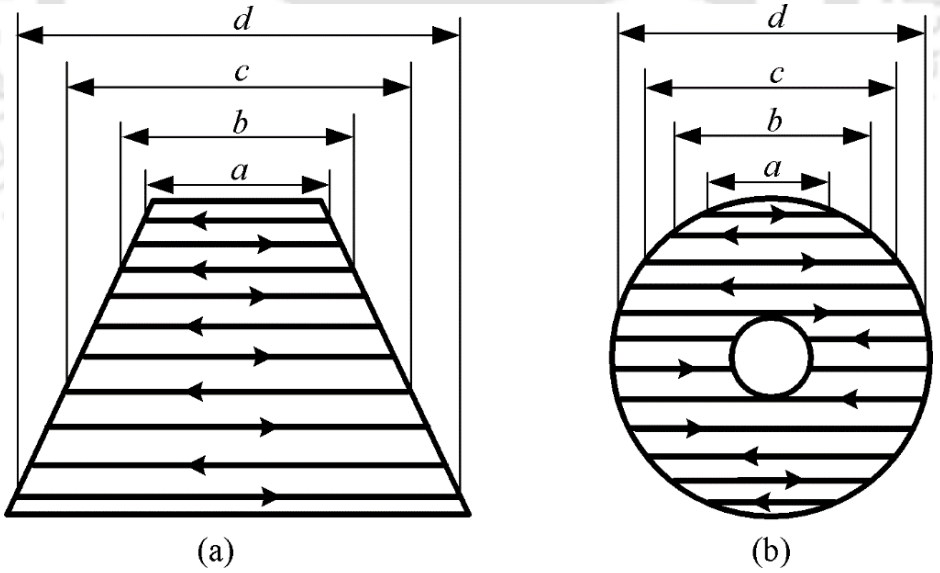

Figure 3.10 Illustration of representative average length (l_n) travelled by the nozzle for (a) a layer to be completely filled, (b) a layer to be partially filled

For determining a proper range of l_n, a statistical approach is adopted in this work. The approach relies on the random measurements of the length at a few places. The following steps are executed:

Step 1: It is decided to take n_s samples for estimating l_n. In each sample, n_d measurements are carried out.

Step 2: For each sample, the mean length ($\bar{l}_j$) is calculated as

$$\bar{l}_j = \frac{\sum_{i=1}^{n_d} l_i}{n_d}, \tag{3.35}$$

where j varies from 1 to n_s.

Step 3: The grand mean ($\bar{\bar{l}}$) is calculated as

$$\bar{\bar{l}} = \frac{\sum_{j=1}^{n_s} \bar{l}_j}{n_s}. \tag{3.36}$$

Step 4: The standard deviation of the means (s_m) is calculated as

$$s_m = \sqrt{\frac{\sum_{j=1}^{n_s} \left(\bar{l}_j - \bar{\bar{l}}\right)^2}{n_s - 1}}. \tag{3.37}$$

Step 5: The final step involves the calculation of confidence interval (C_I). It gives a lower and upper estimate of length as

$$C_I = \bar{\bar{l}} \pm t_{(n_s-1,\alpha/2)} \frac{s}{\sqrt{n_s}}, \tag{3.38}$$

where t-value is a statistics of Student's t-distribution and α is the significance level. Considering 95% confidence, the value of α is 0.05. The t-value is obtained from a standard statistical table. Hence, by using this procedure, lower and upper estimates of length are obtained. This helps in providing interval estimation of build time in FDM.

3.2.3 Cost model

Summation of all the cost elements listed in Table 3.1 gives the total cost (C_{total}) of a part manufactured by an AM process:

$$C_{total} = C_{material} + C_{operator} + C_{slicing} + C_{overhead}, \tag{3.39}$$

where $C_{material}$ is the material cost, $C_{operator}$ is the operator cost, $C_{slicing}$ is the slicing cost including software and involvement of the designer to convert the CAD model to proper format and $C_{overhead}$ is the overhead cost. Denoting material cost per unit mass by $c_{material}$

and time-dependent cost components by lowercase letter c followed by subscript representing the respective cost-element, the total cost (C_{total}) can be written as

$$C_{total} = \left(c_{material} m_r\right) + \left(c_{slicing} t_{design}\right) + \left\{\left(c_{operator} + c_{overhead}\right) t_{build}\right\} + \left(c_{operator} t_{pp}\right), \tag{3.40}$$

where m_r is the mass of raw material needed for fabricating the part, t_{design} is the time required to convert the CAD model to proper STL file format and t_{pp} is the time required to remove the part from the build chamber of the machine and perform finishing operations. When a part is manufactured by powder, some powder always gets wasted and becomes unusable. The waste powder mass should also be included in the estimation of m_r. One simple way for getting the proper estimate of m_r is to multiply the actual mass by a suitable factor. An important element of any AM process is the slicing cost. It comprises the cost of a slicing software that is required to convert a CAD model into a proper STL format. In this process, a designer is involved in the judicious use of the slicing software. For operating an AM based machine, an operator is required for carrying out activities like repositioning the machine bed, removal of the part from the machine bed, ensure proper functioning of the machinery parts and carrying out suitable finishing operations. In some cases, operators are also trained to handle the slicing software in desktop 3D printers. Hence, the role of an operator cannot be ignored although AM based machineries are claimed to be automatic unlike conventional machineries.

Eq. (3.40) is applicable for finding the cost only when a single part is built at the machine chamber. If multiple parts (say n_p) of the same part are built in the machine chamber, the total cost (C_{total}) per part is given by

$$C_{total} = \left(c_{material} m_r\right) + \left(\frac{c_{slicing} t_{design}}{n_p}\right) + \left\{\left(c_{operator} + c_{overhead}\right) t_{build}\right\} + \left(c_{operator} t_{pp}\right). \tag{3.41}$$

Per hour cost-elements are obtained as

$$c_{operator} = \frac{\text{monthly salary}}{\left(\text{working days in a month} \times \text{effective working hours in a day}\right)}, \tag{3.42}$$

$$c_{slicing} = \frac{\text{Annual slicing software cost}}{\text{annual operating hours}} + \frac{\text{monthly salary of the designer}}{\left(\begin{array}{l}\text{working days in a month} \\ \times \text{ effective working hours in a day}\end{array}\right)}, \tag{3.43}$$

$$c_{overhead} = \frac{1}{\text{annual operating hours}} \left(\frac{\text{machine cost} - \text{salvage value}}{\text{machine life}} + \text{annual maintenance cost} + \text{annual factory rent} + \text{annual electricity charge} \right). \quad (3.44)$$

3.3 Implementation of fuzzy set theory for handling uncertainties

The cost estimation procedure described in Section 3.2 is deterministic in nature. To take into account uncertainties, the deterministic cost models can be converted into fuzzy set based cost models. An element in a fuzzy set is characterized by a membership grade, which usually varies between 0 and 1. A fuzzy set is the generalization of a conventional crisp set, in which membership grade of each element of the set is 1. For developing a fuzzy set based model, the uncertain quantities are treated as fuzzy variables. A fuzzy variable is a quantity whose value is imprecise or vague rather than a single crisp value. A fuzzy variable is represented by a fuzzy number that is an agglomeration of interval numbers with a membership grade associated with each interval. There are several ways of obtaining a fuzzy number; the most common way is to construct it based on the inputs from experts. This thesis considers all fuzzy variables as triangular fuzzy numbers. In a triangular fuzzy number, the low (l) and the high (h) estimates of experts are assigned a membership grade of 0.5 while the most likely (m) estimate is assigned a membership grade of 1 (Dixit and Dixit 2008).

Membership grade greater than 0.5 in a fuzzy set indicates the positive association of the element with the set. On the other hand, membership grade lower than 0.5 indicates that the element is more inclined towards being a non-member of the set. Membership grade of 0.5 is a border case, where the degree of association with the set is half. Hence, it is reasonable to assign a membership grade of 0.5 to low (l) and high (h) estimates, which indicates that there is a 50% chance to get such values. Figure 3.11 shows a typical linear triangular fuzzy number. It is to be noted that that most likely estimate m need not be simple mean of l and h. (For example, assuming a worker gets \$ 5 for some task. Due to rising inflation, it may be advisable to keep a provision of \$ 7 for the task. Hence, the high estimate may be kept as \$ 7. However, it is not prudent to fix low estimate as \$ 3, because labour charges usually do not reduce, at least significantly. Hence, the expert might fix low estimate as just \$ 4.8 or so.)

A fuzzy number can be represented by an infinite number of intervals with different membership grades. An α-cut of a fuzzy set is a crisp set containing all the elements having

membership grades greater than or equal to α. The α-cut of a typical convex fuzzy number (say A) is represented by

$$A_{\alpha} = \left[a_1^{\alpha}, a_2^{\alpha} \right], \tag{3.45}$$

where A_α is the interval corresponding to membership grade α, $a_1{}^{\alpha}$ and $a_2{}^{\alpha}$ are the lower and upper limits of the interval, respectively.

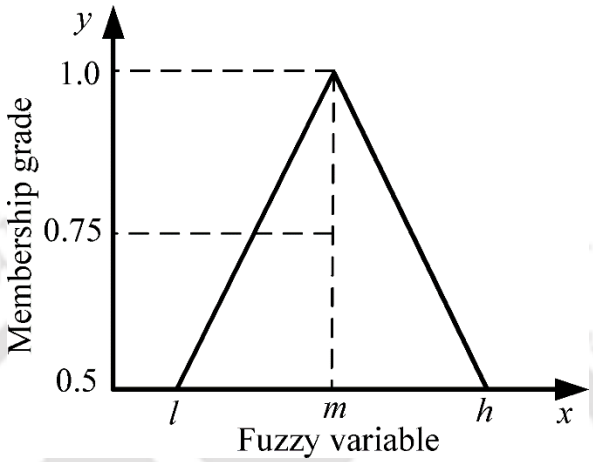

Figure 3.11 Fuzzy variable as a function of membership grade

For developing a fuzzy set based model, arithmetic operations, viz., addition, subtraction, multiplication and division in the deterministic model are replaced by fuzzy operations. Fuzzy arithmetic carries out interval arithmetic at each membership grade α. Suppose a variable A has interval ($a_1{}^{\alpha}$, $a_2{}^{\alpha}$) and B has interval ($b_1{}^{\alpha}$, $b_2{}^{\alpha}$) at membership grade α, then the arithmetic operations at that particular membership grade (α-cut) are carried out in the following manner:

$$\text{Summation: } (a_1^{\alpha}, a_2^{\alpha}) + (b_1^{\alpha}, b_2^{\alpha}) = (a_1^{\alpha} + b_1^{\alpha}, a_2^{\alpha} + b_2^{\alpha}) \tag{3.46}$$

$$\text{Subtraction: } (a_1^{\alpha}, a_2^{\alpha}) - (b_1^{\alpha}, b_2^{\alpha}) = (a_1^{\alpha} - b_2^{\alpha}, a_2^{\alpha} - b_1^{\alpha}) \tag{3.47}$$

$$\text{Multiplication: } (a_1^{\alpha}, a_2^{\alpha}) \times (b_1^{\alpha}, b_2^{\alpha}) = (a_1^{\alpha} \times b_1^{\alpha}, a_2^{\alpha} \times b_2^{\alpha}) \tag{3.48}$$

$$\text{Division: } (a_1^{\alpha}, a_2^{\alpha}) \div (b_1^{\alpha}, b_2^{\alpha}) = (a_1^{\alpha} / b_2^{\alpha}, a_2^{\alpha} / b_1^{\alpha}) \tag{3.49}$$

This way, the interval can be obtained at each α-cut. For illustration, fuzzy addition and subtraction of two fuzzy numbers (A and B) are shown in Figure 3.12. Addition and subtraction of two linear triangular fuzzy numbers will result in linear triangular fuzzy numbers but the same is not true for the multiplication and division. However, as an approximation, the fuzzy numbers obtained by multiplication and divisions can also be treated as linear triangular fuzzy numbers.

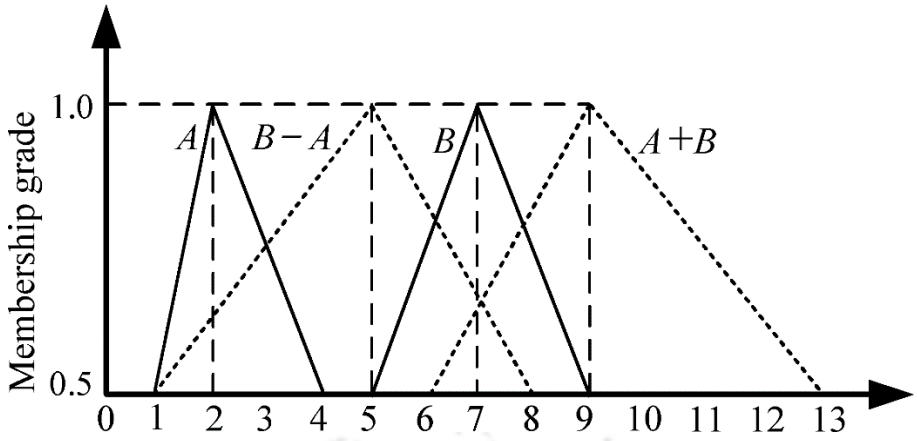

Figure 3.12 Arithmetic operations (addition and subtraction) of two fuzzy numbers

3.4 Illustration of the methodology by examples

The procedure described in Section 3.2 will be implemented to estimate the cost of different parts manufactured by two AM processes, i.e., SLS and FDM. Specific to SLS, two parts, i.e, part A and part B are considered. The parts were earlier considered for manufacturing by Zhang and Bernard (2013). These parts are deliberately selected so that the build time obtained by those authors can be compared with the values obtained by the build time estimation model developed in Section 3.2.1. However, for FDM process, in-house experiments were conducted and parts having different geometrical features were printed in an FDM machine. The purpose was to compare the actual time with the values obtained by the analytical model described in Section 3.2.2. Later, the cost model was implemented to evaluate the cost of both SLS and FDM. The cost estimation for SLS and FDM are illustrated with examples in Section 3.4.1 and Section 3.4.2, respectively.

3.4.1 Cost estimation for SLS

The parts considered for SLS are part A and part B. Part A is a milling cutter of volume 184893 mm^3 contained in a bounding box of dimensions 120 × 120 × 28 mm^3 and part B is a typical 3D shape of volume 9603 mm^3 contained in a bounding box of dimensions 74 × 34 × 34 mm^3 (Zhang and Bernard 2013). The details of the SLS machine parameters are given in Table 3.2. In the estimation of build time, the first step is to calculate the time for spreading powder by the roller. Then, the time to scan each individual layer, and the time to travel at rapid speed is calculated. Finally, the overall build time of both the parts is calculated. Table 3.3 shows different variables for build time calculation. The methodology developed in this study is different due to the consideration of acceleration and deceleration of the roller and the laser nozzle. Also, this study does not consider the surface area of the

product. Nevertheless, the values obtained are fairly close to those of Zhang and Bernard (2013).

Table 3.2 Estimation of build time of the two parts

Parameters	Value	Basis
Distance travelled by the roller in the machine bed, l_r (mm)	230	(SLS SPEC 2017)
Maximum velocity attained by the roller, v_r (mm/s)	700	(Pham and Wang 2000), own judgement
Acceleration of the roller, a_r (mm/s^2)	20000	(CADEM 2017)
Time delay of the roller between two successive layers, t_d (s)	5	(Pham and Wang 2000, Zhang and Bernard 2013), own judgement
Layer thickness, l_t (mm)	0.15	(Zhang and Bernard 2013)
Maximum scan velocity of the laser, v_s (mm/s)	700	(Zhang and Bernard 2013)
Scan spacing of the laser, d_h (mm)	0.33	(Zhang and Bernard 2013)
Laser beam diameter, d_l (mm)	0.6	(Zhang and Bernard 2013)
Acceleration of the laser, a_l (mm/s^2)	20000	(CADEM 2017)
Maximum rapid velocity of the laser, v_{ra} (mm/s)	2100	(Zhang and Bernard 2013), own judgement

Table 3.4 shows the details and the basis of different cost elements. The raw material used in this study is polyamide of density 1.2 gm/cm^3. It is a commonly used material in SLS process. To determine the material cost per kg, the actual volume of the product is increased by 20% to consider the material wastage. Then Eq. (3.42) and Eq. (3.43) are applied to calculate the operator cost and slicing cost, respectively. Lastly, the overhead cost is calculated as per Eq. (3.44). The most dominating part of the overhead cost is the machine depreciation. As the cost of a 3D printer is high, it is considered to have 8 years of useful life and straight-line depreciation technique is followed (Ruffo and Hague 2007).

Finally, the total cost of a part considering single quantity and n_p similar quantities in the machine chamber is obtained as per Eq. (3.40) and Eq. (3.41), respectively. t_{design} and t_{pp} are considered as 1 hr each. Table 3.5 shows the cost of part A and part B when built individually and with two units of the parts in the machine chamber.

Table 3.3 Estimation of build time of the two parts

Considering 1 unit of part at the machine chamber		
Variables	**Part A**	**Part B**
Ratio of the volume of the part to that of bounding box, r_p	0.458	0.112
Time for adding powder by the roller, t_{ap} (s)	1001.20	1215.70
Time for scanning, t_s (s)	1908.70	101.69
Time taken by the laser nozzle to travel at rapid velocity, t_r (s)	1549.30	547.65
Time for machine preparation, t_{mp} (s)	1800	1800
Time for ending operation, t_{eo} (s)	1800	1800
Total build time, t_{build} (hr)	2.24	1.52
Total build time as per Zhang and Bernard (hr)	2.29	1.43
Absolute % difference	2.18	6.29
Considering 2 units of parts at the machine chamber		
Variables	**Part A**	**Part B**
Total build time, t_{build} (hr)	1.60	0.85
Total build time as per Zhang and Bernard (hr)	1.63	0.75
Absolute % difference	1.84	13.33

Table 3.4 Details of different cost components

Cost components	Most likely value	Basis
Material cost per kg ($)	61.28	(Greguric 2019)
Operator cost		
Monthly salary ($)	204.28	(Indeed n.d.)
Working days in a month	25	Typical Industrial practice
Effective working hours in a day (hr)	7	Typical Industrial practice
Slicing cost		
Annual Software fee ($)	175.10	(Locker 2019)
Annual operating hours (hr)	1800	Assuming 6 hours usage in 300 days
Monthly salary of the designer ($)	364.79	(PayScale n.d.)
Working days in a month	25	Typical Industrial practice
Effective working hours in a day (hr)	6	Typical Industrial practice
Overhead cost		
Machine cost ($)	87549.70	(SLS SPEC 2017, Indiamart n.d.)
Machine life (year)	8	(Ruffo and Hague 2007, Baumers et al. 2016)
Salvage value ($)	8754.97	Based on telephonic conversation with industry (10% of machine cost)
Yearly maintenance cost ($)	4377.49	5% of machine cost
Annual factory rent ($)	671.21	Assuming 18.58 square meter of floor space (99 acres n.d.)
Annual electricity charge ($)	1050.60	Assuming $0.15 per kWhr and electricity consumption of 3 kWhr
Annual operating hours (hr)	4300	Two shifts with 90% utilization
Indian currency is converted to US dollar (Xe 2020)		

Table 3.5 Cost per unit with lot sizes of 1 and 2 unit(s) inside the machine chamber

Cost per unit ($)	Part A		Part B	
	1 unit	2 units	1 unit	2 units
	30.89	25.98	11.91	7.38

3.4.1.1 Implementation of fuzzy arithmetic in cost estimation for SLS

The cost is obtained as a single value in Section 3.4.1. In this section, fuzzy set theory will be implemented to obtain the cost as a fuzzy number by considering uncertain variables as fuzzy. Table 3.6 lists the low (l), most likely (m) and high (h) estimates of the fuzzy

variables. In the calculation of build time, four parameters, viz., layer thickness (l_t), scan spacing (d_h), laser beam diameter (d_l) and time delay of the rollers between two successive layers (t_d) are considered fuzzy. The lower and higher estimates of l_t, d_h and d_l are considered to vary by ±20%. On the other hand, the lower estimate of t_d is assumed to deviate by 20% and the high

Table 3.6 Values of fuzzy parameters

Parameter	**(*l*, *m*, *h*)**
Time delay between successive layers, t_d (s)	(4, 5, 7)
Layer thickness, l_t (mm)	(0.12, 0.15, 0.21)
Scan spacing, d_h (mm)	(0.26, 0.33, 0.40)
Laser beam diameter, d_l (mm)	(0.48, 0.60, 0.72)
Monthly salary of the operator ($)	(183.85, 204.28, 224.71)
Monthly salary of the designer ($)	(328.31, 364.79, 401.27)
Slicing software cost ($)	(157.59, 175.10, 192.61)
Machine cost ($)	(78794.73, 87549.70, 96304.67)
Salvage value ($)	(7879.47, 8754.97, 9630.47)
Yearly maintenance cost of the machine ($)	(3939.74, 4377.49, 5252.98)
Annual factory rent ($)	(637.65, 671.21, 704.78)
Annual electricity charge ($)	(998.07, 1050.60, 110.13)

estimate by 40%. The higher value of t_d is expected to deviate more than the most likely value because increasing product height with complex geometrical features increases t_d. For time-dependent cost elements, monthly salary of the operator and designer is considered to vary by ±10%. Also, the machine cost, its salvage value and slicing software cost are assumed to vary by ±10%. However, for machine maintenance cost, the lower estimate is assumed to vary by 10% and upper estimate by 20%. Lastly, the annual factory rent and electricity charge are considered to vary by ±5%.

For obtaining cost as a fuzzy number, triangular membership function is considered for every fuzzy variable as shown in Figure 3.11. After carrying out suitable arithmetic operations, the three estimates of the total cost (in $) of the part ($C_{total}$) are obtained as shown in Table 3.7. Representation of cost as a fuzzy number is shown in Figure 3.13. It shows different values for cost intervals at different membership grades. For the lowest membership grade, i.e., 0.5, the range of interval is the maximum. The upper bound of this interval is the worst estimate of cost.

Table 3.7 Total cost of part as a fuzzy number

	Quantities in the machine chamber	Cost per part ($)		
		Low estimate (*l*)	Most likely estimate (*m*)	High estimate (*h*)
Part A	1	27.71	30.89	36.71
	2	24.00	25.98	31.25
Part B	1	10.06	11.91	15.08
	2	6.26	7.38	9.40

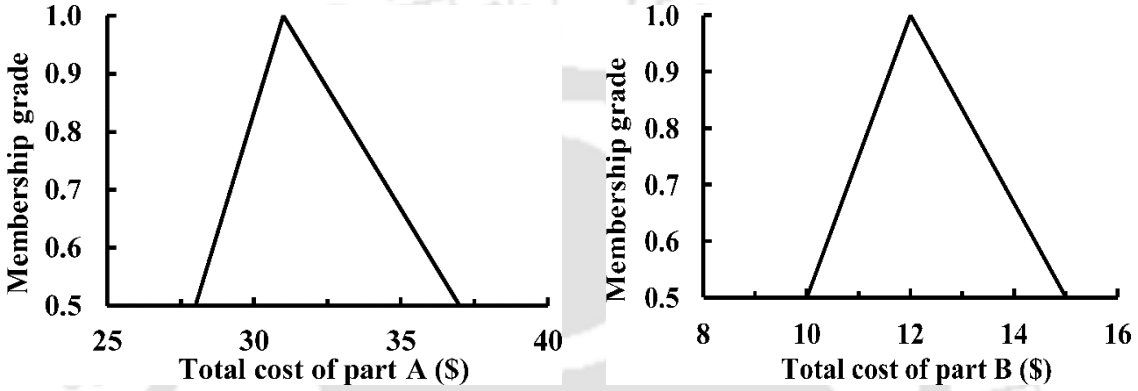

(a)

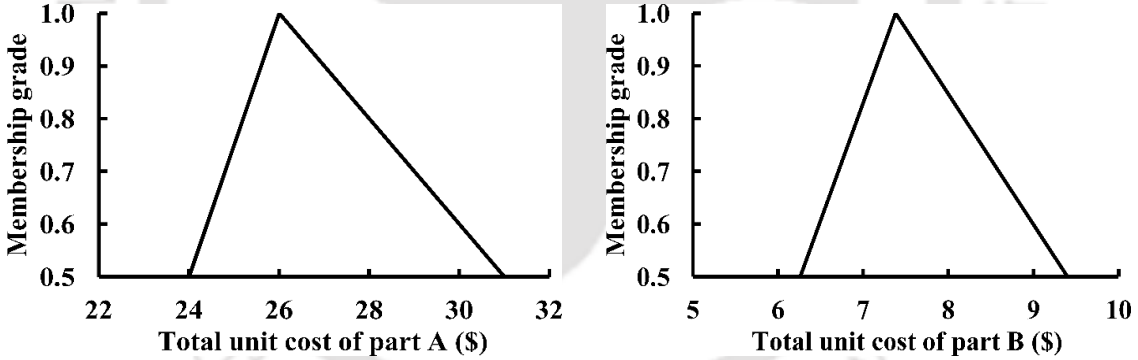

(b)

Figure 3.13 Representation of cost as a fuzzy number: (a) Considering 1 quantity at the machine chamber, (b) Considering 2 quantities at the machine chamber

3.4.2 Cost estimation for FDM

This section presents the cost of the parts by FDM process. Initially, the build time estimation model described in Section 3.2.2 is validated by conducting in-house experiments in Riwell RL 200A, an FDM based 3D printer as shown in Figure 3.14. Some important specifications of this 3D printer are given in Appendix A. Acrylonitrile butadiene styrene (ABS), a widely used thermoplastic material is used for printing the parts. The machine parameters considered for building the parts are given in Table 3.8.

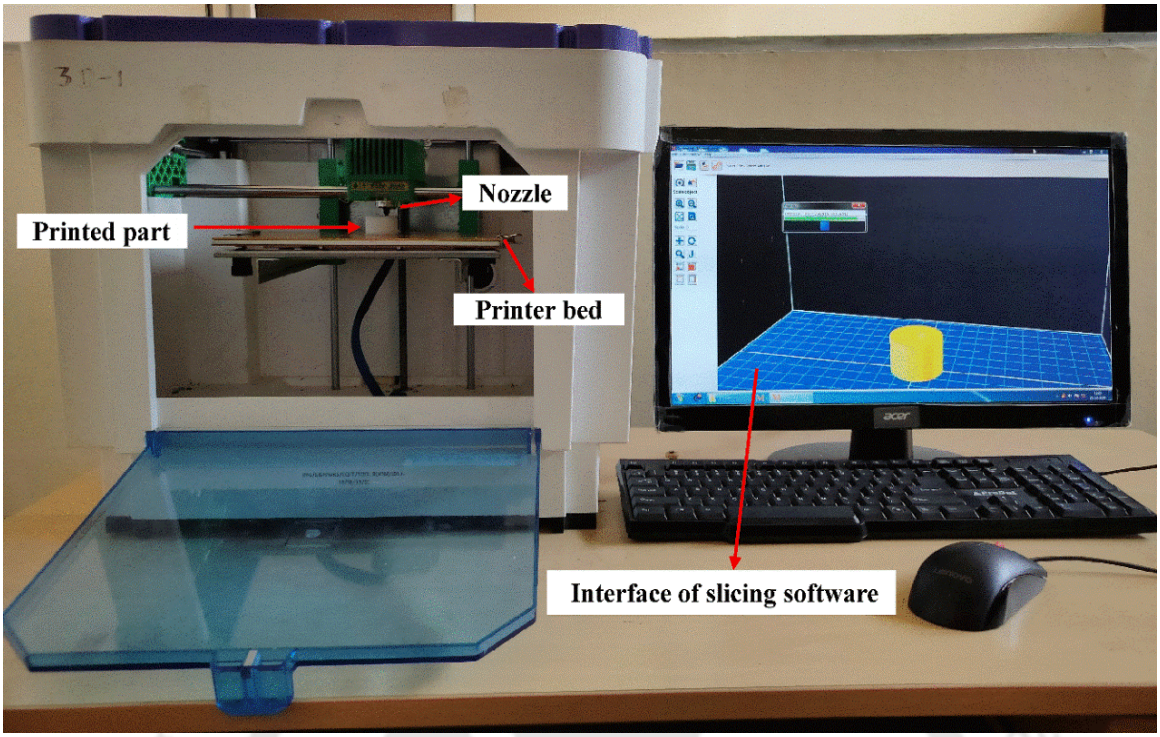

Figure 3.14 Photograph of fused deposition modelling (Make: Riwell RL 200A)

Table 3.8 FDM machine parameters

Parameters	Value
Diameter of the nozzle, d_n (mm)	0.4
Layer thickness, l_t (mm)	0.2
Maximum attainable velocity by the nozzle, v_n (mm/s)	40
Acceleration of the nozzle, a_n (mm/s^2)	40
Filament diamter (mm)	1.75
Infill density, I_d (%)	25

Figure 3.15 shows five different parts printed in Riwell RL 3D printer. These parts are named part 1, part 2, part 3, part 4 and part 5. All these parts are prepared in SOLIDWORKS software, a popular and user-friendly solid modelling CAD software. The purpose was to validate the time estimation model described in Section 3.2.2 with both simple (cuboid, cylinder and pyramid) as well as relatively complex (Lord Ganesh and milling cutter) geometrical parts. Later the digital representation of the models was converted to STL file format. The geometric parameters of the parts are shown in Table 3.9. The details of time estimation are given in Table 3.10. A representative average traverse length was chosen to estimate the correction factor. For each part, the representative length is estimated as the mean of the shortest and the largest distance travelled by the nozzle. The maximum error in time estimation is 7.89% for part 4. For all

other parts, the error in time estimation is less than 5%. The results presented in Table 3.10 are deterministic. The time is estimated only for a single value of traverse length.

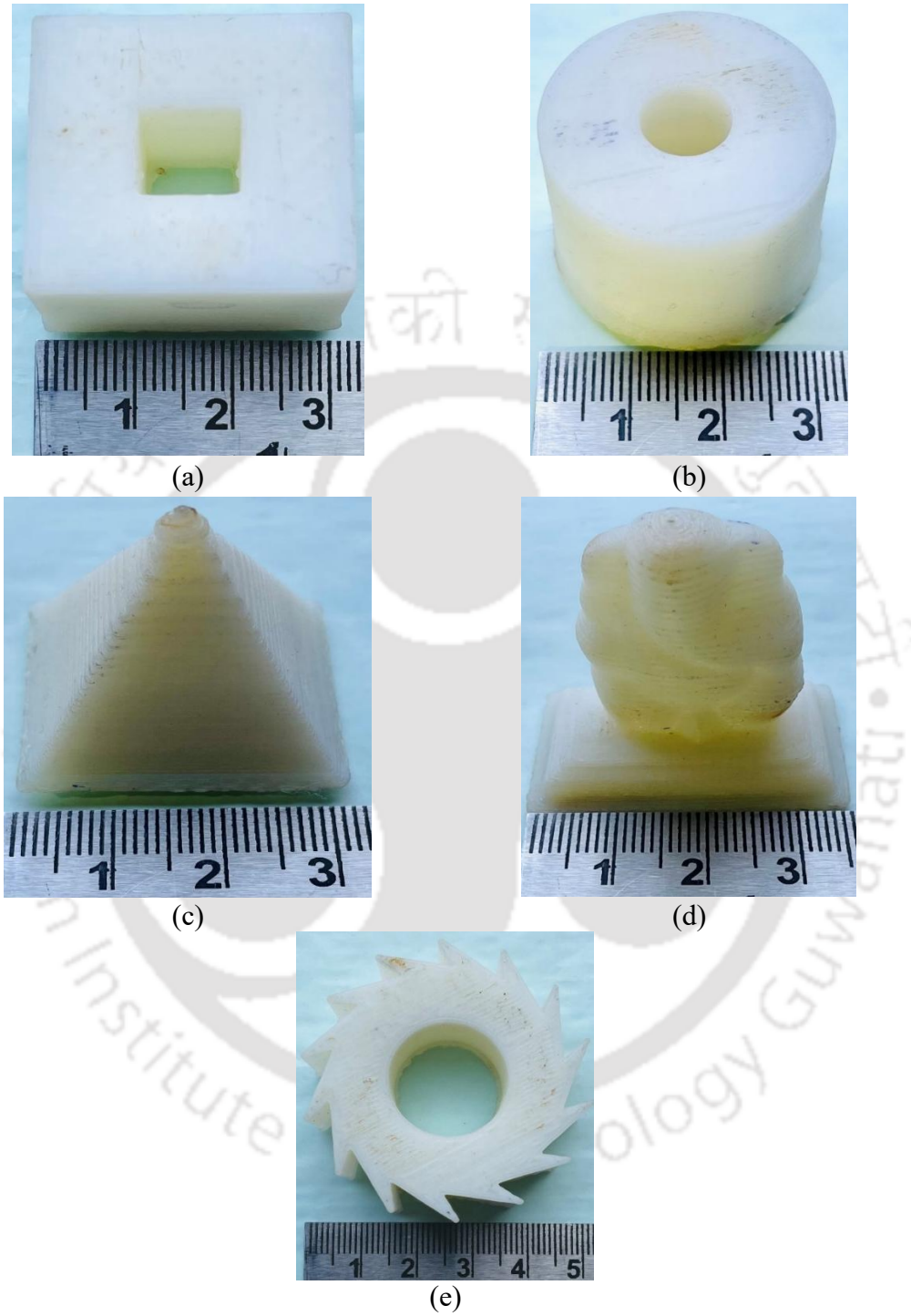

Figure 3.15 Parts printed in FDM based 3D printer: (a) Part 1, (b) Part 2, (c) Part 3, (d) Part 4, and (d) Part 5 (Least count of the scale shown is 1 mm)

Further analysis was carried out taking the interval estimate of representative traverse length as mentioned in Section 3.2.2.1. For each part, the number of samples is taken as five, i.e., $n_s = 5$. It means that measurement was repeated 5 times. For each sample,

five values of measurements are taken, i.e., $n_d = 5$. It means that during each sample, 5 values of lengths are obtained at random locations. This was repeated five times; thus, total number of measured values were 25 for each part. The values of the range of length traversed by the nozzle, standard deviation and confidence interval are listed in Appendix B.

Table 3.9 Geometrical parameters of the parts

Geometrical Parts	Part Volume, V_{part} (mm^3)	Length of bounding box, l_b (mm)	Width of bounding box, w_b (mm)	Height of bounding box, h_b (mm)	Volume of bounding box, V_b (mm^3)	r_p
Part 1	16000	30	30	20	18000	0.89
Part 2	12566.37	30	30	20	18000	0.70
Part 3	9000	30	30	30	27000	0.33
Part 4	8266.06	37	23	39	33189	0.25
Part 5	15831.47	50	50	15	37500	0.42

Table 3.10 Printing time for different parts

Parameters	Geometrical parts				
	Part 1	Part 2	Part 3	Part 4	Part 5
Estimated time to print boundaries (s)	1000	828.32	595.71	775.80	1383.10
Estimated time to print surfaces and volume with infill (s)	1260.5	990.02	713.50	660.11	1283.40
Correction factor, c	3	3.34	3.24	3.58	3.02
Estimated total time, t_{build} (min)	76.36	65.85	46.41	49.74	83.72
Actual printing time, t_{actual} (min)	73	64	47	54	88
% error	–4.60	–2.89	1.26	7.89	4.86

Table 3.11 shows the values of lower as well as upper estimates of time corresponding to different values of traverse length (l_n). The lower, most likely and upper estimates of a parameter are denoted by l_l, m_l and h_l, respectively. It is observed from Table 3.11 that for part 1, part 2 and part 3, the actual build time falls with the interval estimate. For other two parts, i.e., part 4 and part 5, the time estimate is close to the estimated time interval.

Table 3.11 Interval estimation of build time

Tested parts	Parameters		t_{build} (min) (l_l, m_l, h_l)	t_{actual} (min)	% error (with respect to 3 estimates) (l_l, m_l, h_l)
	l_n (mm) (l_l, m_l, h_l)	c (l_l, m_l, h_l)			
Part 1	(16.88, 20, 22.32)	(2.79, 3, 3.08)	(72.34, 76.36, 77.88)	73	(0.90, –4.60, –6.68)
Part 2	(13.14, 14.34, 16.22)	(3.14, 3.34, 3.49)	(62.83, 65.85, 68.12)	64	(1.83, –2.89, –6.44)
Part 3	(13.27, 15.2, 17.13)	(3.06, 3.24, 3.47)	(44.34, 46.41, 48.9)	47	(5.66, 1.26, –4.04)
Part 4	(11.11, 12.5, 13.77)	(3.41, 3.58, 3.79)	(48.05, 49.74, 51.91)	54	(11.02, 7.89, 3.87)
Part 5	(15.35, 17.52, 19.61)	(2.85, 3.02, 3.23)	(80.51, 83.72, 87.74)	88	(8.51, 4.86, 0.30)

After obtaining the build time, the cost of the parts is estimated. The parts are printed individually in the build platform of the 3D printer. First, the most likely value of cost is estimated. For cost estimation, the estimated value of build time is considered. The basis of cost elements is given in Table 3.12. Other cost elements that are common to AM processes are already provided in Table 3.4. The cost of the parts, i.e, part 1, part 2, part 3, part 4 and part 5 are obtained as $ 4.75, $ 4.29, $ 3.52, $ 3.62 and $ 5.00, respectively. The highest and the lowest cost was obtained for part 5 and part 3, respectively. It was observed that the lowest cost was not for the part having the smallest volume, i.e., part 4. Hence, it is evident that unlike the size of the part, geometry and complexity are also responsible for an increased amount of cost.

Table 3.12 Details of different cost components for FDM

Cost components	Most likely value	Basis
Material cost per kg ($)	17.51	(Amazon n.d.)
Machine cost ($)	7295.81	(Myriwell n.d.)
Salvage value ($)	729.58	(10% of machine cost)
Yearly maintenance cost ($)	364.79	5% of machine cost
Indian currency is converted to US dollar (Xe 2020)		

3.4.2.1 Implementation of fuzzy arithmetic in cost estimation for FDM

In Section 3.4.2, the cost is obtained as a single value. This section considers the uncertain cost related parameters as fuzzy variables. Similar to Section 3.4.1.1, the fuzzy variables are represented in the form of low (l), most likely (m) and high (h). To compensate the material loss during extrusion, the extra material is considered to vary by 5%, 20% and 30% for low, most likely and high estimates, respectively. Components of operator, slicing and overhead costs are considered fuzzy as mentioned in Section 3.4.1.1. Applying suitable fuzzy arithmetic operations as per Eqs. (3.46)–(3.49), the estimates of cost are obtained as fuzzy numbers. The cost (in $) for different parts as a fuzzy number is shown in Table 3.13 and the representation of cost as a fuzzy number with different membership grades is shown in Figure 3.16.

Table 3.13 Cost of the parts produced by FDM process

Parts	Cost ($)		
	Low estimate (*l*)	**Most likely estimate (*m*)**	**High estimate (*h*)**
Part 1	4.11	4.75	5.33
Part 2	3.74	4.29	4.85
Part 3	3.09	3.52	4.00
Part 4	3.19	3.62	4.09
Part 5	4.36	5.00	5.70

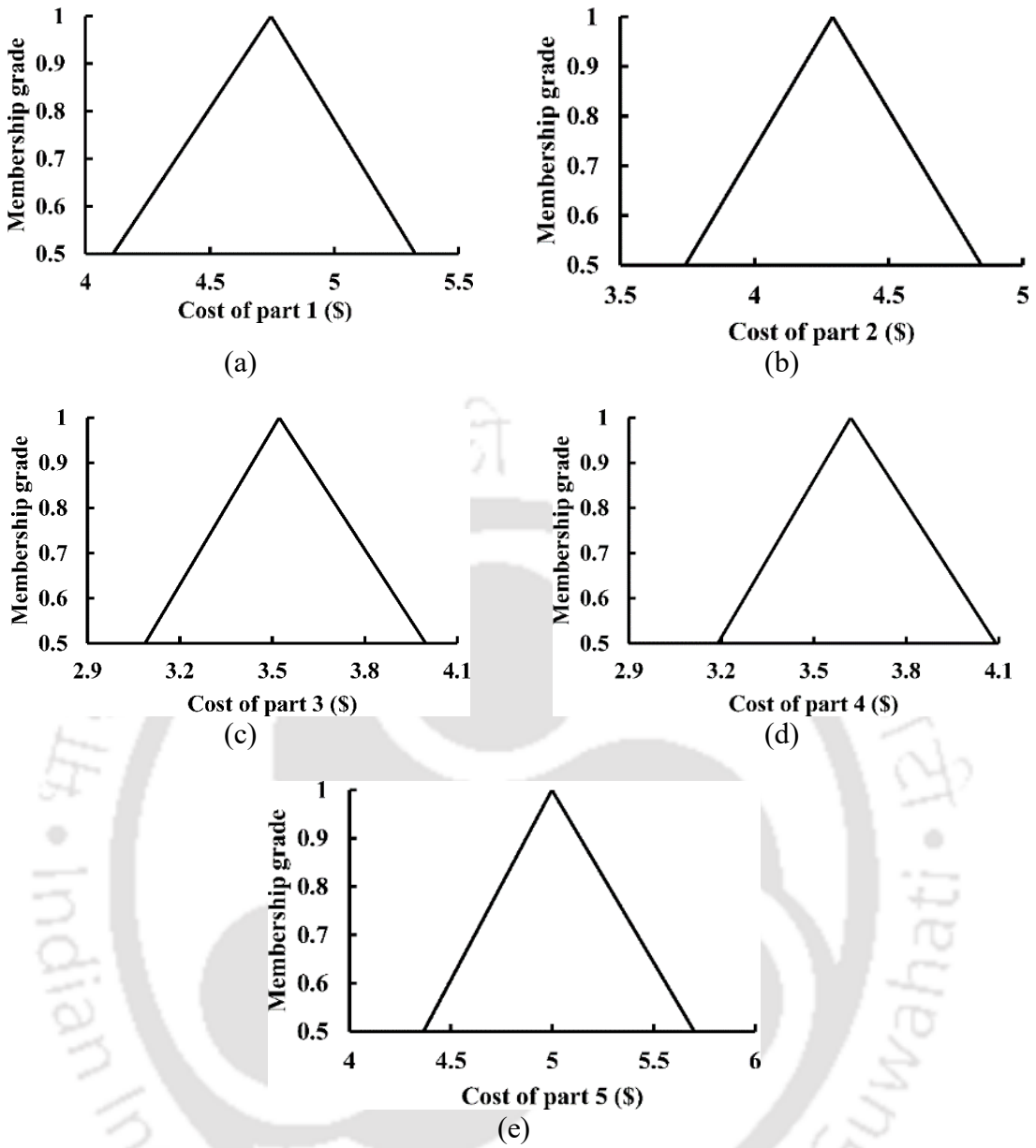

Figure 3.16 Representation of cost as a fuzzy number for parts produced by FDM: (a) Part 1, (b) Part 2, (c) Part 3, (d) Part 4, and (d) Part 5

3.5 Conclusion

In this chapter, a fuzzy set based cost model of AM with specific examples of SLS and FDM in uncertain conditions is proposed. A similar procedure can be adopted for other AM processes by appropriately modifying the parameters related to build time and cost components. Nevertheless, fundamentally, the cost estimation principle is the same as presented in this chapter. Initially, a deterministic cost model is developed considering time-dependent and time-independent cost elements. Build time estimation of a part is an important component in determining the cost. Here, it is approximately estimated by an analytical approach considering machine kinematics and geometrical parameters for both

SLS and FDM processes. The time estimation model has been implemented to calculate the build time of different parts. Also, the build time estimates obtained by the analytical models are validated with the experiments and values available in scientific literature. Later, the cost of the different parts is obtained as a most likely (deterministic) value. It is followed by applying suitable fuzzy arithmetic operations where the cost is obtained as a fuzzy number by considering build time and cost elements as fuzzy variables.

The working condition of a typical industry located in the Indian subcontinent is considered. Apart from the most likely (m) cost evaluated from the deterministic cost model, fuzzy input parameters also gave a realistic value of the low (l) and high (h) estimate of the cost of the product. In fact, cost is predicted as interval numbers with varying degrees of membership grade. It is also necessary to estimate a fuzzy reliability to get an indication if a part can be fabricated at a particular value of fuzzy cost. In Chapter 4, a reliability estimation of fuzzy cost is carried out to explore the influence of uncertainty.

Chapter 4

Cost Comparison of Additive Manufacturing with Traditional Manufacturing in the Presence of Uncertainties

4.1 Introduction

The application of additive manufacturing (AM) has increased exponentially in the recent years. This disruptive technology has now taken a special position in the field of manufacturing. Industries are keen to explore this innovative technology and avail the potential benefits by adopting it as a manufacturing route. However, adopting any new technology in the presence of conventionally established technology is a challenging task. Also, industries are apprehensive about the high processing cost of the process. In the present cost-competitive era, the management needs to ascertain that the preferred technology is profitable as well as sustainable under any circumstance. Hence, a proper cost estimation structure is essential to guide the decision-makers to choose a manufacturing route that is capable of using economic means of production.

Based on cost estimation of AM and other manufacturing processes, researchers have conducted several studies to guide the selection of an economical process. Several researchers, for example, Hopkinson and Dickens (2003), Ruffo et al. (2006), Atzeni et al. (2010), Atzeni and Salmi (2012), Achillas et al. (2017) and Laureijs et al. (2017) performed a comparative analysis based on economy. Their work demonstrated choosing a favourable manufacturing process (either AM or other) based on the production of quantities of a typical part.

The comparative studies based on the cost assessment of additive and traditional manufacturing processes done so far have not yet addressed the issues of uncertainties. This chapter attempts to fill up this gap by comparing SLS process with injection moulding (IM) in the presence of uncertainties. SLS is one of the most popular additive manufacturing processes for producing components made of polymeric materials, which are traditionally manufactured using the IM. The working principle of SLS and its cost model is already described in Chapter 3. The remaining sections are arranged as follows. Sections 4.2 describes the deterministic cost model of IM process. Section 4.3 introduces the concept of reliability and presents a detailed methodology to compare two uncertain fuzzy costs.

Section 4.4 illustrates the methodology with the help of examples. Section 4.5 concludes the chapter.

4.2 Cost estimation of injection moulding (IM)

Cost of an injection moulded part comprises material cost ($C_{material}$), mould cost (C_{mould}) and processing cost ($C_{processing}$). The total cost of an injection moulded part (C_{IM}) is given by

$$C_{IM} = C_{material} + \frac{C_{mould}}{n_p} + C_{processing}, \tag{4.1}$$

where n_p is the identical quantities of parts produced during the lifetime of the mould. The raw materials used in injection moulding are thermoplastic polymers. The material cost ($C_{material}$) per part is given by

$$C_{material} = c_m \rho_m V_p \left(1 + \frac{l_s}{100}\right), \tag{4.2}$$

where c_m is the material cost per unit mass, ρ_m is the density of the raw material, V_p is the volume of the injection moulded part and l_s is the percentage loss of the material. As some material is always wasted, a suitable factor is multiplied by the actual mass. The procedure for determining the other two components of cost, i.e, mould cost and processing cost are described in Section 4.2.1 and Section 4.2.2, respectively.

4.2.1 Estimation of mould cost in injection moulding

The mould cost is the most dominating cost component in an injection moulding process. Boothroyd et al. (2010) described the complete mould costing methodology that comprises the cost of the mould base and the cost associated with its manufacturing. The manufacturing cost of the mould is the cost required to convert it into a working mould. The mould cost is given by

$$C_{mould} = C_{mb} + C_{mm}, \tag{4.3}$$

where C_{mb} is the cost of mould base and C_{mm} is the cost of mould manufacturing. A typical mould comprises a cavity plate, core plate, support plate, ejector plate and clamping plate as shown in Figure 4.1.

The material considered for the mould is steel of various categories such as stainless steel and hot-rolled steel. The molten material is injected into a stationary cavity plate. On the other hand, the movable core plate holds the core that facilitates the shaping of the inner side of the part. The core plate is attached to the support plate. Adjacent to the core plate

, there lie the support and the ejector plates. The ejector plate comprises ejection pins to push the part off

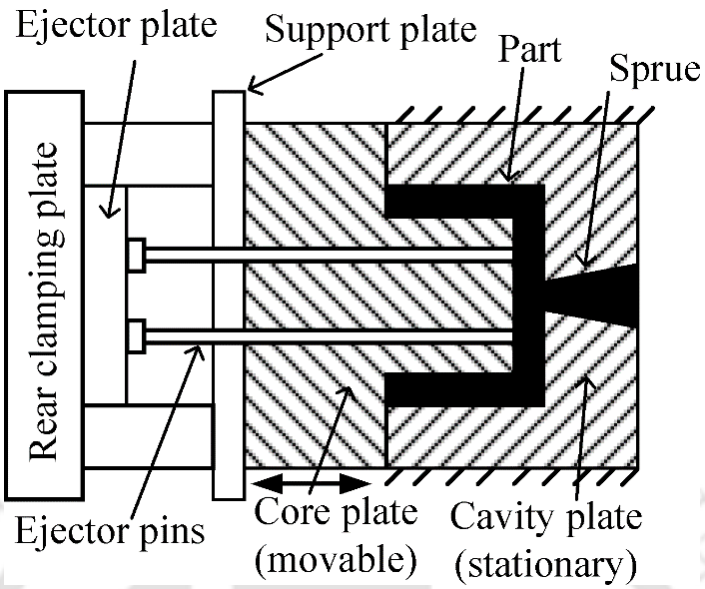

Figure 4.1 A schematic of a typical mould

the core during the opening of the mould. The rear clamping plate holds the mould with necessary force during the injection of the polymer material as well as ejection of the part. To obtain an approximate cost of the mould base, Boothroyd et al. (2010) presented an empirical relation:

$$C_{mb} = 1000 + 0.45 A_b h_p^{0.4}, \tag{4.4}$$

where C_{mb} is the cost of the mould base in \$, A_b is the area of mould base cavity in cm and h_p is the combined thickness of cavity and core plates in cm. Eq. (4.4) was developed in the year 1989 applicable to the United States of America (USA). The relation was developed based on a survey where several data were accumulated for different mould bases from industries in USA. For developing a similar formula from the perspective of an Indian manufacturer, it is necessary to obtain requisite set of data from Indian industry. However, for simplicity, Eq. (4.4) will be used for analysis in this thesis. It was observed that this equation provides reasonable values based on limited and approximate information. This equation is converted into Indian currency and its right-hand side is multiplied by the ratio of consumer price index (CPI) of India in 2019 to that in 1989. The obtained equation is again converted to dollar. Thus, Eq. (4.4) is modified, based on the data in references as (Inflation tool n.d., Thomas Cook n.d.)

$$C_{mb} = 1940 + 0.87 A_b h_p^{0.4}. \tag{4.5}$$

An appropriate mould base is selected based on the geometry of the part (area and depth) and the number of cavities contained in the mould. The minimum clearance between two adjacent cavities as well as the edges of the plate should be 7.5 cm. Thickness plate is taken as 15 cm larger than the cavity-depth (Boothroyd et al. 2010). The number of cavities to be fabricated in the mould base is inversely proportional to the size of the part. Increasing the number of cavities may increase the production output in one cycle, but it results in increased running cost due to the larger size of the injection moulding machine. The number of cavities for a large part (maximum dimension more than 100 mm) is usually taken as one (Chin and Wong 1996). In this work, only one cavity has been taken.

C_{mm} in Eq. (4.3) is the cost of manufacturing during the conversion of the mould base into a working mould. Mould manufacturing involves the cost associated with ejector pins, ejector systems and geometrical complexities of the part. The list of equations for estimating the mould manufacturing cost is provided in Appendix C.

4.2.2 Estimation of processing cost in injection moulding

The processing cost is based on the type of moulding machine, the setup time of the machine, moulding cycle time and the involvement of the operator during different stages of the manufacturing process. The processing cost ($C_{processing}$) per part is given by

$$C_{processing} = \left(\frac{t_{setup}}{n_p} + \frac{t_{cycle}}{n_c p_y} \right) \left(c_{operator} + c_{labour} + c_{overhead} \right), \tag{4.6}$$

where t_{setup} is the setup time of the machine, n_p is the required number of parts, t_{cycle} is the cycle time, n_c is the number of cavities in the mould and p_y is the production yield (fraction of non-defective parts to all parts produced). Further, $c_{operator}$, c_{labour} and $c_{overhead}$ are the operator, labour and overhead costs, respectively. The labour cost is calculated similar to the operator cost. Similar to the SLS process, overhead cost comprises machine depreciation, annual maintenance contract, factory rent and electricity charge. The expressions to estimate these cost components are given in Chapter 3.

Cycle time (t_{cycle}) in Eq. (4.6) is given by the algebraic summation of the three components— injection time (t_f), cooling time (t_c) and mould resetting time (t_{rs}). Thus,

$$t_{cycle} = t_f + t_c + t_{rs}. \tag{4.7}$$

Injection time is the time taken to fill the molten plastic material inside the mould via the sprue, runners and gates. Cooling time is of the longest duration amongst all three components due to the low thermal conductivity of the polymers. The cooling process takes place by the conduction mode of heat transfer. Mould resetting time involves the opening

of the mould, ejection of the moulded part and closing of the mould. A low value of t_{rs} seems to be economical, but this involves the fast movement of the mould that causes vibration in the machine and failure of the part. The equations for determining t_f and t_c are presented in Appendix D. Based on the Shing (1999), t_{rs} is taken as 10 s.

4.3 Methodology to compare two uncertain costs

This section proposes a method to compare two uncertain costs for choosing a favourable manufacturing process (either SLS or IM). Following the calculations, if the low (l), most likely (m) and high estimates (h) of a process (say SLS) are less than the corresponding estimates of the other process (say IM), then undoubtedly, the SLS process is less expensive than IM process. Confusion arises when some estimates of a process are lower and some are higher in comparison to the other process. For this purpose, the concept of fuzzy reliability is used. It gives a clue about the chance of manufacturing a part within a particular cost. As the highest value at a membership grade of 0.5 is a worst-case estimate, reliability of 100 % can be assigned to this estimate. By spending a lesser amount also, there is a chance to get the part fabricated with some reduced reliability.

The fuzzy reliability of a quantity is based on the idea of entropy, a measure of uncertainty. Mathematically, the degree of uncertainty is given by (De Luca and Termini 1972, Dixit and Dixit 2008)

$$d(\mu)=\begin{cases}-\{\mu\log_2\mu+(1-\mu)\log_2(1-\mu)\} & \text{for } 0<\mu<1\\ 0 & \text{for } \mu=0,1\end{cases}, \tag{4.8}$$

where μ is the membership grade. In Eq. (4.8), the base of the logarithm is taken as 2. This guarantees that the magnitude of entropy is confined between 0 and 1. The maximum value of uncertainty is equal to 1 at μ = 0.5. On the other hand, the minimum value of uncertainty is 0 at μ = 0, i.e., when there is no chance of occurrence of an event at all. Also, the value of uncertainty is 0 at μ = 1, i.e., when there is 100% chance of an occurrence of an event. As $d(\mu)$ is a measure of uncertainty, $\{1–d(\mu)\}$ is a measure of certainty. Before arriving at the expression for reliability estimates, the next step is to define a possibility index (P_I). This gives the fractional possibility that a part can be manufactured at a particular value of cost, say C^*. P_I is estimated based on C^*, the lower limit of cost and the upper limit of cost. The left or the lower limit of cost represented by $C_L(\mu)$ as a function of μ is given by

$$C_L(\mu)=2(m-l)(\mu-1)+m, \tag{4.9}$$

where m and l are the most likely and lower values of fuzzy cost estimates, respectively. On the other hand, the right or the upper limit of cost represented by $C_R(\mu)$ as a function of μ is given by

$$C_R(\mu) = 2(m-h)(\mu-1)+m, \tag{4.10}$$

where h is the upper value of the fuzzy cost estimate. When C^* lies between m and h, P_I is given by

$$P_I(\mu, C^*) = \begin{cases} \dfrac{C^* - C_L(\mu)}{C_R(\mu) - C_L(\mu)} & \text{if } C^* < C_R(\mu) \\ 1 & \text{otherwise} \end{cases}. \tag{4.11}$$

On the other hand, when C^* lies between l and m, P_I is given by

$$P_I(\mu, C^*) = \begin{cases} 0 & \text{if } C^* < C_L(\mu) \\ \dfrac{C^* - C_L(\mu)}{C_R(\mu) - C_L(\mu)} & \text{otherwise} \end{cases}. \tag{4.12}$$

After obtaining P_I, the next step is to evaluate the reliability at C^*. Now, a reliability index (β) which is a function of both C^* and μ is given by

$$\beta(\mu, C^*) = P_I(\mu, C^*)\{1 - d(\mu)\}. \tag{4.13}$$

Based on different values of μ, different values of β can be computed. As the lower estimate of a variable corresponds to a membership grade of 0.5 and as per fuzzy set theory, an element having a membership grade of less than 0.5 tends towards non-member class. Hence, it is appropriate to find out reliability index for membership grades varying between 0.5 and 1. The integrated effect of reliability indices is obtained by integrating β with respect to membership grade within the limit of 0.5 and 1. It is compared with the ideal case (corresponding to 100% reliability) in which P_I is 1 at each membership grade. Thus, the reliability (R_e) is given by

$$R_e(\%) = \frac{\int_{0.5}^{1} \beta(\mu, C^*)\,\mathrm{d}\mu}{\int_{0.5}^{1} (1 - d(\mu))\,\mathrm{d}\mu} \times 100. \tag{4.14}$$

The reliability value at a particular cost can be considered as a cumulative probability that the part can be manufactured at that cost. By knowing the cost at different values of reliabilities (cumulative probabilities), one can know the probability distribution and evaluate the expected cost of manufacturing. The expected cost of manufacturing is the

total area under the cost-reliability curve from zero to the cost corresponding to 100% reliability.

The concept of reliability can also be used for subjective comparison of two different values of fuzzy cost and choose a favourable manufacturing process (either SLS or IM). It is possible that the SLS process is better at a particular value of reliability but for other values of reliability IM comes out to be better. Such a case will be illustrated with an example.

Generally, an industry manufactures several quantities of a part as per the demand. Usually, the sales and marketing department can estimate a probability distribution of demand. Based on the probability distribution, the expected cost can be estimated. In this study, two types of distribution are used— uniform distribution and normal distribution. In uniform distribution, the probability of demand for each quantity is the same. For example, if the demand varies from 1 to n_p quantities as per uniform distribution, the probability of each quantity is equal to $1/n_p$. Hence, the cost per quantity (unit cost), C_u is given by

$$C_u = \left[\begin{array}{l} \left\{ \left(\frac{1}{n_p} \right) \times \text{unit cost of 1 quantity} \right\} + \left\{ \left(\frac{1}{n_p} \right) \times \text{unit cost of 2 quantities} \right\} \\ + \left\{ \left(\frac{1}{n_p} \right) \times \text{unit cost of 3 quantities} \right\} + \ldots\ldots + \left\{ \left(\frac{1}{n_p} \right) \times \text{unit cost of } n_q \text{ quantities} \right\} \end{array} \right]. \tag{4.15}$$

However, in the normal distribution, the probability of demand for each quantity is different. The probability of each quantity, $P(x)$ is given by

$$P(x) = \frac{1}{\sigma\sqrt{2\pi}} \exp\left\{ \frac{-(x-\bar{x})^2}{2\sigma^2} \right\}, \tag{4.16}$$

where x varies from 1 to n_p quantities, σ is the standard deviation and $\bar{x}$ is the mean. Although this expression is valid only if x is a continuous variable, it can also be used for discrete values for large x. Here, σ is taken as equal to $(n_p-1)/6$ (considering that all possible values of demand are within 6σ range) and $\bar{x}$ is the average of 1 and n_p, i.e., $\bar{x} = (1+ n_p)/2$. The quantity that lies in the middle of the range has the highest probability. On the other hand, the quantity that lies at either of the extreme ends has the lowest probability. The cost per quantity, i.e., unit cost (C_u) is given by

$$C_u = \left[\begin{array}{l} \left\{ P(1) \times \text{unit cost of 1 quantity} \right\} + \left\{ P(2) \times \text{unit cost of 2 quantities} \right\} \\ + \left\{ P(3) \times \text{unit cost of 3 quantities} \right\} + \ldots\ldots + \left\{ P(n_p) \times \text{unit cost of } n_p \text{ quantities} \right\} \end{array} \right]. \tag{4.17}$$

4.4 Illustration of the methodology by examples

The methodology presented in this chapter will be illustrated by examples of two different parts: part A and part B The details of these parts are already described in Chapter 3. For both processes, an excel spreadsheet is prepared listing all the cost parameters. The spreadsheet is prepared in such a way that the cost (including fuzzy estimates of cost) can be estimated as a function of quantities of the part.

4.4.1 Cost estimation of the parts by selective laser sintering

The overall procedure to estimate the cost by SLS process is described in Chapter 3. The cost of a quantity manufactured by SLS process depends on the utilization of the machine chamber. The cost per quantity is the least when the entire area of the machine chamber (230×230 mm^2) is used. This is also referred to as full utilization of the machine. Considering the size of part A, full utilization of the machine occurs when two quantities are manufactured at a time. The variation of deterministic unit cost with the quantities of part A is illustrated in Figure 4.2a. The deterministic curve with μ=1 is represented by black colour. In deterministic case, for producing only one quantity of part A, the unit cost is $ 28.95. For producing two quantities, the unit cost is reduced to $ 24.62; which is a reduction of approximately 15% in the unit cost. This is because the total build time and the slicing costs get divided among the quantities. As already stated, in one setting, only two quantities of part A can be manufactured. If more than two quantities of part A are produced, then the entire build area of the machine has to be again filled up by the powder. In this case, only the slicing cost gets reduced as per Eq. (3.41). On the other hand, the total build time of a part increases. Therefore, as represented in Figure 4.2a, the unit cost increases from $ 24.62 to $ 25.23. This type of fluctuation in cost continues between an even and odd number of parts. For even number of parts, the cost is lower compared to the preceding odd number. With an increase in the number of part, slicing cost keeps on reducing and eventually becomes negligible. In that case, cost per quantity does not vary much with an increase in the number of parts.

On the other hand, for part B the full utilization of the machine occurs when eighteen quantities are manufactured simultaneously. It is assumed in this study that only one SLS machine is utilized for manufacturing. The processing cost per quantity (when the part is actually fabricated inside the machine chamber) is dependent on the build time per quantity. This also depends on the number of quantities of the part manufactured in the chamber. For producing only one quantity of part B, the unit cost is $ 11.63. When eighteen

quantities are produced simultaneously, the unit cost is reduced to $ 3.57; i.e., a reduction of approximately 69% in the unit cost. The deterministic cost curve with μ=1 of part B is represented by black colour in Figure 4.2b. For producing more than eighteen quantities, a new setting of the 3D printer is required. Hence, for manufacturing the nineteenth part, the unit cost increases as illustrated in Figure 1b. However, with an increase in the number of quantities, the fluctuation in the unit cost diminishes.

After determining the deterministic cost, the fuzzy cost is obtained by considering the variables as fuzzy. In this work, the material cost per kg (l = $ 55.15, m = $ 61.28, h = $ 67.41) and the material loss in percentage (l = 5, m = 10, h = 15) are also considered fuzzy. In Figure 4.2, the representation of fuzzy cost at different membership grades, i.e., μ=0.8 and μ=0.5 is illustrated by red and blue colour, respectively. It is observed that as the quantities of a part (either part A or part B) increase, the cost per quantity remains almost constant.

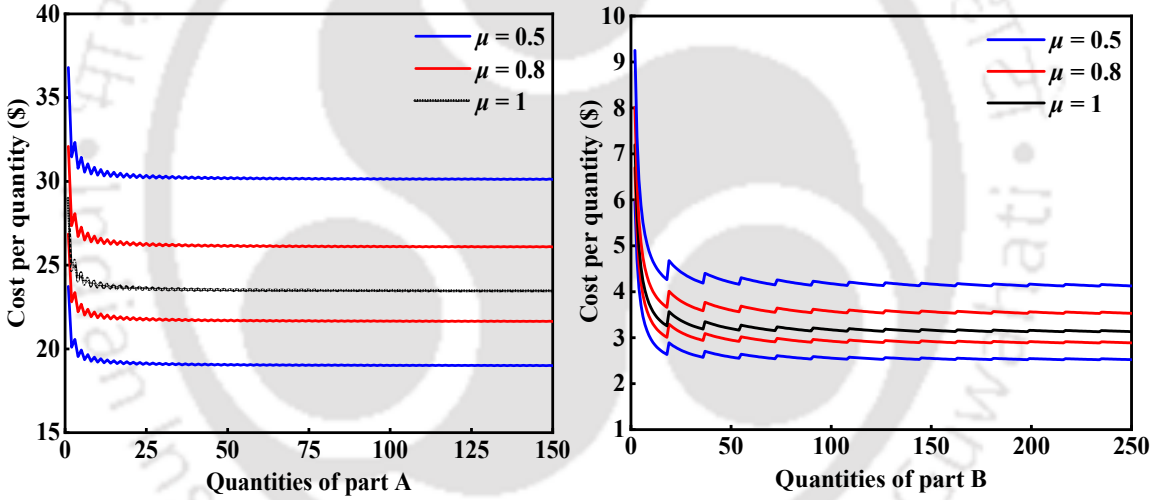

(a) (b)

Figure 4.2 SLS cost at different membership grades: (a) cost versus quantities of part A, (b) cost versus quantities of part B

4.4.2 Cost estimation of the parts by injection moulding

The deterministic cost of injection moulding (IM) is estimated as per the procedure described in Section 4.2. Initially, the material cost is estimated as per Eq. (4.2). An extra 10% of the material is considered to compensate for the material loss during the moulding process. The details and the basis of the different cost elements (material, operator, labour and overhead cost) of IM are listed in Table 4.1 and Table 4.2. Along with the most likely (m) values of parameters used in the deterministic model, the values of those parameters that are considered fuzzy, i.e., low (l) and high (h) estimates are also listed.

After estimating the material cost, the next step involves the estimation of mould cost. First, the mould base cost is estimated as per Eq. (4.5). Next, the mould manufacturing cost requires the calculation of the projected area of the part. For part A, it has been approximately obtained by multiplying the area of the bounding box with the ratio of the actual volume of the part to the volume of the bounding box. The ratio is obtained as 0.46 for part A. For part B, the ratio is 0.11. A low value of the ratio indicates that there is more empty space in the bounding box. For part B, the empty space is not uniform in any of the three axes (x, y and z) unlike part A. The ratio (for part B) is modified by obtaining its cube root and then squaring it. Finally, this modified ratio is multiplied with the area of the bounding box to estimate the projected area. The variables (deterministic and fuzzy values) for mould cost estimation are listed in Table 4.2. After obtaining the mould manufacturing time, this quantity is multiplied by the average hourly rate of mould manufacturing. Finally, the processing cost is estimated as per the procedure. The IM machine has 10 years of useful life and a straight-line depreciation technique is followed. Table 4.3 lists the parameters for the estimation of cycle time in injection moulding. Following the complete procedure, the deterministic cost per quantity and fuzzy cost estimates are obtained.

The representation of cost with the number of quantities is shown in Figure 4.3. The mould cost (the most dominating cost component) and the processing cost are divided among the quantities. It is observed that unlike SLS, the cost per quantity (either part A or B) decreases continuously. Similar to Figure 4.2, the black coloured curves represent the deterministic cost with μ=1 whereas the fuzzy costs with μ=0.8 and μ=0.5 are represented by red and blue colour.

Table 4.1 Details of material cost, operator, labour and overhead cost in injection moulding

Cost components	Value (*l*, *m*, *h*)	Basis for most likely estimate
Material cost per kg ($)	(1.29, 1.43, 1.57)	(Indiamart, n.d., a)
Material loss (%)	(5, 10, 15)	(ACO mould, n.d.)
Machine setup time (hr)	2	(Shing 1999)
Number of cavities, n_c	1	(Chin and Wong 1996)
Production yield, p_y	0.9	(Shing 1999)
Operator/labour cost		
Monthly salary of a mould operator ($)	(270, 300, 330)	(Indeed, n.d., a)
Monthly salary of labour ($)	(154.29, 171.43, 188.58)	(Indeed, n.d., b)
Working days in a month	25	Typical Indian condition
Effective working hours (hr)	7	Typical Indian condition
Overhead cost		
Machine cost ($)	(9000, 10000, 11000)	(Indiamart, n.d., b)
Machine life (year)	10	(Injection Molding, n.d.)
Salvage value ($)	(900, 1000, 1100)	10% of machine cost
Yearly maintenance cost ($)	(450, 500, 550)	5% of machine cost
Annual factory rent ($)	(624.29, 657.14, 690)	Assuming 18.58 square metres of floor space (99 acres, n.d.)
Annual electricity charge ($)	(651.43, 685.71, 720)	Assuming $0.15 per kW.hr and electricity consumption of 2kW.hr
Annual operating hours (hr)	4300	Two shifts with 90% utilization

Table 4.2 Estimation of mould cost

Parameters	Values (*l*, *m*, *h*)	
	Part A	**Part B**
Mould plate area (cm^2)	(689.06, 729, 900)	(382.12, 412.16, 543.56)
Cavity and core plate thickness (cm)	(17.05, 17.8, 20.8)	(17.65, 18.4, 21.4)
Mould base cost ($)	(3810.64, 3953.43, 4585.46)	(2991.87, 3093.59, 3556.07)
Manufacturing time for an ejector pin, t_e (hr)	(1.5, 2.5, 3.5)	(1.5, 2.5, 3.5)
Manufacturing time for ejection system (ejector pins + plate), M_e (hr)	(12.19, 20.32, 28.44)	(11.93, 15.41, 18.89)
Number of surface segments	18	16
Manufacturing time associated with geometrical features of the part, M_x (hr)	12.06	9.96
Manufacturing time for one cavity and core, M_{po} (hr)	17.98	6.70
Manufacturing time for imparting surface finish to the part (hr)	(4.22, 10.07, 17.54)	(2.19, 5.07, 8.66)
Average rate for mould manufacturing per hour ($)	(65.96, 77.6, 89.25)	(65.96, 77.6, 89.25)
Mould manufacturing cost ($)	(3063.63, 4688.68, 6784.1)	(1588.23, 2362.79, 3347.85)
Total mould cost (mould base + mould manufacturing) ($)	(6881.73, 8650.51, 11378.95)	(4580.1, 5456.39, 6903.91)

Table 4.3 Estimation of cycle time in injection moulding

Parameters	Values (*l*, *m*, *h*)	
	Part A	**Part B**
Injection pressure of polymer considering losses, p_j (N/m^2)	(330.9×10^5, 551.5×10^5, 772.1×10^5)	(330.9×10^5, 551.5×10^5, 772.1×10^5)
Part volume, V_p (mm^3)	184893	9603
Projected area, A_p (cm^2)	66.033	12.137
% increase in runner area	(10, 15, 20)	(10, 15, 20)
Clamp force, F_{clamp} (kN)	(262.20, 418.8, 560.75)	(48.19, 76.98, 103.08)
Injection power, P_j (kW)	(5.5, 7.5, 18.5)	(5.5, 5.5, 5.5)
Injection time, t_f (s)	(2.205, 5.438, 7.416)	(0.385, 0.385, 0.385)
Maximum wall thickness, b (mm)	28	34
Thermal diffusivity, α (mm^2/s)	(0.095, 0.1, 0.105)	(0.095, 0.1, 0.105)
Injection temperature, T_i (°C)	291	291
Mould temperature, T_m (°C)	91	91
Ejection temperature, T_e (°C)	129	129
Cooling time, t_c (s)	(1213.0, 1331.7, 1439.1)	(1788.6, 1963.6, 2122)
Mould resetting time, t_r (s)	(8, 10, 12)	(8, 10, 12)
Cycle time, t_{cycle} (hr)	(0.34, 0.374, 0.405)	(0.499, 0.548, 0.593)

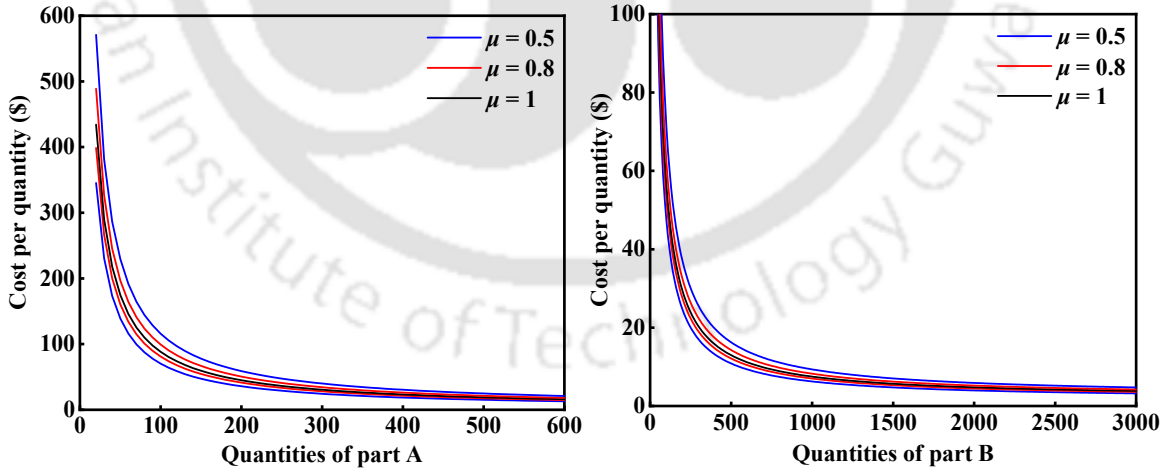

(a) (b)

Figure 4.3 IM cost at different membership grades: (a) cost versus quantities of part A, (b) cost versus quantities of part B

Figure 4.4 shows the cost comparison of IM and SLS. The curves represent the most likely values of cost for both the processes. For part A, beyond 400 quantities, IM is preferable. For producing 400 quantities, the cost of both IM and SLS is same, i.e., $ 23.4.

On the other hand, for part B, it is found that producing 5120 quantities yield the same cost both IM and SLS, i.e., $ 3.12. These points as indicated by the circles are referred as break-even point.

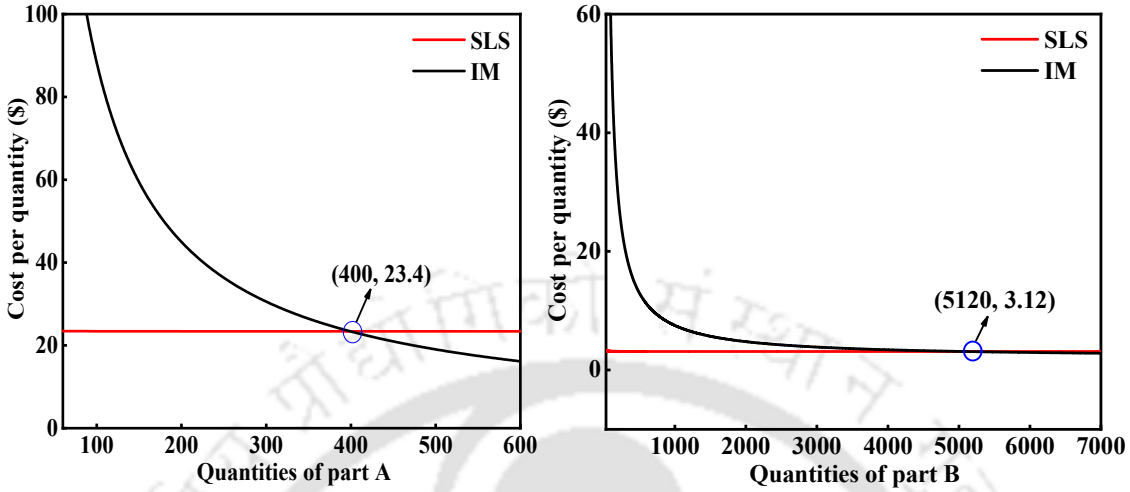

Figure 4.4 Cost comparison of IM and SLS: (a) part A, (b) part B

4.4.3 Estimation of reliability of fuzzy cost

After obtaining the fuzzy values of cost, the reliability estimates of fuzzy costs are carried out. This helps in understanding the influence of uncertainty. The reliability estimates at different estimates of cost are obtained by developing a code in MATLAB, R2018. The code is provided in Appendix E. For SLS process, considering a single quantity of part in the machine chamber, at the extreme right limit of C_{SLS}, i.e., $ 36.71 and $ 15.08 for part A and part B, respectively; the reliability comes out to be 100%. This implies that by spending this particular amount of cost, the part can be manufactured. At the highest membership grade, the reliability is very low, i.e., 35.35 % and 36.81 % for part A and part B, respectively. It is observed from Figure 4.5 that the greater the cost of the part, the greater is the reliability. However, the rate of the increase of reliability decreases with increasing amount of total cost. This is consistent with the reliability behaviour of most of the systems. That is to say that one needs more effort or cost for enhancing the reliability from 0.97 to 0.98 than that required for enhancing the reliability from 0.96 to 0.97. It is because as the cost interval widens, the corresponding membership grades reduce indicating less likelihood of the estimates. Hence, each additional enhancement of cost contributes to reliability to a lesser degree compared to its predecessor. When C_{SLS} is equal to the right limit of cost at the membership grade of 0.7, the reliability of both the parts is more than 99%. Hence, the cost estimate at this membership grade can be considered appropriate for manufacturing a part.

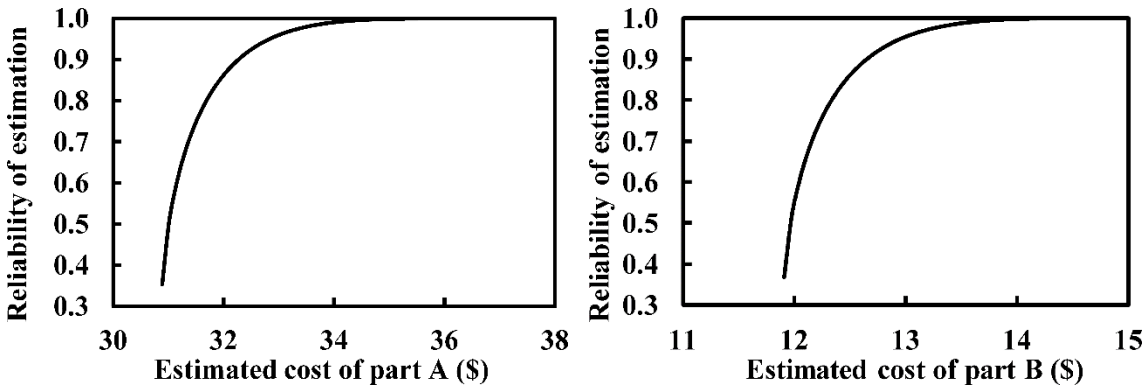

Figure 4.5 Variation of fuzzy reliability with cost considering 1 quantity at the machine chamber for (a) part A, (b) part B

The reliability estimates of cost can also be extended to the concept of probability. Although there is a difference between membership grades and probabilities, as a special case, membership grades can be considered as probabilities. In that case, fuzzy reliabilities can be treated as probabilistic reliability. Thus, the reliability can be considered as the cumulative density function of probability of the cost variable. From the cumulative density function, probability density can be easily obtained. By knowing probability density function, expected value of cost can be obtained. Expected value is the average value of cost in a statistical sense.

4.4.4 Comparison of two uncertain costs and choosing a favourable manufacturing process

The fuzzy-based approach helps in obtaining the lower (l), most likely (m) and higher (h) estimates of cost. By estimating the fuzzy cost, it is seen that for 390 quantities, the cost per quantity (l, m and h) of part A for SLS process is lesser than the cost of IM process. The values of cost estimates (in $) for SLS process are l = 18.99, m = 23.38 and h = 30.10, whereas for IM process are l = 19.08, m = 23.91 and h = 31.22. Hence, it indicates that up to 390 quantities, SLS is a favourable process irrespective of the uncertainties. On the other hand, for 406 quantities of part A, the cost estimates (in $) obtained for SLS process are l = 18.99, m = 23.38 and h = 30.10, whereas for IM process these are l = 18.38, m = 23.04 and h = 30.07. Hence, IM is more favourable as it incurs less cost per quantity irrespective of the uncertainties. When the part A to be manufactured lies in the range of 390–406 quantities, choosing the economic manufacturing process requires a careful consideration. In such situations, the reliability estimates of fuzzy cost can help to choose a favourable process. Table 4.4 shows the low (l), most likely (m) and high (h) estimates of cost for 390–406 quantities considering probability distribution.

Table 4.4 Cost per quantity when the demand for part A varies from 390–406 quantities

SLS cost ($)			IM cost ($)		
Uniform distribution					
l	***m***	***h***	***l***	***m***	***h***
18.99	23.39	30.11	18.73	23.47	30.64
Normal distribution					
l	***m***	***h***	***l***	***m***	***h***
18.97	23.36	30.07	18.70	23.43	30.60

It is observed from Table 4.4 that for both uniform and normal distribution, the low (l) cost estimates of SLS are more than that of IM. However, the most likely (m) and upper estimate (h) cost of SLS are lesser than that of IM. In such a situation, the industry can estimate the expected cost. The expected cost of manufacturing is obtained by computing the total area under the cost and reliability curve. By considering uniform distribution, the expected cost of manufacturing for SLS and IM processes are obtained as $ 23.67 and $ 23.76, respectively, showing the superiority of SLS. Figure 4.6 shows the cost-reliability curve (considering uniform distribution) for the SLS process.

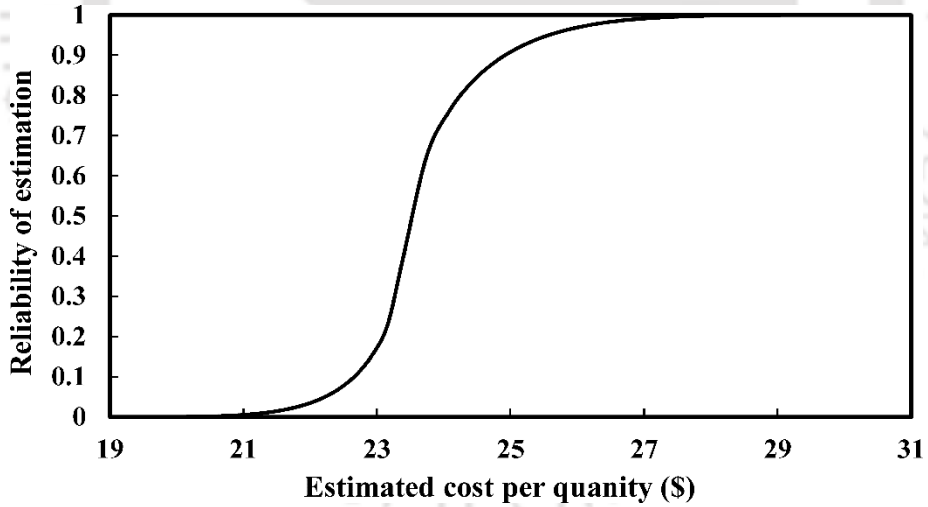

Figure 4.6 Reliability at different values of fuzzy costs for SLS process

By estimating the fuzzy cost of part B, it is seen that for 4100 quantities, the values of cost (in $) per quantity for SLS process are l = 2.52, m = 3.12 and h = 4.12, whereas for IM process, the cost per quantity is l = 2.80, m = 3.38 and h = 4.13. It indicates that up to 4100 quantities, SLS is a favourable process irrespective of the uncertainties. On the other hand, for 5600 quantities of part B, the cost (in $) obtained for SLS process are l = 2.52, m = 3.12 and h = 4.12, whereas for IM process are l = 2.50, m = 3.02 and h = 3.67. Hence,

IM is more favourable as it incurs less cost per quantity irrespective of the uncertainties. For part B, choosing the economic manufacturing process lying in the range of 4100–5600 quantities requires careful consideration. The cost per quantity of part B varying from 4500–5000 quantities (considering probability distribution) is listed in Table 4.5.

Table 4.5 Cost per quantity when the demand for part B varies from 4500–5000 quantities

SLS cost ($)			IM cost ($)		
Uniform distribution					
l	***m***	***h***	***l***	***m***	***h***
2.52	3.13	4.12	2.65	3.20	3.89
Normal distribution					
l	***m***	***h***	***l***	***m***	***h***
2.51	3.12	4.11	2.64	3.19	3.88

It is observed that the most likely (m) cost estimates of SLS are less than that of IM as shown in Table 4.5. However, the upper cost (h) estimate of SLS is greater than that of IM. The expected cost of manufacturing (considering uniform distribution) for SLS and IM are $ 3.22 and $ 3.18, respectively. In such a situation, reliability estimates at different values of cost (upper estimates) can guide in choosing the proper manufacturing route. Table 4.6 shows the reliability estimates at different values of fuzzy cost for both SLS and IM processes. It can be inferred that if the situation is more uncertain, IM is a favourable process. At relatively less uncertain situations (μ = 0.9), SLS is economical. The management can also favour the SLS process if it is willing to take less risk due to uncertainty.

Table 4.6 Reliability estimates at different values of upper estimates of cost for part B corresponding to respective membership grades

Membership grade (μ)	**Upper estimates of SLS cost ($)**	**Reliability `(%)**	**Upper estimates of IM cost ($)**	**Reliability (%)**	**Economical process**
1	3.13	38.13	3.20	44.35	SLS
0.9	3.33	87.63	3.34	88.87	SLS
0.8	3.53	97.12	3.48	97.41	IM
0.7	3.72	99.54	3.61	99.59	IM
0.6	3.92	99.98	3.75	99.98	IM
0.5	4.12	100	3.89	100	IM

4.5 Conclusion

This chapter presents a method to quantify the cost-competitiveness of SLS with the IM process in the presence of uncertainties. The deterministic cost estimation models are presented for both SLS and IM processes and are converted into fuzzy set based cost models by considering uncertain variables as fuzzy. The costs per quantity for two parts produced by two processes (SLS and IM) are computed for a variable demand scenario. The following conclusions are drawn:

- For SLS process, the cost per quantity (for both the parts) decreases up to a certain number of quantities of production (with some fluctuations depending on the machine utilization) and then becomes constant. Full utilization of the SLS machine yields the minimum cost.
- For IM process, the cost per quantity keeps on decreasing monotonically with increasing the number of quantities of production. Apart from the most likely estimates of cost, the fuzzy cost estimates in the uncertain conditions for both the processes give an idea of the lower and upper bound estimates of the cost.
- A reliability estimation is carried out to infer the influence of uncertainty. The reliability estimates at different values of fuzzy cost (both lower and upper limits) are considered as cumulative probabilities. This probability-based concept helps in computing the expected cost of manufacturing.

The content of this chapter contributes to operations management of AM by exploring its cost-competitiveness considering the demand scenario. Overall, the subjective decision-making tool proposed in this chapter will guide the production planners in choosing a favourable manufacturing process (considering economy as well as reliability) in the presence of uncertainties. The methodology presented in this chapter can also be extended for other traditional processes for knowing up to what extent and in which scenarios they can compete with an AM process.

Chapter 5

An Analytical Method for Assessing the Proper Utilization of Additive Manufacturing

5.1 Introduction

There is an apprehension about AM revolutionizing the entire manufacturing sector. The term '3D printing' is now the buzzword in technical discussions, brainstorming sessions and business meetings pertinent to the manufacturing sector. No doubt, the applications of additive manufacturing (AM) are continuously increasing, but unless used judiciously, it cannot compete with traditional manufacturing processes. Also, after three decades since the inception of AM, its utilization by the industries is not as high as per the claims made by the developers and supporters of this technology (Yeh and Chen 2018). Hence, its adoption and effective utilization remain a challenging task for an organization.

Before adopting and utilizing a new technology, an organization wants to ensure its profit and sustainability. In context to AM, an organization attempts to get answers to the following questions:

1. What are the factors that need to be considered before purchasing a 3D printer?
2. Based on the analysis of these factors, how can one assess the suitability of a 3D printer for the organisation?

The objective of this chapter is to provide an analytical guideline for an organization willing to adopt AM. For proper analysis of the utility of AM, the organization must have some idea about the variety, complexity and production volume of its product. Given this information, a cost-benefit analysis, as well as comparison with competing processes, can be carried out. Section 5.2 presents a procedure for utility assessment of AM. The issue of uncertainty in the utility assessment is described in Section 5.3. Section 5.4 presents a method to compare manufacturing processes considering different factors. Section 5.5 presents a quantitative method for evaluating the penalty due to reduction in employment. The overall methodology is demonstrated in Section 5.6. Section 5.7 concludes the chapter.

5.2 Deterministic analysis of utility assessment for a process

It is assumed that an organization has complete knowledge of the products to be fabricated in a particular financial year. There may be several types of products with different production volumes. If the detailed drawing of a product and its production volume is

given, the time to produce that part can be estimated. With this information, analysis of the utility of a 3D printing machine can be carried out as explained in sequel.

5.2.1 Evaluation of utilization factor

Utilization factor (U_f) of a 3D printing machine can be expressed as the ratio of total time required to produce the products to total available time (De Ron and Rooda 2006; Kumar and Soni 2015). Thus,

$$U_f = \frac{\text{Time required for production}}{\text{Total available time}}. \tag{5.1}$$

If U_f is less than 1, the machine is under-utilized. In that case, management should plan to get job orders from outside, so that the machine can be fully utilized. If U_f is more than 1, the machine is over-utilized. Management may have to outsource the jobs or plan to procure additional machines. Typically, the total available annual time in an organization is significantly less than total available hours in a year. For example, an organization may have a policy to run only one shift in a day and may have some holidays in a year. In that case, if U_f is more than 1 but less than a threshold value, the products can be manufactured on the machine with provision for overtime. To illustrate this point, it is considered that a company works effectively for 300 days and on each day, machine is operated for 6 hours. The maximum possible hours in a year are 365×24. Hence, the threshold U_f up to which the operation can be managed by overtime alone is given by

$$U_{f\max} = \frac{365 \times 24}{300 \times 6} = 4.87. \tag{5.2}$$

Thus, for this particular industry, the production plan can be as follows:

- If U_f<1, the industry should try to get job orders from outside.
- If U_f=1, machine is getting utilized properly.
- If 1< U_f<4.87, possibility of overtime should be explored.
- If U_f≥4.87, vendors should be explored for outsourcing the job or another machine should be procured.

5.2.2 Impact of utilization factor on cost

Utilization factor affects the overhead component in an additive manufacturing process. Compared to other components of cost, overhead component is high due to high cost of industrial 3D printing machines. There are several cost models in literature (Hopkinson and Dickens 2003; Ruffo et. al. 2006; Ruffo and Hague 2007; Atzeni and Salmi 2012; Baumers et al. 2016; Thomas 2016; Baumers et al. 2017; Li et al. 2017) but except the work of Fera

et al. (2017), the concept of utilization factor has not been imbibed in the cost models. Fera et al. (2017) suggested to use an overall equipment effectiveness index (OEE) in the cost estimation but did not provide a formulation for its evaluation. OEE is similar to U_f used in this work. For U_f=1, i.e., for full utilization, a generic cost formula as per Eq. (3.41) is given by

$$C_{total} = \left(c_{material} m_r\right) + \left(\frac{c_{slicing} t_{design}}{n_p}\right) + \left\{\left(c_{operator} + c_{overhead}\right) t_{build}\right\} + \left(c_{operator} t_{pp}\right). \tag{5.3}$$

In order to understand the impact of U_f, it is better to express Eq. (5.3) as

$$C_{total} = c_{overhead} t_{build} \left(1 + \frac{c_{material} m_r}{c_{overhead} t_{build}} + \frac{c_{slicing} t_{design}}{n_p c_{overhead} t_{build}} + \frac{c_{operator}}{c_{overhead}} + \frac{c_{pp} t_{pp}}{c_{overhead} t_{build}}\right). \tag{5.4}$$

Utilization factor will affect the overhead cost in an inverse manner; lesser the U_f, the more will be C_{total}, and vice versa. Incorporating the utilization factor, Eq. (5.4) gets modified to

$$C_{total} = \frac{c_{overhead} t_{build}}{U_f} \left(1 + \frac{U_f c_{material} m_r}{c_{overhead} t_{build}} + \frac{U_f c_{slicing} t_{design}}{n_p c_{overhead} t_{build}} + \frac{U_f c_{operator}}{c_{overhead}} + \frac{U_f c_{pp} t_{pp}}{c_{overhead} t_{build}}\right). \tag{5.5}$$

From Eq. (5.4) and Eq. (5.5), ratio (r_u) of actual cost to the cost with U_f=1 is given by

$$r_u = \frac{\frac{1}{U_f}\left(1 + \frac{U_f c_{material} m_r}{c_{overhead} t_{build}} + \frac{U_f c_{slicing} t_{design}}{n_p c_{overhead} t_{build}} + \frac{U_f c_{operator}}{c_{overhead}} + \frac{U_f c_{pp} t_{pp}}{c_{overhead} t_{build}}\right)}{\left(1 + \frac{c_{material} m_r}{c_{overhead} t_{build}} + \frac{c_{slicing} t_{design}}{n_p c_{overhead} t_{build}} + \frac{c_{operator}}{c_{overhead}} + \frac{c_{pp} t_{pp}}{c_{overhead} t_{build}}\right)}. \tag{5.6}$$

Some of the industrial 3D printers are expensive; hence overhead cost dominates other components of cost. In that scenario,

$$r_u \approx \frac{1}{U_f}. \tag{5.7}$$

However, at times, material cost is also significant. In that case, it is better to use Eq. (5.6) instead of Eq. (5.7). This simple equation suggests that for minimizing the cost of production, the utilization factor of a 3D printing machine should be increased.

5.2.3 Scheduling issues

One distinct advantage of AM over several other manufacturing processes is that the time to manufacture a complex product is less because there is no requirement of special tooling.

This is helpful when most of the products are of customized nature. The mean flow time (F_m) can be estimated by (Buffa and Sarin 2007)

$$F_m = \frac{\sum_{i=1}^{n_p} F_i}{n_p}, \tag{5.8}$$

where F_i is the amount of time spent on i^{th} job and n_p is the number of jobs or parts.

Tardiness (t_d) of the job is defined as the difference between completion date and due date, provided the completion date is more than the due date (Buffa and Sarin 2007). If the job is completed before the due date, the tardiness is considered zero. Mathematically,

$$t_d = \max\{0, c_d - d_d\}, \tag{5.9}$$

where c_d is the completion date of the product and d_d is the due date. Mean tardiness can be defined similar to Eq. (5.8). Calculation of mean flow time and tardiness is case-specific. However, in general, mean flow time and tardiness are going to increase with the increase in U_f.

5.3 Incorporation of uncertainty in the analysis

The procedure described in Section 5.2 is a deterministic analysis. In general, estimates are highly uncertain. Uncertainty can be handled through probability or fuzzy set theory. The procedure to convert a deterministic model to fuzzy set based model is described in Chapter 3.

To consider the fuzzy representation of total available time, an expert can estimate most likely, lower bound and upper bound of the total available time. Based on these three values, a linear triangular fuzzy membership function can be constructed as illustrated in Figure 3.10. The total available time can also be represented as a triplet (t_{al}, t_{am}, t_{au}), where three quantities represent the lower, most likely and upper bound, respectively. Similarly, the time required for production can be represented as (t_{pl}, t_{pm}, t_{pu}). In that case, the utility factor can be computed as follows:

$$U_f = \frac{(t_{pl}, t_{pm}, t_{pu})}{(t_{al}, t_{am}, t_{au})} = \left(\frac{t_{pl}}{t_{au}}, \frac{t_{pm}}{t_{am}}, \frac{t_{pu}}{t_{al}}\right). \tag{5.10}$$

Eq. (5.10) provides the value of U_f in the form of triplet, which can be used to plot a linear triangular membership function. This representation of U_f will be an approximation only, as the division of two linear triangular fuzzy numbers yields a nonlinear triangular fuzzy number. However, often the deviation from linearity is not high. To assist the decision

process about the utilization of a 3D printing machine, U_f is subtracted by 1 and is denoted by β_f. Thus,

$$\beta_f = U_f - 1 = \left(\frac{t_{pl}}{t_{au}} - 1, \frac{t_{pm}}{t_{am}} - 1, \frac{t_{pu}}{t_{al}} - 1 \right). \tag{5.11}$$

Now, the decision strategy can be as follows:

- If all the elements of the triplet β_f are negative, then the machine is underutilized. In that case, try to get job orders from outside.
- If all the elements of the triplet β_f are positive, then the machine is over-utilized. Possibility of overtime, outsourcing and procuring another machine should be considered.
- Case of some elements of β_f being positive and some negative needs careful consideration. Here, at some value of α-cut, the machine is underutilized and at others it is over-utilized. The decision is dependent on how much risk management wants to take. In a simplistic way, the centroid of β_f can be evaluated. The machine is underutilized for negative value of centroid and vice versa.

Ratio (r_u), given by Eq. (5.6), and costs can also be computed in the fuzzy form. However, care has to be taken when a particular variable occurs more than once in an expression. In that case, blind application of fuzzy arithmetic will provide a wider range (Dixit and Dixit 2008). Dong and Shah (2008) suggested using a vertex method in which all the combinations of lower and upper limits need to be evaluated and extreme values are taken as lower and upper bounds. For the convenience of evaluating the fuzzy value of r_u, it is convenient to express it as

$$r_u = \frac{\text{other cost} + \dfrac{\text{overhead cost}}{U_f}}{\text{other cost} + \text{overhead cost}} = \frac{1 + \dfrac{r_o}{U_f}}{1 + r_o}, \tag{5.12}$$

where r_o is the ratio of overhead cost to other cost. According to vertex method, expression r_u has to be evaluated at four combinations of r_o and U_f. The lower limit of Eq. (5.12) will be the lowest amongst the values estimated from all possible four combinations. Similarly, the largest value at all possible combinations will provide the upper limit of Eq. (5.12). However, a careful analysis makes it clear that the following strategy requires the evaluation only at two combinations:

- For U_f<1, the lower limit of r_u is obtained at lower limit of r_o along with upper limit of U_f. For U_f>1, the lower limit of r_u is obtained at upper limit of r_o along with upper limit of U_f.
- For U_f<1, the upper limit of r_u is obtained at upper limit of r_o along with lower limit of U_f. For U_f>1, the upper limit of r_u is obtained at lower limit of r_o along with lower limit of U_f.

5.4 Factors for comparing additive manufacturing with other processes

Estimation of U_f will help to decide about owning a 3D printing machine or outsourcing a job. However, various factors need to be considered for ascertaining if 3D printing is indeed the better alternative compared to conventional processes. Based on the review of literature, some deciding factors are product cost, mean tardiness, energy consumption and waste generation. Product cost can be further divided into processing cost and total raw material cost. It is possible that for a certain product, the processing cost of 3D printing may be large but raw material cost may be minimized due to weight reduction of the product. As complex shapes can be easily produced by 3D printing, shape and topology optimization can be carried out to reduce the weight.

As multiple factors need to be considered for comparing two manufacturing processes, a fuzzy set based method can be employed for taking a suitable decision. Each manufacturing process can be rated based on various factors in terms of membership grade and obtain an overall membership grade. If there are n_f deciding factors and a process gets a membership grade of μ_i for the factor i, then the overall membership grade μ_o of the process can be obtained as

$$\mu_o = s_f \times \min(\mu_1, \mu_2, ..., \mu_i, ..., \mu_n) + (1 - s_f) \times \left(\prod_{i=1}^{n_f} \mu_i \right)^{\frac{1}{n_f}}, \tag{5.13}$$

where s_f is a strategy factor. There can be two distinct strategies for obtaining overall membership grade— non-compensating and compensating. In the non-compensating strategy, overall membership grade is just the minimum membership grade out of the membership grades for various factors. Here, good performance in one factor cannot compensate for the poor performance in the other factor. Putting s_f equal to 1 in Eq. (5.13), a pure non-compensating strategy is obtained. However, in the compensating strategy, the overall membership grade is the n_f^{th} root of the products of all n_f membership grades. Here, good performance in one factor can compensate for the poor performance in the other

factor. Putting s_f equal to 0 in Eq. (5.13), a pure compensating strategy is obtained. In general, any value of s_f can be chosen between 0 and 1 depending on the preference of management. The process that provides the highest overall membership grade is the suitable process.

5.5 A quantitative method for evaluating the penalty due to reduction in employment

AM is well suited for fabricating parts having complex geometrical features. The parts that are difficult to manufacture by conventional manufacturing can be easily manufactured by 3D printing owing to the automatic characteristics. This may have an adverse impact on the labour in terms of employment. However, if the job of the labour is permanent and there is no policy of salary reduction, the organization has to pay full salary to the labour or the operator in spite of their reduced involvement in the production process. Government may also enforce the organization to pay some unemployment allowance to state exchequer as a part of corporate social responsibility (CSR).

The time taken to manufacture a complex part by 3D printing is less than that by conventional manufacturing. However, the salary payable to the labour will be same for both conventional and 3D printing although the latter involves less labour engagement. The amount payable to the manpower head can be referred as labour penalty cost. Let t_{cm} be the time for conventional manufacturing and t_{3D} the time for 3D printing for a product. The labour penalty cost attributed to a product can be obtained as

$$\text{Labour penalty cost} = \left(\frac{t_{cm}}{t_{3D}} - 1 \right) \times (\text{Labour cost}). \tag{5.14}$$

The organization can reduce the labour penalty cost by enhancing the production, provided there is a sufficient market for the product. A ratio r is defined as

$$r = \frac{\text{Demand potential}}{\text{Current annual production}}. \tag{5.15}$$

Incorporating r in Eq. (5.14), the modified labour penalty cost is obtained as

$$\text{Labour penalty cost} = \left(\frac{t_{cm}}{t_{3D} r} - 1 \right) \times (\text{Labour cost}). \tag{5.16}$$

Maximizing the value of r, the labour penalty cost can be minimized. It is to be noted that in some cases, the penalty cost may be negative also, implying that AM is in fact going to provide more employment. The calculation of labor penalty cost for a product needs t_{cm}, t_{3D} and r. Depending on these values, labor penalty cost can be positive or negative. As these parts have been chosen for the purpose of illustration and are not being produced in

industry, there is no information available regarding t_{3D} and r. With the availability of the values of t_{3D} and r, labor penalty cost can be easily estimated.

5.6 Illustration of the methodology by examples

The methodologies developed in this work is illustrated by means of some examples. In order not to lose focus, only relevant details of these examples are provided. This section is divided into three subsections. In Subsection 5.5.1, an example of fabricating a polymer cutter (referred as part A in Chapter 3) in varying quantities is presented. In the next subsection, an example is taken in which 3D printing machine is required to print two different parts (referred as part A and part B in Chapter 3) in varying quantities. The last subsection compares a SLS process with an IM process. Only the results of fuzzy set based analysis are discussed as the deterministic analysis is a special case of fuzzy set based analysis, in which the values are computed at a membership grade of 1.

5.6.1 Case of producing multiple quantities of a single part

It is considered that an industry produces a polymer milling cutter (part A) on a SLS machine. It is assumed that the machine operates for 6 hours daily, 300 days in a year. However, the lower estimate for machine operation is only 4 hours due to maintenance etc. and the upper estimation is 9 hours daily, considering some overtime.

Table 5.1 Details of machine utilization and costs for producing different quantities of polymer cutters on an SLS 3D printing machine

Annual production (unit)	**Production time (hr)** (t_{pl}, t_{pm}, t_{pu})	**Utilization factor** (U_{fl}, U_{fm}, U_{fu})	β_f (β_{fl}, β_{fm}, β_{fu})	**Unit cost ($) for U_f=1** (C_l, C_m, C_u)	**Actual unit cost ($)** ($C_{al}$, C_{am}, C_{au})	r_u (r_{ul}, r_{um}, r_{uu})
100	(126, 159, 223)	(0.05, 0.09, 0.19)	(–0.95,–0.91,–0.81)	(19.01, 23.40, 30.12)	(36.89, 83.01, 217.86)	(1.75, 3.55, 8.48)
300	(378, 477, 669)	(0.14, 0.27, 0.56)	(–0.86, –0.74, –0.44)	(18.99, 23.39, 30.11)	(22.23, 39.40, 86.60)	(1.14, 1.68, 3.25)
600	(756, 954, 1338)	(0.28, 0.53, 1.12)	(–0.72, –0.47, 0.12)	(18.99, 23.38, 30.10)	(18.57, 28.50, 53.75)	(0.96, 1.22, 1.95)
1000	(1260, 1590, 2230)	(0.47, 0.88, 1.86)	(–0.53, –0.12, 0.86)	(18.99, 23.38, 30.10)	(17.10, 24.14, 40.61)	(0.83, 1.03, 1.42)
1500	(1890, 2385, 3345)	(0.70, 1.33, 2.79)	(–0.30, 0.33, 1.79)	(18.99, 23.38, 30.10)	(16.37, 21.96, 34.04)	(0.77, 0.94, 1.16)
2100	(2646, 3339, 4683)	0.98, 1.86, 3.90)	(–0.02, 0.86, 2.90)	(18.99, 23.38, 30.10)	(15.95, 20.72, 30.29)	(0.73, 0.89, 1.01)
2620	(3301, 4166, 5843)	(1.22, 2.31, 4.87)	(0.22, 1.31, 3.87)	(18.99, 23.38, 30.10)	(15.74, 20.10, 28.42)	(0.71, 0.86, 0.97)

Table 5.1 presents the results for different annual production volume. It also depicts the impact of uncertainties on the production time and cost. Pictorial representation is provided in Figures 5.1 and 5.2. Figure 5.2 has been obtained by carrying out computations at various α-cuts. Due to fuzzy division operation, the membership function for U_f is nonlinear. However, it can be approximated as a linear membership function, as nonlinearity is not high. When the production volume increases from 100 units to 300 units, the utilization factor increases from 0.09 to 0.27 with a consequent reduction in the unit cost from $ 83.01 to $ 39.40. This cost is still more than the achievable cost of $ 23.39 for full utilization. This is also indicated by r_u, which is the ratio of actual cost to the cost for full utilization. The value of r_u for the production of 300 units is 1.68 and becomes 1.03

(close to 1) at a production volume of 1000 units. At production volume of 1500, the machine gets over utilized with further reduction in the unit cost.

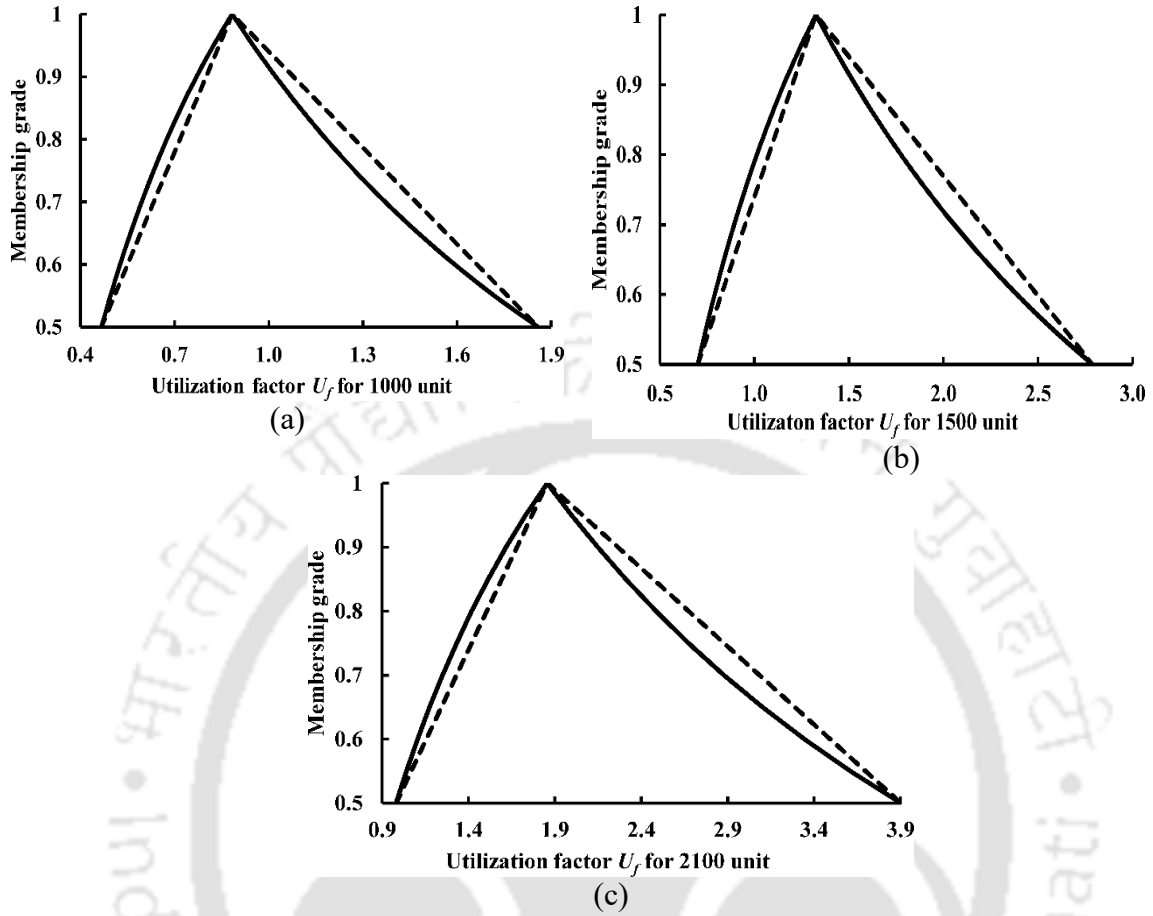

Figure 5.1 Variation of U_f with membership grade for the production of (a) 1000, (b) 1500 and (c) 2100 units

It is observed that there is a lot of uncertainty in the estimation of utilization factor and costs. At high production volume, uncertainty in the costs reduces; albeit it is still significant. This is due to the low impact of overhead cost at high utilization factor, although the uncertainty in utilization factor remains high. For the production volume of 2620, utilization factor may vary from 1.22 to 4.87, most likely value being 2.31. As per Eq. (5.2), the maximum possible value of utilization factor is 4.87; hence, considering the worst cost scenario, production volume should not be increased beyond 2620 units. The worst case cost estimate is $ 28.42, which is only slightly more than the most likely estimate at full utilization, i.e., $ 23.38.

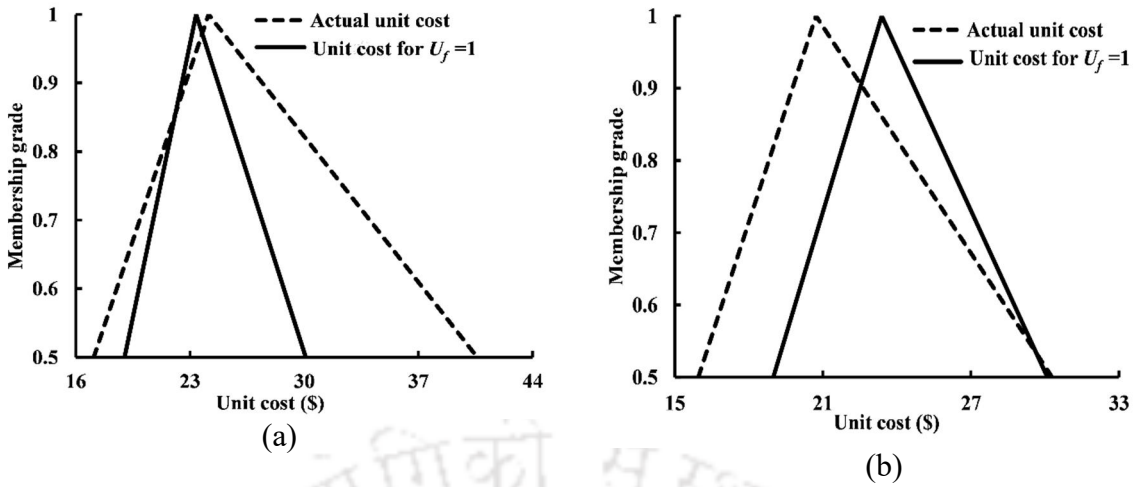

Figure 5.2 Variation of unit cost with membership grade for the production of (a) 1000, and (b) 2100 units

Coming to decision in the presence of uncertainty, it is clear that at a production volume of 300, the 3D printer is underutilized as the upper estimate is also less than 1; this is also indicated by the negative values of β_f at all estimates. The situation at a production volume of 600 is not clear; here from deterministic analysis, the utilization factor is 0.53 but its upper estimate is 1.12. Based on the centroid method of defuzzification, utilization factor can be stated as (0.28 + 0.53+1.12)/3=0.64, which favours the decision in favour of underutilization. The more refined analysis can be carried out by considering the reliability of each estimate, as mentioned in Chapter 4.

Figure 5.2(a) shows that for the production of 1000 units, the most likely estimate of actual unit cost is almost same as that for the full utilization. However, uncertainty in the actual cost is more than that in case of full utilization. In fact, in the worst case scenario, the actual cost can be higher by about 35%. On the other hand, Figure 5.2(b) depicts a case of over-utilization. Here, the actual cost is less than the cost for full utilization. However, uncertainty analysis reveals that there is a chance that difference may not be significant, as evident from the right hand side of two curves.

5.6.2 Case of producing multiple quantities of different parts

This subsection considers the case of producing two parts, i.e, part A and part B. Table 5.2 provides the details of machine utilization and costs for producing different quantities of two parts. The purpose of showing this table is to highlight that when overall production volume increases, the utilization factor increases. A worth noting fact is that an increase in the quantities of one part reduces the cost of both the parts. For comparison of the values in the table, unit costs for full utilization were also estimated. For 1000 units, these are ($

18.99, $ 23.38, $ 30.10) for Part A and ($ 2.52, $ 3.12, $ 4.12) for part B. For 100 units, these are ($ 19.01, $ 23.40, $ 30.12) for Part A and ($ 2.56, $ 3.15, $ 4.18) for part B. It is seen that for full utilization of the machine, the cost is not dependent on the production volume, but it is dependent on the production volume if it affects utilization. Hence, it is stressed that an organization should attempt to enhance the utilization of a 3D printing machine.

Table 5.2 Details of machine utilization and costs for producing different quantities of two parts on an SLS 3D printing machine

Annual production (unit)		**Production time (hr)** (t_{pl}, t_{pm}, t_{pu})		**Utilization factor** (U_{fl}, U_{fm}, U_{fu})	**Actual unit cost ($)** ($C_{al}$, C_{am}, C_{au})	
Part A	**Part B**	**Part A**	**Part B**		**Part A**	**Part B**
100	100	(126, 159, 223)	(19.97, 26.06, 37.50)	(0.05, 0.10, 0.22)	(33.72, 73.79, 190.92)	(4.89, 11.43, 31.22)
100	200	(126, 159, 223)	(39.95, 52.11, 74.99)	(0.06, 0.12, 0.25)	(31.36, 66.85, 170.46)	(4.50, 10.28, 27.76)
200	100	(252, 318, 446)	(19.97, 26.06, 37.50)	(0.10, 0.19, 0.40)	(25.04, 47.83, 112.24)	(3.52, 7.18, 17.99)
200	200	(252, 318, 446)	(39.95, 52.11, 74.99)	(0.11, 0.21, 0.43)	(24.31, 45.70, 105.99)	(3.39, 6.82, 16.92)
600	600	(756, 954, 1338)	(117.39, 153.66, 221.82)	(0.32, 0.41, 1.30)	(17.78, 26.99, 49.33)	(2.37, 3.71, 7.31)
600	1000	(756, 954, 1338)	(194.82, 255.21, 368.65)	(0.35, 0.67, 1.42)	(17.78, 26.20, 47.02)	(2.33, 3.58, 6.92)
1000	600	(1260, 1590, 2230)	(117.39, 153.66, 221.82)	(0.51, 0.97, 2.04)	(16.90, 23.57, 38.93)	(2.20, 3.16, 5.59)
1000	1000	(1260, 1590, 2230)	(194.82, 255.21, 368.65)	(0.54, 1.03, 2.17)	(16.79, 23.24, 37.97)	(2.18, 3.10, 5.42)

5.6.3 Comparison of additive manufacturing with injection moulding

Table 5.3 presents the results of unit cost (considering full utilization) and total production time for injection moulding and 3D printing. For different lot sizes, the unit cost and total production time are provided. Membership grades for suitability are provided based on cost

and time. Assignment of membership grades is subjective and may vary from organization to organization and context to context. However, for the purpose of illustration, a scheme is used for assigning membership grades. As per the scheme, for each lot size, the process providing the lowest cost is assigned a membership of 0.9 from cost perspective. Corresponding membership for other process is obtained by ensuring that membership grades from cost perspective are inversely proportional to unit cost.

Table 5.3 Details of cost (considering full utilization) and production time for injection moulding and 3D printing associated with membership grade

Lot size	Unit Cost ($)		Total time (hr)		Membership grade					
	IM	3DP	IM	3DP	IM			3DP		
					μ_{cost}	μ_{time}	$\mu_{overall}$	μ_{cost}	μ_{time}	$\mu_{overall}$
1	8650.51	28.96	62.79	2.24	0	0.25	0	0.9	1	0.92
10	866.61	23.65	66.16	15.9	0.02	0.25	0.05	0.9	1	0.92
100	88.22	23.40	107.85	159	0.24	1	0.36	0.9	0.5	0.59
1000	10.38	23.38	534.70	1590	0.9	1	0.92	0.4	0	0

IM: Injection moulding, 3DP: 3D printing

Production time affects the tardiness. A process providing less production time is likely to minimize tardiness. Tardiness depends on the due date. Even if a process takes a lot of time to manufacture, there may not be any tardiness if the activities can be planned well in advance. However, for the purpose of illustration, it is assumed that a customer needs the final produced part within minimum possible time. Hence, the process taking the minimum time is assigned a membership grade of 1. Each delay of 1 day is assumed to reduce the membership grade by half. With this logic, the membership grades are generated. Overall membership grade is evaluated by giving equal weightage to compensating and non-compensating strategy. In Table 5.3, overall membership grade is calculated by putting $s_f = 0.5$ in Eq. (5.13). Table 5.4 shows the overall membership grade for pure compensating strategy, i.e, $s_f = 0$ as well as pure non-compensating strategy, i.e, $s_f = 1$. The overall membership grade obtained for $s_f = 0$ is greater than $s_f = 1$. However, for some cases, the overall membership grade is equal, i.e., 0 for both $s_f = 0$ and $s_f = 1$.

Table 5.4 Details of cost (considering full utilization) and production time for injection moulding and 3D printing associated with membership grade

Lot size	Membership grade							
	Injection moulding				3D Printing			
	μ_{cost}	μ_{time}	$s_f = 0$	$s_f = 1$	μ_{cost}	μ_{time}	$s_f = 0$	$s_f = 1$
			$\mu_{overall}$	$\mu_{overall}$			$\mu_{overall}$	$\mu_{overall}$
1	0	0.25	0	0	0.9	1	0.95	0.9
10	0.02	0.25	0.07	0.02	0.9	1	0.95	0.9
100	0.24	1	0.49	0.24	0.9	0.5	0.67	0.5
1000	0.9	1	0.95	0.9	0.4	0	0	0

It is observed that up to a lot size of 100, 3D printing is greater over membership grade than that of injection moulding. Hence, the deployment of 3D printing is recommended. For a lot size of 1000, it is preferable to use injection moulding based on the overall membership grade. It is interesting to note that for the lot size of 100, although the production time for injection moulding is less than that for 3D printing, from cost perspective it is not a favourable process. This is reflected by greater overall membership grade for 3D printing.

5.7 Conclusion

In this chapter, an analytical methodology has been proposed for assessing the utility of 3D printing for an organization. Based on the concept of utilization factor, the proper use of a 3D printing machine is evaluated. Further, the effect of utilization factor on production cost for different production volume of parts is presented. The effect of uncertainties on the utilization factor and cost are discussed. In addition, a fuzzy set based technique to choose a process based on several deciding factors is described. The overall methodology proposed in this chapter is illustrated by some examples. The following conclusions are drawn from the case studies:

- The increase in the production volume of a part increases the utilization factor with a reduction in the unit cost. A lot of uncertainty is observed in the utilization factor as well as unit cost. However, the uncertainty in the unit cost for high production volume reduces due to the low impact of overhead cost.
- For the production of two different parts, the increase in the production of one quantity decreases the cost of both the parts. This is due to overall utilization of the machine.
- Comparison of 3D printing with injection moulding demonstrates that decision to choose one process over the other is dependent on the production volume. For higher lot

size, injection moulding is preferable due to low production cost as well as low production time.

Chapter 6
Energy Consumption in Additive Manufacturing

6.1 Introduction

To assess the sustainability of a manufacturing process, the environmental aspects are equally important as economic aspects. Energy consumption results in several environmental issues and has been the concern of the global community for years. Hence, the proper investigation of the energy requirement of a manufacturing process and reducing it is a significant strategy for achieving sustainability. During the process of converting a raw material to the final product, energy is consumed at every stage. Although additive manufacturing (AM) is claimed to be environmentally friendly, it can have an adverse effect on the environment if it is not utilised judiciously. Hence, it is necessary to understand the role of every energy consuming element of an AM based machinery.

In the past, researchers conducted several studies to investigate the energy consumption in AM by different approaches. For example, Mongol et al. (2006), Baumers et al. (2011), Paul and Anand (2012), Kellens et al. (2014) and Ma et al. (2020) studied the effect of geometrical parameters like orientation, position, height and layer thickness of a part on the energy consumption of AM processes. On the other hand, Sreenivasan (2010), Meteyer et al. (2014) and Yeng et al. (2017) investigated the involvement of different machinery components of AM in energy consumption. Peng et al. (2016) investigated the energy consumption of an extrusion based AM process by considering the melting of raw material as a primary energy and the energy consumed by machinery components as a secondary energy. Recently, Ma et al. (2021) explored the energy consumption of three popular AM processes, viz., fused deposition modelling (FDM), stereolithography and selective laser melting. To improve the energy efficiency, an approach to obtain the optimal process parameters is also proposed.

This chapter presents the energy consumption models of two popular AM processes, i.e., selective laser sintering (SLS) and fused deposition modelling (FDM). Based on the involvement of different energy consuming components, the procedure to estimate the energy consumption is described. After this brief introduction, Sections 6.2 and 6.3 describe the energy estimation model of SLS and FDM, respectively. Section 6.4 illustrates the methodology by examples. Section 6.5 concludes the chapter.

6.2 Energy consumption model of selective laser sintering

This section describes the deterministic energy consumption model of SLS. For estimating the energy consumption of any AM process, it is necessary to have proper information on different energy consuming components of a 3D printing machine. A brief description of SLS is provided in Chapter 3. There are several machinery components in SLS machine that consumes energy. Table 6.1 lists the energy consuming elements of SLS. All the energy consuming components are described in the next subsections.

Table 6.1 Energy consuming components of SLS

Energy consuming components	Purpose
Laser system	Sintering of powder in layer-by-layer manner
Heater system	Maintaining the chamber at an elevated temperature and heating the powder
Rotating roller	Supplying and levelling the powder in bed
Pistons in the movable platform	One piston for lowering of the powder bed and the other piston for supplying the powder in front of the roller

6.2.1 Energy consumed by laser system

The energy consumed by the laser beam during the sintering of the powder is dependent on laser parameters, geometrical parameters of the part as well as material properties. The estimation of the energy requirement by the laser system considering all parameters simultaneously by an analytical model is a tedious task. Franco and Romoli (2012) analysed the effect of different laser parameters on the energy requirement for polyamide polymer powder, which is also considered as a raw material in this study. The interaction of laser beam and the powder is characterised by a basic parameter, viz., the energy density. The energy density (E_d) is given by

$$E_d = \frac{P_l}{v_s d_l}, \tag{6.1}$$

where P_l is the power rating of the laser, v_s is the scan velocity of the laser and d_l is the diameter of the laser beam. Franco and Romoli (2012) conducted experiments on an SLS machine and provided data to estimate laser energy consumed per unit mass based on different values of E_d. Based on those data, the laser energy consumption can be estimated.

6.2.2 Energy consumed by heater system

The heater system is composed of an infrared heater and a resistive heater (Gibson et al. 2014). The closed chamber is maintained at a high temperature by the infrared heater. On

the other hand, the resistive heater is used to maintain an elevated temperature of the build platform throughout the fabrication of the part. The energy consumed by the infrared heater (E_{ir}) is given by (Metreyer et al. 2014)

$$E_{ir} = \frac{P_{ir} t_{build}}{\eta_{ir}}, \tag{6.2}$$

where P_{ir} is the power rating of the infrared heater, t_{build} is the time involved in warming up the machine chamber and building the part and η_{ir} is the efficiency of the infrared heater. On the other hand, a resistive heater is required to heat the powder in the build platform for proper sintering to occur. The energy is required in the form of heat. It depends on the powder material properties. The heat input (Q_r) to maintain the elevated temperature of the powder during building of the part is given by

$$Q_r = m_p c_p \left(T_f - T_i\right), \tag{6.3}$$

where m_p is the mass of the powder, c_p is the specific heat of the powder, T_f is the final attainable temperature of the powder and T_i is the initial temperature of the powder. The heat input is provided by the resistive heater and its energy consumption (E_{rh}) is given by

$$E_{rh} = \frac{Q_r}{\eta_r}, \tag{6.4}$$

where η_r is the efficiency of the resistive heater. The total energy consumed by the heater system (E_{heater}) is given by

$$E_{heater} = E_{ir} + E_{rh}. \tag{6.5}$$

6.2.3 Energy consumed by roller

The roller spreads the powder and forms a layer in the machine bed. The mechanical energy of the roller is estimated as per the kinematic profile shown in Figure 6.1.

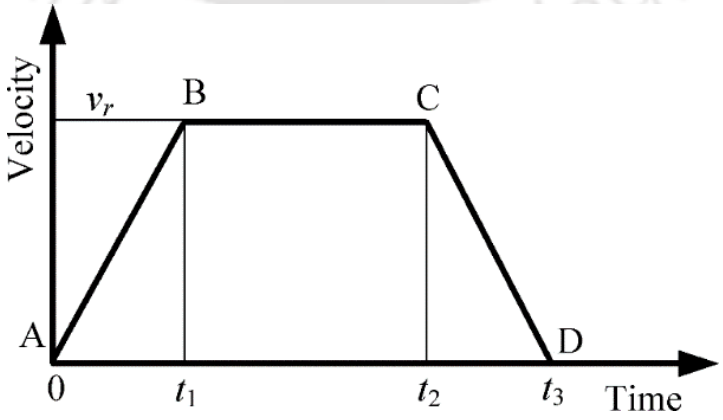

Figure 6.1 Velocity versus time diagram of the roller

The energy spent in portion AB (E_1) is given by the change in kinetic energy and work done against powder:

$$\begin{aligned} E_1 &= \frac{1}{2} m_r v_r^2 + \frac{1}{2} I_r \omega_r^2 + F_r s_{ab} \\ &= \frac{1}{2} m_r v_r^2 + \frac{1}{2} I_r \omega_r^2 + \frac{1}{2} F_r v_r t_1, \end{aligned} \tag{6.6}$$

where m_r is the mass of the roller, v_r is the maximum attainable translational velocity by the roller, I_r is the moment of inertia of the roller about its centre and ω_r is the maximum attainable angular velocity by the roller. The term F_r is the resistive force provided by the powder to the roller, s_{ab} is the distance travelled by the roller from point A to B and t_1 is the time spent by the roller to reach the point B. The roller is considered to be a solid cylinder. Its moment of inertia is given by

$$I_r = \frac{1}{2} m_r r_r^2, \tag{6.7}$$

where r_r is the radius of the cylindrical roller. During travelling of the roller, it is assumed that rolling takes place without slipping that satisfies the relation

$$v_r = \omega_r r_r. \tag{6.8}$$

At point B, the roller attains its maximum velocity and continues to move until point C. The energy spent in portion BC (E_2) is given by

$$\begin{aligned} E_2 &= F_r s_{bc} \\ &= F_r v_r \left(t_2 - t_1 \right), \end{aligned} \tag{6.9}$$

where t_2 is the time required by the roller to reach point C. From point C, the roller decelerates and comes to rest at point D. For bringing the roller to rest, it requires some amount of kinetic energy. However, during this period, the powder also offers resistance. Hence, the energy spent in portion CD (E_3) is less than the energy spent in portion AB. E_3 is given by

$$E_3 = \frac{1}{2} m_r v_r^2 + \frac{1}{2} I_r \omega_r^2 - F_r s_{cd}, \tag{6.10}$$

where s_{cd} is the distance travelled by the roller from point C to D. The total energy spent (E_r) is given by

$$\begin{aligned} E_r &= E_1 + E_2 + E_3 \\ &= \frac{1}{2} m_r v_r^2 + \frac{1}{2} I_r \omega_r^2 + F_r s_{ab} + F_r s_{bc} + \frac{1}{2} m_r v_r^2 + \frac{1}{2} I_r \omega_r^2 - F_r s_{cd}. \end{aligned} \tag{6.11}$$

However, $s_{ab} = s_{cd}$, hence

$$E_r = m_r v_r^2 + I_r \omega_r^2 + F_r v_r \left(t_1 - t_2\right). \tag{6.12}$$

The study conducted by Nan et al. (2020) revealed that the roller force is approximately 20 times the total weight of the heap of powder generated in front of the roller. This heap of powder is generated approximately up to the half the diameter of the roller (Haeri et al. 2016). The diameter of the roller is evaluated based on the size of the polymer powder. In SLS, the size of the roller is related to the size of the powder particle as (Haeri et al. 2016)

$$\frac{d_{roller}}{d_{powder}} = \left[500, 1000\right], \tag{6.13}$$

where d_{roller} and d_{powder} are diameters of the roller and powder, respectively, and square bracket contains interval number. Overall, the energy required by the roller is provided by a motor. Hence, the energy requirement by the motor to operate the roller (E_{roller}) is given by

$$E_{roller} = \frac{E_r}{\eta_m}, \tag{6.14}$$

where η_m is the efficiency of the motor.

6.2.4 Energy consumed by the movable platform

The part fabricated in a build platform moves in the downward direction according to the prescribed layer thickness. Apart from this, a powder delivery platform is also present on the other side that supplies the powder in front of the roller. Both the platforms are controlled by piston. The piston moves and stops repeatedly according to the number of layers present in the part. Assuming that no energy is required in stopping, the mechanical energy of the piston (E_{ps}) is given by the summation of potential and total kinetic energy:

$$E_{ps} = m_{ps} g h_{ps} + \frac{1}{2} m_{ps} v_{ps}^2 N_l, \tag{6.15}$$

where m_{ps} is the mass of the piston, g is the acceleration due to gravity, h_{ps} is the total height travelled by the piston, v_{ps} is the velocity of the piston and N_l is the number of layers present in the part. Similar to the energy required by the motor, the energy required by the piston (E_{piston}) is also provided by the motor:

$$E_{piston} = \frac{E_{ps}}{\eta_m}, \tag{6.16}$$

where η_m is the efficiency of the motor.

Apart from the energy consumption mentioned in Sections 6.2.1–6.2.4, some additional energy is also consumed by the computer, workstation and some amount of energy are also lost during the process. This extra amount of miscellaneous energy (E_{misc}) is considered to be 5% of the total energy:

$$E_{misc} = 0.05\left(E_{laser} + E_{heater} + E_{roller} + E_{piston}\right). \tag{6.17}$$

6.3 Energy consumption model of fused deposition modelling (FDM)

This section describes the deterministic energy consumption model of FDM. Amongst all AM processes, the market share of FDM is the highest in terms of machinery sold, thanks to the economy of this extrusion-based technology. A brief description of FDM is provided in Chapter 3. The energy consumption in FDM can be categorized in the following stages:

- Energy consumed during melting of filament
- Energy consumed during extrusion
- Energy consumed in heating the baseplate
- Energy consumed by the movable platform
- Miscellaneous energy consumption (standby, losses)

6.3.1 Energy consumed during melting of the filament

The thermoplastic filament is extruded in the molten form through the nozzle of the machine. The molten extruded material is maintained at a temperature 1 °C above the melting point (Huang et al. 2013). After extrusion, the material is fused with the previously formed layer. The total heat energy (Q_m) required during melting of the filament is given by

$$Q_m = m_e c_{ps}\left(T_m - T_i\right) + m_e q_f + m_e c_{pm}\left(T_f - T_m\right), \tag{6.18}$$

where m_e is the mass of the extruded material, c_{ps} is the specific heat of solid polymer, T_m is the melting temperature of the material, T_i is the initial temperature, q_f is the heat of fusion, c_{pm} is the specific heat of melted polymer and T_f is the final temperature. The heat input is provided by the heater and its energy consumption (E_m) is given by

$$E_{melting} = \frac{Q_m}{\eta_r}, \tag{6.19}$$

where η_r is the efficiency of the heater.

6.3.2 Energy consumed during extrusion

At this stage, the molten thermoplastic material is pushed through the nozzle to the baseplate. The required force for extrusion should overcome the pressure drop across the

extruder. The pressure drop is dependent on the viscosity of the molten material and several geometrical parameters like length and diameter of the liquefier, diameter of the filament, length and diameter of the nozzle, and nozzle angle. Figure 6.2 illustrates different zones of the extruder where the filament is melted and extruded from the nozzle. The material behaviour of thermoplastic filament obeys shear thinning where the viscosity of the material decreases with an increase in the shear rate (Bellini et al. 2004). A power law is adopted to model the dependence of viscosity on shear rate (Turner et al. 2014):

$$\eta = K\dot{\gamma}^{n-1}, \tag{6.20}$$

where η is the viscosity of the material, $\dot{\gamma}$ is the shear rate, K and n are the power law fit parameters. Also, the flow of the molten material in the extruder is non-isothermal. Hence, the dependence of viscosity on temperature should also be considered along with shear rate (Bellini et al. 2004, Turner et al. 2014):

$$\eta = H(T)\eta_{T_0}(\dot{\gamma}), \tag{6.21}$$

where $H(T)$ is the temperature-dependent term for viscosity. The term T_0 is the reference temperature at which the power law fit parameters K and n are determined. The Arrhenius relation to model the temperature-dependent term is given by (Turner et al. 2014)

$$H(T) = \exp\left\{\alpha\left(\frac{1}{T} - \frac{1}{T_0}\right)\right\}, \tag{6.22}$$

where α is the activation energy and T is the temperature at the end of the extruder.

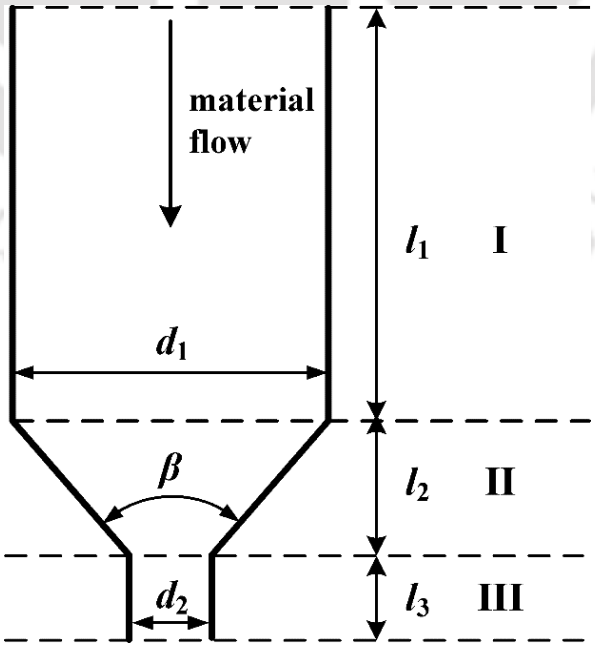

Figure 6.2 Different zones of the extruder. With permission from Turner et al. (2014). Copyright 2014, Emerald Publishing Company.

Applying Eqs. (6.21) and (6.22) to the momentum balance on the extruder, Bellini et al. (2004) estimated the pressure drop in the extruder by dividing it into three different zones as illustrated in Figure 6.2. For simplicity, the model was developed considering several assumptions: (a) the melt, i.e. the molten material, is incompressible, (b) no-slip boundary condition is applicable at the wall of the extruder, and (c) the flow of the melt is uniform, steady and laminar. The pressure drops at each sections of the extruder are given by (Bellin et al. 2004, Turner el al. 2014)

$$\begin{aligned}
\Delta P_1 &= 2l_1\left(\frac{v_f}{\phi}\right)^{1/m_f}\left\{\frac{m_f+3}{(d_1/2)^{m_f+1}}\right\}^{1/m_f}\exp\left\{\alpha\left(\frac{1}{T}-\frac{1}{T_0}\right)\right\},\\
\Delta P_2 &= \left\{\frac{2m_f}{3\tan(\beta_n/2)}\right\}\left(\frac{1}{d_2^{3/m_f}}-\frac{1}{d_1^{3/m_f}}\right)\left\{\left(\frac{d_1}{2}\right)^2(m_f+3)2^{m_f+3}\right\}^{1/m_f}\exp\left\{\alpha\left(\frac{1}{T}-\frac{1}{T_0}\right)\right\},\\
\Delta P_3 &= 2l_3\left(\frac{v_f}{\phi}\right)^{1/m_f}\left\{\frac{(m_f+3)(d_1/2)^2}{(d_1/2)^{m_f+3}}\right\}^{1/m_f}\exp\left\{\alpha\left(\frac{1}{T}-\frac{1}{T_0}\right)\right\},
\end{aligned} \tag{6.23}$$

where ΔP_1, ΔP_2 and ΔP_3 are the pressure drops in zone I, II and III, respectively, l_1 and l_3 are the lengths of the extruder corresponding to zone I and III, respectively, v_f is the velocity of the filament at the entry, β_n is the nozzle angle, ϕ and m_f are the material constants, and d_1 and d_2 are diameters of the filament and nozzle, respectively. The constants ϕ and m_f represent the fluidity and flow exponent, respectively. ϕ and m_f are related to the power law fit parameters as (Bellin 2002)

$$\begin{aligned}
\phi &= K^{-\frac{1}{n}},\\
m_f &= \frac{1}{n}.
\end{aligned} \tag{6.24}$$

The total pressure drop (ΔP) is given by the algebraic summation of the pressure drops at all the three zones:

$$\Delta P = \Delta P_1 + \Delta P_2 + \Delta P_3. \tag{6.25}$$

The force (F_e) required to push the molten thermoplastic material through the extruder is given by

$$F_e = \Delta P A_f, \tag{6.26}$$

where A_f is the cross-sectional area of the filament. The energy required in extrusion ($E_{extrusion}$) is given by

$$E_{extrusion} = F_e s_m, \tag{6.27}$$

where s_m is the distance travelled by the molten material in the extruder. The distance travelled (s_m) is given by

$$s_m = v_e t_e, \tag{6.28}$$

where v_e is the extrusion velocity and t_e is the extrusion time. The extrusion time (t_e) is assumed to be equal to the printing time. The energy required in extrusion ($E_{extrusion}$) is provided by the motor:

$$E_{extrusion} = \frac{E_e}{\eta_m}, \tag{6.29}$$

where η_m is the efficiency of the motor.

6.3.3 Energy consumed in heating the baseplate

The extruded material is deposited in a baseplate that is heated by the resistive heater. The baseplate where the printing takes place is made of a thermosetting plastic. The heat input (Q_b) to raise the temperature of the base plate during printing is given by

$$Q_b = m_b c_{pb} \left(T_f - T_i\right), \tag{6.30}$$

where m_b is the mass of the base plate, c_{pb} is specific heat of the baseplate, T_f is the final attainable temperature by the baseplate and T_i is the initial temperature of the baseplate. The heat input provided by the resistive heater and the energy consumption ($E_{baseplate}$) is given by

$$E_{baseplate} = \frac{Q_b}{\eta_r}. \tag{6.31}$$

6.3.4 Energy consumed by the movable platform

After a layer is formed, the baseplate moves in the downward direction according to the predetermined layer thickness. The baseplate along with the platform moves and stops repeatedly according to the number of layers present in the part. Assuming that no energy is required in stopping, the mechanical energy of the movable platform (E_{pl}) is given by the summation of potential and total kinetic energies:

$$E_{pl} = m_{pl} g h_{pl} + \frac{1}{2} m_{pl} v_{pl}^2 N_l, \tag{6.32}$$

where m_{pl} is the mass of platform, g is the acceleration due to gravity, h_{pl} is the total height travelled, v_{pl} is the velocity of the platform and N_l is the number of layers present in the part. The energy required by the platform ($E_{platform}$) is provided by the motor:

$$E_{platform} = \frac{E_{pl}}{\eta_m}, \tag{6.33}$$

where η_m is the efficiency of the motor.

6.3.5 Miscellaneous energy consumptions

Apart from the energy consumption sources mentioned in Sections 6.3.1–6.3.4, energy is also consumed by the computer, workstation and some energy are also lost in the form of heat and machine error (Song and Telenko 2017, Yosofi et al. 2018). The energy consumed by miscellaneous sources (E_{misc}) is approximated as 5% of the total energy consumed by all other sources, i.e.,

$$E_{misc} = 0.05 \left(E_{melting} + E_{baseplate} + E_{platform} + E_{extrusion} \right). \tag{6.34}$$

6.4 Illustration of the methodology by examples

The methodology described in Sections 6.2 and 6.3 will be demonstrated by examples. The next subsequent sections (Sections 6.4.1 and 6.4.2) present energy estimation of parts by SLS and FDM, respectively.

6.4.1 Energy consumption calculation by selective laser sintering

The energy consumption model of SLS will be implemented to estimate the energy consumption for manufacturing two parts, viz., part A and part B. Those two parts and the same SLS machine were considered for cost estimation in Chapter 3. The details of the parts, build time and machine parameters are given in Section 3.4.1. Same parameters are used for energy estimation in this section.

The first step is to estimate the energy consumption by the laser system. The laser parameters used in this study are listed in Table 6.2. Based on these parameters, the energy density (E_d) is 0.07 J/mm^2. As per this value of E_d, the energy required for both the parts is obtained from the findings of Franco and Romoli (2012). Then, the energy consumed by the infrared and resistive heaters is estimated. The infrared heater consumes energy for heating the chamber during the machine warm-up and building the part. On the other hand, the resistive heater consumes energy for heating the powder in the machine bed. It depends on the mass of the powder and its material properties. The mass of the powder is estimated based on the size of the powder bed and height of the part. Table 6.2 lists the necessary parameters of the heater system used in this study.

Table 6.2 Parameters for energy consumed by the laser and heater system

Parameters	Value	Basis
Power rating of the laser (W)	30	(SLS SPEC 2017), own judgement (based on literature review)
Scan velocity of the laser (mm/s)	700	(Pham and Wang 2000), own judgement
Laser beam diameter (mm)	0.6	(Zhang and Bernard 2013)
Power of infrared heater (W)	1000	(Deziel 2018)
Efficiency of infrared/resistive heater	0.9	Own judgement
Specific heat of powder (kJ/kgK)	2.5	(Franco and Romoli 2012)
T_{final} of powder (°C)	185	(Franco and Romoli 2012)
$T_{initial}$ of powder (°C)	20	(Franco and Romoli 2012)

The next step involves the energy estimation by the roller for spreading and levelling the powder. The kinematic behaviour of the roller is illustrated in Figure 6.1. The roller travels to-and-fro across the platform based on the number of layers present in the part. For each travel, the roller consumes energy. The procedure to estimate the time taken by the roller to travel from one end of the platform to the other is explained in Chapter 3. The data used for estimating roller energy is given in Table 6.3.

Table 6.3 Parameters for estimating the roller energy

Parameter	Value	Basis
Distance travelled by roller (mm)	506	(SLS SPEC 2017), own judgement
Velocity of roller (mm/s)	700	(Pham and Wang 2000), own judgement
Acceleration of the roller (mm/s^2)	20000	(CADEM 2017)
Time, t_1–t_2 (s)	0.69	By calculation
Mass of roller (kg)	5	Own judgement
Diameter of powder (μm)	100	(Duraform n.d.)
Radius of the roller (mm)	50	(Haeri et al. 2016)
Force required by roller (N)	326.94	(Nan et al. 2020)
Efficiency of the motor	0.75	Own judgement considering part load operation

Lastly, the energy consumed by the moving pistons is estimated. The total vertical distance travelled by the piston of the build platform is equal to the height of the part. For the build piston, an additional 20% increase is included in the mass of the piston to consider the mass of the powder deposited. The parameters for estimating the energy consumed by piston is given in Table 6.4. The piston lowers down according to the prescribed layer thickness and the number of layers present in the part. An additional 5% increase is included

in the number of times the piston is lowered. However, the total distance travelled by piston of the powder delivery piston is much more than the piston of the build platform. The powder delivery piston feeds the powder to the height equal to the radius of roller, i.e., 50 mm. This process is repeated for every number of layers of the part. Also, the piston has to travel to the bottom frequently for complete filling of the feedstock with powder. This is done by an external delivery source. Considering these effects, an additional increase of 50% of the mass of the piston is also included. Hence, the energy of the piston for powder delivery is much more than the piston of the build platform. Finally, based on Eqs. (6.32) and (6.33), the energy consumed by the pistons

Table 6.4 Parameters for estimating the energy consumed by the pistons

Parameters	Value	Basis
Mass of the platform (kg)	10	Own judgement
Velocity of the platform (mm/s)	700	Own judgement
Efficiency of the motor	0.75	Own judgement considering part load operation

Table 6.5 Energy consumption by different sources for part A and part B

Energy components	Value	
	Part A	Part B
Energy consumed by laser system (kJ)	45.04	2.34
Energy consumed by infrared heater (kJ)	6954.67	4072.27
Energy consumed by resistive heater (kJ)	570.26	692.46
Energy consumed by the roller in spreading the powder (kJ)	80.19	144.95
Energy consumed by the piston by build platform (kJ)	0.78	0.94
Energy consumed by the piston for powder delivery (kJ)	4.58	4.89
Miscellaneous energy consumption (computer, losses)	382.78	245.89
Total energy consumption of the part (kJ)	8038.29	5163.74
Total energy consumption of the part (kWhr)	2.23	1.43
Total energy consumption per unit mass of the part (kJ/kg)	51756.42	639868.65
Total energy consumption per unit build time (kJ/hr)	4623.25	5072.1

is estimated. The energy consumed by every component for manufacturing part A and part B considering a single quantity is listed in Table 6.5. As evident from the last two rows of the table, mass of the part and build time may give some indication about the energy consumption, but it also depends on the part complexity.

6.4.1.1 Estimation of energy considering multiple quantities of a part in the machine chamber

The energy required by the laser and the infrared heater varies with the number of quantities manufactured in the machine chamber. However, the energy consumed by the resistive heater, roller and the pistons is independent of the number of quantities manufactured in the machine chamber. Hence, if more than one quantity of a part is manufactured, the overall unit energy requirement is less as the energy is reduced amongst the resistive heater, roller and pistons. As per the size of part A, only two quantities can be manufactured at a single setting of the machine chamber. In such a case, the total consumed energy is estimated as 12119.91 kJ whereas unit energy consumption is 6059.96 kJ. Hence, in manufacturing two quantities of part A, energy consumption is reduced by approximately 25% for a part. On the other hand, considering the smaller sized part B, a maximum of eighteen quantities can be manufactured in a single setting. This is also referred to as full utilization of the machine. The energy consumed for manufacturing a single quantity of part B is 5163.74 kJ whereas the unit energy consumed for eighteen quantities is 1004.67 kJ reducing the energy consumption by 81%. The variation of energy with the quantities of part B is shown in Figure 6.3.

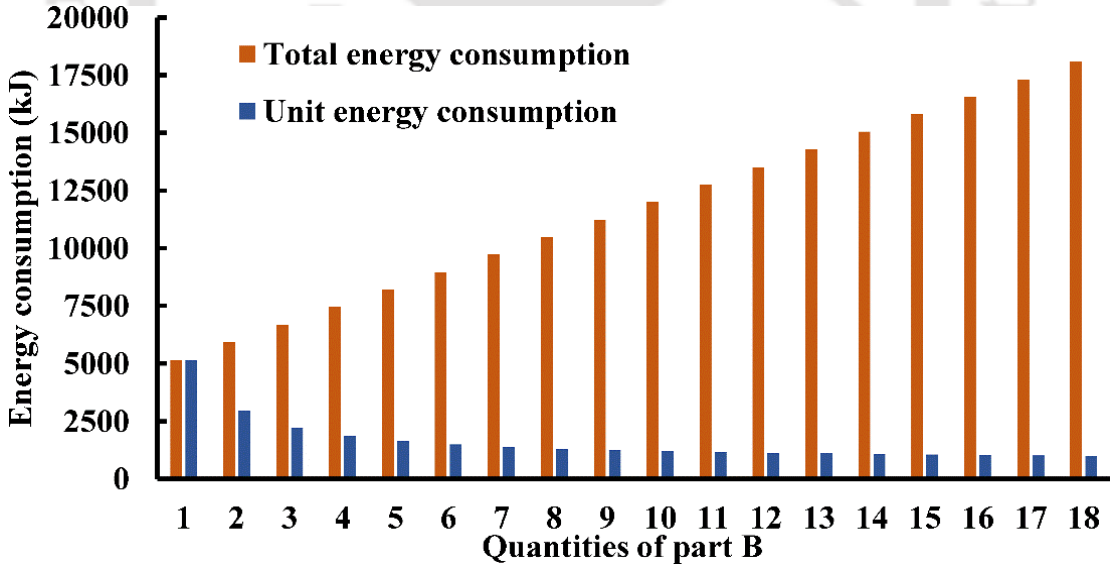

Figure 6.3 Variation of energy consumption with quantities of part B

6.4.1.2 Implementation of fuzzy arithmetic in energy consumption calculation of SLS

This section considers uncertain parameters as fuzzy and the energy consumption in SLS is obtained as a fuzzy number. The fuzzy parameters are expressed as low (l), most likely (m) and high (h) estimates in Table 6.6. In the estimation of energy consumed by the roller, the lower limit of roller force is assumed to deviate by 20% whereas the upper limit by 10%

than the most likely estimate. The height of the heap of powder accumulated in front of the roller is assumed to vary by 10% and 20% of the radius of the roller for the lower and upper estimates, respectively. Also, the lower and upper limit of the size of the roller is considered to be 500 and 1000 times that of the size of the powder. In the estimation of energy consumed by the pistons for build platform, the lower and upper limits of mass of the piston are additionally increased by 10% and 30% of the actual mass of the piston, respectively. However, for the piston of the powder delivery platform, the lower and upper limits are increased by 30% and 70%, respectively. This piston has to accumulate relatively more mass of the powder that is continuously fed by the feedstock.

Table 6.6 Fuzzy parameters considered for estimation of energy consumption in SLS

Parameter	**(*l*, *m*, *h*)**
Power rating of the laser (W)	(20, 30, 50)
Scan velocity of the laser (mm/s)	(500, 700, 1000)
Power of infrared heater (W)	(800, 1000, 1200)
Efficiency of infrared/resistive heater	(0.8, 0.9. 0.95)
Diameter of the roller (mm)	(50, 75, 100)
Mass of roller (kg)	(4.5, 5, 5.5)
Force required by roller (N)	(313.86, 435.92, 527.46)
Layer thickness (mm)	(0.12, 0.15, 0.21)

Table 6.7 shows the unit energy consumption of the parts considering a single quantity and full utilization of the machine chamber, i.e., two and eighteen quantities of part A and part B, respectively. The energy as a fuzzy number is obtained by applying the procedure mentioned in Section 3.3. The variation of energy as a fuzzy number with different membership grades is shown in Figure 6.4.

Table 6.7 Unit energy consumption as a fuzzy number considering a single part and full utilization of the machine

		Unit energy consumption (kJ)		
	Quantities in the machine chamber	**Low estimate (*l*)**	**Most likely estimate (*m*)**	**High estimate (*h*)**
Part A	1	4930.94	8038.29	14970.4
	2	3534.51	6059.96	11776.59
Part B	1	4160.02	5163.74	7637.45
	18	714.87	1004.67	1659.19

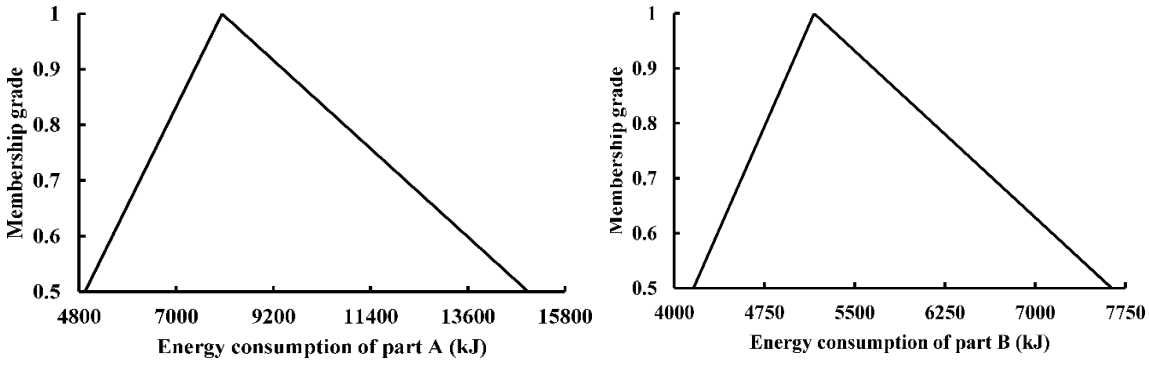

(a)

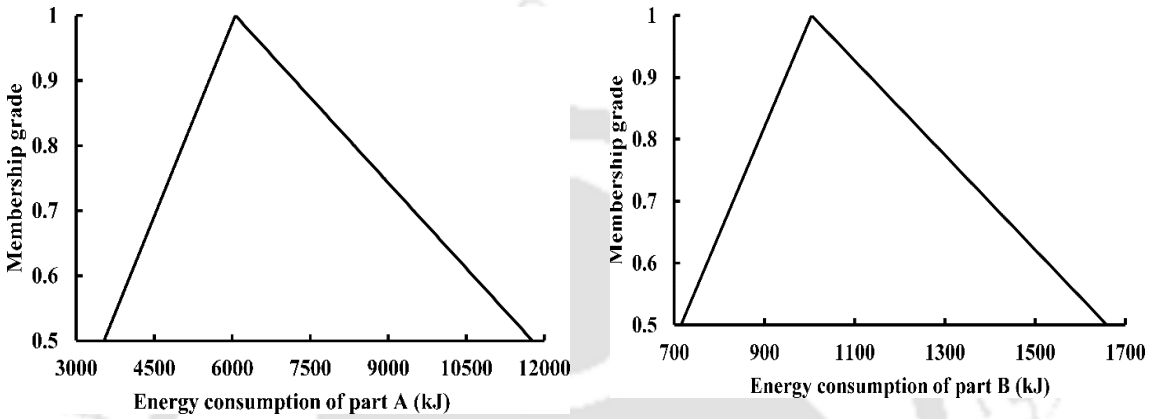

(b)

Figure 6.4 Representation of energy consumption as a fuzzy number for parts produced by SLS: (a) Considering a single quantity, (b) considering full utilization of the machine chamber (two and eighteen quantities of part A and part B, respectively)

6.4.2 Energy consumption calculation by fused deposition modelling

The energy consumption model will be implemented to estimate the energy consumption for manufacturing five parts, viz., part 1, part 2, part 3, part 4 and part 5. The energy consumption for the parts by FDM is estimated as per the procedure described in Section 6.3. The geometrical details of the parts are given in Chapter 3. The first step is to estimate the energy consumed during melting of the filament as per Eq. (6.18). The necessary parameters for estimating the energy in melting are listed in Table 6.8. An extra 20 % is included in the mass of the extruded material to consider the material loss. After the melting of solid polymer, energy is also consumed in the fusion process. The specific heat of a molten polymer is greater than the solid form. For an amorphous polymer like ABS, the specific heat of the molten form is considered to be 50 % more than the solid form (Osswald and Hernández-Ortiz 2006).

Table 6.8 Parameters for estimating the energy consumed during melting of the filament and heating the base plate

Parameters	Most likely value (*m*)	Basis
Specific heat of solid ABS, c_{ps} (kJ/kg°C)	1.92	(ABS characteristics 2019)
Specific heat of molten ABS, c_{pm} (kJ/kg°C)	2.88	(Osswald and Harnandez 2006)
Melting temperature of ABS, T_m (°C)	230	(PlasticRanger 2000)
Initial temperature, T_i (°C)	25	Room temperature
Heat of fusion of ABS, q_f (kJ/kg)	205	(Osswald and Harnandez 2006)
Final temperature, T_f (°C)	231	(Huang et al. 2013, PlasticRanger 2000)
Efficiency of the heater, η	0.9	Assuming 10 % heat loss
Mass of the baseplate, m_b (gm)	500	Own judgement
Specific heat of the baseplate, c_{pb} (kJ/kg.°C)	1.3	(Glass Epoxy characteristics 2019)
Initial temperature of the baseplate, T_i (°C)	25	Room temperature
Final temperature of the baseplate, T_f (°C)	110	(Rahman et al. 2018)

The next step is to estimate the energy consumed during extrusion. It depends on several parameters including the geometry of the extruder, pressure drop in the extruder, cross-sectional area of the filament, extrusion time and extrusion velocity. The procedure to determine the extrusion time (assuming to be equal to printing time) is described in Chapter 3. Also, the extrusion velocity is assumed to be equal to printing velocity. The parameters for estimating the energy consumed during extrusion are listed in Table 6.9. The next step comprises the estimation of energy consumption in heating the base plate. The resistive heater consumes energy for heating the base plate during the entire printing process. Lastly, the energy consumed by the movable platform in the vertical direction is estimated as per Eq. (6.32). The movable platform lowers down vertically according to the layer thickness of the part. The total vertical distance travelled by the platform is equal to the height of the part.

The energy consumed by different sources for the parts is listed in Table 6.10. It is observed that the maximum energy is consumed during heating the baseplate. The mass of the parts, printing time and the geometrical features give indications on the energy consumption.

Table 6.9 Parameters for estimating the energy consumed during extrusion of the molten filament and the movable platform

Parameters	Most likely value (*m*)	Basis
Total length of the extruder (mm)	150	(Bellini et al. 2004)
Length of zone I, l_1 (mm)	97.5	(Bellini et al. 2004)
Length of zone II, l_2 (mm)	37.5	(Bellini et al. 2004)
Length of zone III, l_3 (mm)	15	(Bellini et al. 2004)
Velocity of the filament at the entry, v_f (mm/s)	10	(Shadvar et al. 2021)
Power law fit parameter, K	3760.97	(Shadvar et al. 2021)
Power law fit parameter, n	0.57	(Shadvar et al. 2021)
Diameter of zone I (mm)	1.75	(Precision, n.d.)
Diameter of zone II (mm)	0.4	(Precision, n.d.)
Nozzle angle, β (°)	120	(Turner et al. 2014)
Temperature at the end of the extruder, T (K)	540	(Bellini et al. 2004)
Temperature, T_0 (K)	513.15	(Shadvar et al. 2021)
Energy of activation, α	0.9652	(Shadvar et al. 2021)
Extrusion velocity, v_e (mm/s)	40	(Precision, n.d.)
Mass of the platform, m_p (kg)	5	Own judgement
Velocity of the platform, v_p (mm/s)	40	(Precision, n.d.), by calculation

Table 6.10 Energy consumption by various sources for the parts

Energy consuming source	Most likely value				
	Part 1	**Part 2**	**Part 3**	**Part 4**	**Part 5**
Energy consumed during melting the filament (kJ)	15.53	12.19	8.73	8.02	15.36
Energy consumed in heating the baseplate (kJ)	61.39	61.39	61.39	61.39	61.39
Energy consumed during extrusion (kJ)	5.54	4.78	3.37	3.61	6.08
Energy consumed by the movable platform (J)	1.87	1.87	2.8	3.64	1.4
Miscellaneous energy consumption (kJ)	4.12	3.92	3.67	3.65	4.14
Total energy consumption (kJ)	86.58	82.28	77.17	76.68	86.97
Total energy consumption (Whr)	24.05	22.86	21.44	21.30	24.16
Total energy consumption per unit mass (kJ/kg)	3726.96	4509.66	5905.26	6388.51	3783.56
Total energy consumption per unit build time (kJ/hr)	68.03	74.97	99.77	92.49	62.33

6.4.2.1 Implementation of fuzzy arithmetic in energy consumption calculation of FDM

This section considers the uncertain energy related parameters in FDM as fuzzy. The fuzzy parameters are listed in Table 6.11. In the estimation of energy consumed during melting, the lower estimate of the extra material consumed is varied by 5 % whereas the upper limit by 30 %. For specific heat of the molten ABS, the lower and upper estimate of the specific heat of molten ABS is considered to be greater than the solid form by 30 % and 80 %, respectively. For estimating the pressure drop in the extruder, the lower and upper limit of the length of the extruder is considered to vary by 10 %. Considering heat loss in different forms, the lower and upper limit of efficiency of the heater is considered as 80 % and 95 %, respectively. The total energy consumption (in kJ) of different parts are shown in Table 6.12 and the variation of energy consumption with membership grades is shown in Figure 6.5.

Table 6.11 Fuzzy parameters considered for estimation of energy consumption in FDM

Parameters	**(*l*, *m*, *h*)**
Extra material consumed during extrusion (%)	(5, 20, 30)
Specific heat of molten polymer, c_{pm} (kJ/kg°C)	(2.50, 2.88, 3.46)
Efficiency of the resistive heater, η_r (%)	(80, 90, 95)
Total length of extruder (mm)	(148.5, 150, 151.5)
Velocity of the material at the entry, v_f (mm/s)	(14.85, 15, 15.15)
Reference temperature, T_o (K)	(493.15, 513.15, 533.15)
Power law fit parameter, K	(2434.44, 3760.97, 10779.53)
Power law fit parameter, n	(0.45, 0.57, 0.6)
Efficiency of the motor, η_m (%)	(70, 75, 80)

Table 6.12 Energy consumption of the parts produced by FDM

Parts	**Energy consumption as a fuzzy number (kJ)**		
	Low estimate (*l*)	**Most likely (*m*)**	**High estimate (*h*)**
Part 1	75.29	86.58	109.22
Part 2	72.44	82.28	102.61
Part 3	69.19	77.17	94.09
Part 4	68.77	76.68	93.62
Part 5	75.44	86.97	110.79

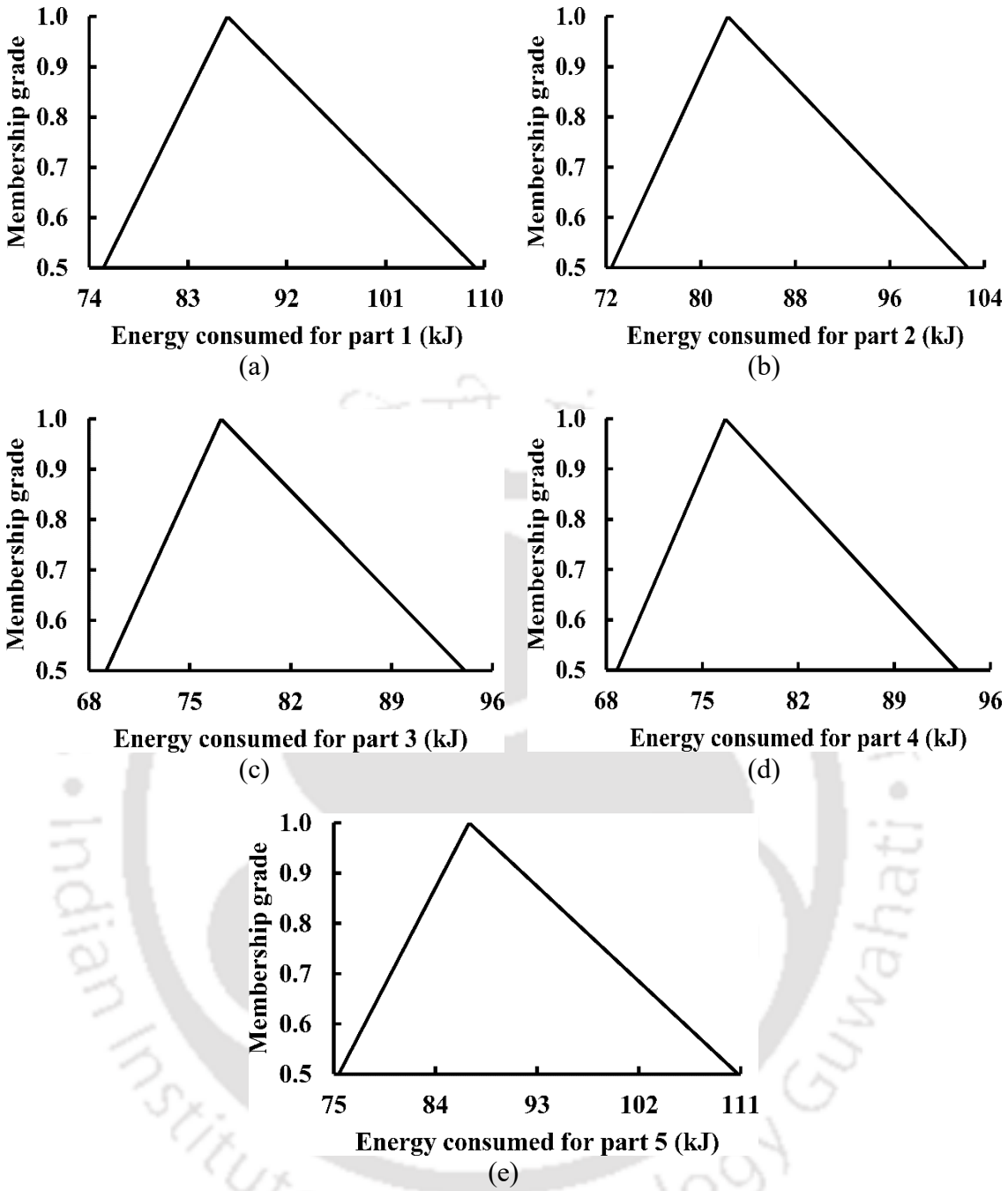

Figure 6.5 Representation of energy consumption as a fuzzy number for parts produced by FDM: (a) Part 1, (b) Part 2, (c) Part 3, (d) Part 4, and (d) Part 5

6.5 Overall sustainability analysis

It is considered that an industry works effectively for 300 days in a year and the 3D printer operates for 6 hours a day, i.e., 1800 hours is available in a year. Based on this assumption, the maximum quantities of a part that can be manufactured in a year can be estimated. For the purpose of illustration, five parts, i.e., part 1, part 2, part 3, part 4 and part 5 manufactured by FDM based 3D printing is considered. Based on the build time of these

parts, the maximum quantities that can be manufactured annually is estimated. Finally, the manufacturing cost on an annual basis is estimated as shown in Table 6.13.

The energy consumption of the parts can be used to estimate the energy cost and the amount of CO_2 emission. The energy cost is estimated based on the values of energy consumption and electricity rate given in Table 6.10 and Table 3.4, respectively. For simplicity, it is taken as cost of electricity. The amount of CO_2 emission in kg based on the energy input is given by (Telang 2011):

$$Amount\ of\ CO_2\ emission = Energy\ input \times Emission\ factor, \tag{6.35}$$

where the energy input is considered in terms of kWhr/year and emission factor is taken as 0.85. Table 6.13 shows the manufacturing cost, energy usage, energy cost and the amount of CO_2 emission for five different parts.

Table 6.13 Cost, energy usage and CO_2 emission of the parts on an annual basis

Parts	Annual production (quantities)	Manufacturing cost ($)	Energy usage (kWhr/year)	Energy cost ($)	CO_2 emission (kg)
Part 1	1414	6711.53	34.02	5.1	28.91
Part 2	1640	7038.2	37.49	5.62	31.86
Part 3	2327	8197.09	49.88	7.48	42.40
Part 4	2171	7860.04	46.25	6.94	39.31
Part 5	1290	6447.21	31.17	4.67	26.49

6.6 Conclusion

This chapter presents a methodology to estimate the energy consumption for producing parts by two popular AM processes, i.e., SLS and FDM. The role of different energy consuming elements is briefly described and represented mathematically. The deterministic energy estimation model based on the working principle is developed. The methodology is illustrated through examples. The amount of energy consumed for SLS and FDM is obtained as a fuzzy number to get an idea of the lower and upper estimates of the energy. The following salient conclusions are drawn:

- For SLS, the energy consumed for building a single part and multiple quantities of the part in the machine is estimated. It is observed that the maximum energy is consumed by the heater system. Considering multiple quantities, unit energy consumption is the least when the full machine chamber is utilized.

- For FDM, production of a single part is considered in the baseplate. The energy consumption for building a part individually is estimated. It is observed that the maximum energy is consumed in heating the baseplate where the molten thermoplastic is deposited to print the part.
- It can be inferred that although the mass and build time of the product can give some indication of the energy consumption, but in only an approximate way; energy consumption is also influenced by the part complexity.
- The CO_2 emission of a part is minimum for the part having the least build time. However, on an annual basis, the emission of the same part is the maximum as the annual production is the maximum.

Chapter 7
Epilogue

7.1 Introduction

Additive manufacturing (AM) is gaining enormous popularity due to its unique ability to produce a complex-shaped product by depositing material in a layer by layer manner. It provides several technological benefits and hence its application is increasing in different sectors, viz., automobile, aerospace and medical. Despite some exceptional advantages offered by AM, there is an apprehension about adopting this technology as a manufacturing route. Also, the speed of adoption and its utilisation is not as high as expected. In the present era of sustainability, the adoption of AM is a challenging task. It is necessary to ensure under conditions and up to what extent is AM cost-efficient. For this, a proper cost analysis is a necessity. It helps in assessing its competitiveness in the market and making it more economically sustainable. A major portion of this thesis is inclined towards the cost aspect of AM. Apart from cost analysis, the energy usage of AM is also investigated.

As reported in Chapter 2, researchers have carried out several works in the domain of sustainability aspects of AM. However, the issue of uncertainties in the estimation is not addressed. The parameters are often ambiguous, differs from place to place and varies with management policies. This thesis utilizes the concept of fuzzy set theory to address uncertainties in the estimation. It is one of the most widely used soft computing methods. The uncertain or the fuzzy variables are assigned suitable membership grades. Based on the low, most likely and high estimates of an uncertain variable, triangular membership functions are constructed. Such functions are linear and computations can be performed at ease. The content and outcomes of various subparts of this thesis are briefly summarised in the following sections. Finally, the overall conclusions and the scope of future work are highlighted.

7.2 Cost estimation of additive manufacturing in the presence of uncertainties

Cost estimation requires information of different activities and their associated cost elements to produce the part. The cost elements are often uncertain and vary from place to place, planning and management policies. Hence, to tackle uncertainties, apart from the deterministic cost model, a fuzzy set based cost model is also proposed. Two popular AM processes, i.e., SLS and FDM are considered. One of the most important parameters for cost estimation is build time. Analytical models for build time estimation are proposed for

both the processes. For the specific cases of SLS and FDM, build time estimation procedures are proposed analytically. For FDM, in-house experiments are conducted to validate the analytical build time model with the experimental build time. To evaluate the cost, the working conditions of a typical Indian industry is considered. However, all the cost parameters are finally reported in dollar as it is considered a universal currency. The cost estimation procedure presented in this work can also be applied for other AM processes if a proper build time estimation model is available.

7.3 Cost comparison of additive manufacturing with traditional manufacturing in the presence of uncertainties

For a prudent cost analysis of any manufacturing process, its comparison with other processes is a necessity. In the past, researchers carried out cost comparison of AM with other processes mostly based on break-even analysis. In this work, a conventional manufacturing process, i.e., injection moulding (IM) is considered. For the sake of completeness, the procedure to estimate the cost of IM is presented. The fuzzy costs of SLS and IM are compared under a variable demand scenario. A method to evaluate the reliability of a particular cost estimate and its significance is introduced. The concept of reliability is suitably utilised and variability in demand is tackled from probability theory. Variable demand is assumed to follow uniform as well as normal distribution. Based on the low, most likely and high estimates of cost, the expected cost of manufacturing is evaluated. The proposed methodology is illustrated by examples.

7.4 An analytical approach for assessing the utility of additive manufacturing in an organisation

An approach for assessing the utility of additive manufacturing in an organization is proposed. The concept of utilization factor is introduced. Its effect on production planning and its associated cost are discussed. The uncertainty in the estimation of utilization factor and costs is addressed by fuzzy set based theory. Also, a methodology is proposed for comparing SLS and IM. For the purpose of comparison, two decision making parameters, i.e., cost and time are considered. A quantitative approach to estimate the labour penalty cost due to reduction in employment is presented. This work demonstrated how proper utilisation of the machine can lower the unit costs of a product produced by AM. It is observed that the unit cost of a part produced also reduces for SLS if the utilisation factor is enhanced. A lot of uncertainty was observed in the utilization factor as well as unit cost. However, the uncertainty in the unit cost for high production volume reduces due to the low impact of overhead cost.

7.5 Energy estimation of additive manufacturing

The energy consumption of any manufacturing process is essential for comparison of its efficiency with other competitive processes. Every AM process follows the pattern of layer by layer deposition for manufacturing a finished part, but the energy consumption varies according to the working principle of individual AM processes. The energy consumption models of SLS and FDM are presented. The role of every energy consuming element is described. The methodology is demonstrated with the help of examples. Energy consumption is obtained for a single quantity as well as multiple quantities of the same part. The energy consumed for building a single part and multiple quantities of the part in the machine is estimated. For SLS, the maximum energy is consumed by the heater system. Based on the annual production of parts, the energy usage and CO_2 emission are evaluated. A procedure to quantify the overall sustainability based on manufacturing cost, energy cost and CO_2 emission is also presented.

7.6 Overall Conclusions

The salient conclusions of this thesis are listed as follows:

- A general cost model was proposed for AM by considering time-dependent and time-independent cost parameters. To tackle uncertainties and vagueness, the concept of fuzzy sets is implemented in cost estimation.
- Build time is one of the most important parameters for cost estimation. The time estimated by the analytical model is validated by conducting in-house experiments for FDM process. The maximum and the minimum deviation from the experimental results are 7.89% and 1.26%, respectively.
- Apart from the most likely estimate of the cost obtained from the deterministic cost model, fuzzy input parameters also gave a realistic value of the low and high estimate of the cost.
- In the cost comparison of SLS and IM, it is found that the unit cost of IM decreases with an increase in the number of quantities. However, the unit cost of SLS decreases up to a certain quantity but remains almost constant thereafter.
- For SLS, the cost per quantity is the least when the entire area of the machine chamber is used. This is also referred to as full utilization of the machine.
- In the cost analysis, for some cases considering uncertainties, the most likely and the high estimates cost of SLS were less than that of IM. However, the low estimate cost of

SLS is higher than that of IM. In such cases, the concept of reliability was implemented to choose a favourable process.

- The increase in the production volume of a part increases the utilization factor with a reduction in the unit cost of the part.
- For the production volume of two different parts, the increase in the production of one quantity decreases the cost of both the parts. This is due to the overall utilization of the machine.
- Comparison of 3D printing with injection moulding demonstrates that the decision to choose one process over the other is dependent on the production volume. For higher lot size, injection moulding is preferable due to low production cost as well as low production volume.
- In the estimation of energy consumption, for SLS, the maximum energy was consumed by the heater system. On the other hand, for FDM, the highest amount of energy was consumed in heating the baseplate. The minimum energy was consumed by the movable platform for both SLS and FDM.
- Full utilization of the machine chamber yields the minimum energy consumption per quantity. For SLS, the energy consumption of a part was reduced by 81% when the entire machine chamber was utilised instead of building a single part.

7.7 Scope for future work

Based on the work content of this thesis, there are some possibilities for further exploration and investigation. Some of these are as follows:

- In-house experiments need to be carried out in different 3D printers to validate the build time and energy consumption models. Also, the effect of jerk settings in build time estimation and energy consumption can be carried out for more detailed analysis.
- This thesis considered only linear triangular membership function. Estimates can be obtained also by non-linear membership functions, i.e., trapezoidal membership functions.
- The decision-making process is made based on cost and time. Some other parameters like waste generation, recycling of powder can also be included in the decision-making process.
- A popular decision-making method based on fuzzy set theory is defuzzification. Some popular techniques such as height method, centroid method, weighted method, average method and mean-max method can be explored.

- The work carried out in this thesis is limited to selective laser sintering (SLS) and fused deposition modelling (FDM). Both these processes use raw material in the form of polymer. Metallic based AM processes should also be investigated. The methodology can be extended for other manufacturing processes. This will help in arriving at a sustainability index for each of the processes.

References

- 99 acres, n.d., 2228 Properties, Accessed on March 4, 2019, <https://www.99acres.com/factory-land-for-rent-in-delhi-ncr-ffid>
- A.S.T.M., F2792-12a. 2012. Standard terminology for additive manufacturing technologies, 10.
- ABS characteristics, 2019, Custom Plastic & Metal Solutions, Accessed on September 11, 2020 <https://dielectricmfg.com/knowledge-base/abs/>
- Achillas, C., Aidonis, D., Iakovou, E., Thymianidis, M. and Tzetzis, D., 2015. A methodological framework for the inclusion of modern additive manufacturing into the production portfolio of a focused factory. *Journal of Manufacturing Systems*, *37*, pp.328–339.
- ACO mold, n.d., Mold and Molding Solutions, Accessed on December 21, 2019, <http://www.injectionmoldchina.net/cost-analysis.html>
- Alexander, P., Allen, S. and Dutta, D., 1998. Part orientation and build cost determination in layered manufacturing. *Computer-Aided Design*, *30*(5), pp.343–356.
- Amazon, n.d., Natural ABS 3D Printer Filament 1.75mm, Accessed on November 15, 2019, <https://www.amazon.in/s?k=abs+filament+1.75mm+1kg&crid=1SCZWI8MH9AY4&sprefix=ABS+filament%2Caps%2C496&ref=nb_sb_ss_i_4_12>
- Andrade, M.C., Pessanha Filho, R.C., Espozel, A.M., Maia, L.O.A. and Qassim, R.Y., 1999. Activity-based costing for production learning. *International Journal of Production Economics*, *62*(3), pp.175–180.
- Armijo, P.R., Markin, N.W., Nguyen, S., Ho, D.H., Horseman, T.S., Lisco, S.J. and Schiller, A.M., 2021. 3D printing of face shields to meet the immediate need for PPE in an anesthesiology department during the COVID-19 pandemic. *American journal of infection control*, *49*(3), pp.302–308.
- Atzeni, E. and Salmi, A., 2012. Economics of additive manufacturing for end-usable metal parts. *The International Journal of Advanced Manufacturing Technology*, *62*(9–12), pp.1147–1155.
- Atzeni, E., Iuliano, L., Minetola, P. and Salmi, A., 2010. Redesign and cost estimation of rapid manufactured plastic parts. *Rapid Prototyping Journal*.16 (5), pp. 308–317.
- Baldinger, M., Levy, G., Schönsleben, P. and Wandfluh, M., 2016. Additive manufacturing cost estimation for buy scenarios. *Rapid Prototyping Journal*, *22*(6), pp.871–877.

- Ballardini, R.M., 2019. Intellectual Property Rights and Additive Manufacturing. In *Additive Manufacturing–Developments in Training and Education* (pp. 85-97). Springer, Cham.
- Baumers, M., Beltrametti, L., Gasparre, A. and Hague, R., 2017. Informing additive manufacturing technology adoption: Total cost and the impact of capacity utilisation. *International Journal of Production Research*, *55*(23), pp.6957–6970.
- Baumers, M., Dickens, P., Tuck, C. and Hague, R., 2016. The cost of additive manufacturing: machine productivity, economies of scale and technology-push. *Technological Forecasting and Social Change*, *102*, pp.193–201.
- Baumers, M., Tuck, C., Bourell, D.L., Sreenivasan, R. and Hague, R., 2011. Sustainability of additive manufacturing: measuring the energy consumption of the laser sintering process. *Proceedings of the Institution of Mechanical Engineers, Part B: Journal of Engineering Manufacture*, *225*(12), pp.2228–2239.
- Baumers, M., Tuck, C., Wildman, R., Ashcroft, I., Rosamond, E. and Hague, R., 2012, August. Combined build-time, energy consumption and cost estimation for direct metal laser sintering. In *From Proceedings of Twenty Third Annual International Solid Freeform Fabrication Symposium—An Additive Manufacturing Conference* (Vol. 13).
- Baumers, M., Tuck, C., Wildman, R., Ashcroft, I., Rosamond, E. and Hague, R., 2013. Transparency built-in: Energy consumption and cost estimation for additive manufacturing. *Journal of Industrial Ecology*, *17*(3), pp.418–431.
- Bellini, A., 2002. *Fused Deposition of Ceramics: A Comprehensive Experimental, Analytical and Computational Study of Material Behavior, Fabrication Process and Equipment Design* (Doctoral dissertation, Drexel University).
- Bellini, A., Gu¨ c¸ eri, S.U. and Bertoldi, M., 2004. Liquefier dynamics in fused deposition. *Journal of Manufacturing Science and Engineering*, *126*(2), pp.237–246.
- Boothroyd, G., 2010. Product design for manufacture and assembly. *Computer-Aided Design*, *26*(7), pp.505–520.
- Bours, J., Adzima, B., Gladwin, S., Cabral, J. and Mau, S., 2017. Addressing hazardous implications of additive manufacturing: complementing life cycle assessment with a framework for evaluating direct human health and environmental impacts. *Journal of Industrial Ecology*, *21*(S1), pp.S25–S36.
- Buffa, E.S., Sarin, R.K., 2007. Modern Production / Operations Management, 8th ed. John Wiley & Sons, Singapore.
- Byun, H.S. and Lee, K.H., 2005. A decision support system for the selection of a rapid prototyping process using the modified TOPSIS method. *The International Journal of Advanced Manufacturing Technology*, *26*(11-12), pp.1338–1347.
- CADEM 2017, CNC acceleration, deceleration and cycle time, Accessed on March 15, 2019, <https://www.cadem.com/single-post/cnc-axes-acceleration-cycle-time>

- Chacón, J.M., Caminero, M.A., García-Plaza, E. and Núnez, P.J., 2017. Additive manufacturing of PLA structures using fused deposition modelling: Effect of process parameters on mechanical properties and their optimal selection. *Materials & Design*, *124*, pp.143–157.
- Chen, T.C.T. and Tsai, H.R., 2018. Multilayer fuzzy neural network for modeling a multisource uncertain unit-cost learning process in wafer fabrication. *Rapid Prototyping Journal*, *24*(3), pp. 521–531.
- Chin, K.S. and Wong, T.N., 1996. Developing a knowledge-based injection mould cost estimation system by decision tables. *The International Journal of Advanced Manufacturing Technology*, *11*(5), pp.353–365.
- Comminal, R., Serdeczny, M.P., Pederson, D.B. and Spangenberg, J., 2018. Numerical modeling of the material deposition and contouring precision in fused deposition modeling. In *2018 International Solid Freeform Fabrication Symposium*. University of Texas at Austin.
- Cunico, M.W.M. and de Carvalho, J., 2013. Design of an FDM positioning system and application of an error-cost multiobjective optimization approach. *Rapid Prototyping Journal*, *19*(5), pp. 244–352.
- De Luca, A. and Termini, S., 1972. A definition of a nonprobabilistic entropy in the setting of fuzzy sets theory. *Information and Control*, *20*(4), pp.301–312.
- De Ron, A.J. and Rooda, J.E., 2006. OEE and equipment effectiveness: an evaluation. *International Journal of Production Research*, 44(23), pp.4987–5003.
- Deziel, C. 2018, How Much Electricity Does a Quartz Infrared Heater Use?, Accessed on July 5, 2020) <https://homeguides.sfgate.com/much-electricity-quartz-infrared-heater-use-87458.html>
- Di Angelo, L. and Di Stefano, P., 2011. A neural network-based build time estimator for layer manufactured objects. *The International Journal of Advanced Manufacturing Technology*, *57*(1–4), pp.215–224.
- Ding, D., Pan, Z.S., Cuiuri, D. and Li, H., 2014. A tool-path generation strategy for wire and arc additive manufacturing. *The international Journal of Advanced Manufacturing technology*, *73*(1), pp.173–183.
- Dixit, P.M. and Dixit, U.S., 2008. *Modeling of Metal Forming and Machining Processes: by Finite Element and Soft Computing Methods*. Springer Science & Business Media, London.
- Dong, W. and Shah, H.C., 1987. Vertex method for computing functions of fuzzy variables. *Fuzzy Sets and Systems*, *24*(1), pp.65–78.
- Duraform, n.d., Duraform PA and GF, Accessed on July 5, 2020 <https://www.arptech.com.au/data/sls-duraform.pdf>

- Faludi, J., Bayley, C., Bhogal, S. and Iribarne, M., 2015. Comparing environmental impacts of additive manufacturing vs traditional machining via life-cycle assessment. *Rapid Prototyping Journal*, *21*(1), pp.14–33.
- Fera, M., Fruggiero, F., Costabile, G., Lambiase, A. and Pham, D.T., 2017. A new mixed production cost allocation model for additive manufacturing (MiProCAMAM). *The International Journal of Advanced Manufacturing Technology*, *92*(9), pp.4275–4291.
- Fera, M., Macchiaroli, R., Fruggiero, F. and Lambiase, A., 2018. A new perspective for production process analysis using additive manufacturing—complexity vs production volume. *The International Journal of Advanced Manufacturing Technology*, *95*(1), pp.673–685.
- Franco, A. and Romoli, L., 2012. Characterization of laser energy consumption in sintering of polymer based powders. *Journal of Materials Processing Technology*, *212*(4), pp.917–926.
- Gardan, J., 2016. Additive manufacturing technologies: state of the art and trends. *International Journal of Production Research*, 54(10), pp.3118–3132.
- Gibson, I., Rosen, D.W. and Stucker, B., 2014. *Additive manufacturing technologies* (Vol. 17). New York: Springer.
- Glass Epoxy characteristics, 2019, Custom Plastic & Metal Solutions, Accessed on September 12, 2020 < https://dielectricmfg.com/knowledge-base/glass-epoxy/>
- Goodridge, R.D., Tuck, C.J. and Hague, R.J.M., 2012. Laser sintering of polyamides and other polymers. *Progress in Materials science*, *57*(2), pp.229–267.
- Greguric L 2019, How Much Do 3D Printing Materials Cost?, Accessed on March 2, 2019, <https://all3dp.com/2/how-much-do-3d-printer-materials-cost/>
- Haeri, S., Wang, Y., Ghita, O. and Sun, J., 2017. Discrete element simulation and experimental study of powder spreading process in additive manufacturing. *Powder Technology*, *306*, pp.45–54.
- Haghighi, A. and Li, L., 2018. Study of the relationship between dimensional performance and manufacturing cost in fused deposition modeling. *Rapid Prototyping Journal*, *24*(2), pp. 395–408.
- Han, W., Jafari, M.A. and Seyed, K., 2003. Process speeding up via deposition planning in fused deposition-based layered manufacturing processes. *Rapid Prototyping Journal*, *9*(4), pp.212–218.
- Hapuwatte, B., Seevers, K.D., Badurdeen, F. and Jawahir, I.S., 2016. Total life cycle sustainability analysis of additively manufactured products. *Procedia CIRP*, *48*, pp.376–381.

- Hopkinson, N. and Dicknes, P., 2003. Analysis of rapid manufacturing—using layer manufacturing processes for production. *Proceedings of the Institution of Mechanical Engineers, Part C: Journal of Mechanical Engineering Science*, *217*(1), pp.31–39.
- Hornick, J. and Roland, D., 2013. 3D printing and intellectual property: initial thoughts. *The Licensing Journal*, *33*(7), p.12.
- Huang, R., Riddle, M., Graziano, D., Warren, J., Das, S., Nimbalkar, S., Cresko, J. and Masanet, E., 2016. Energy and emissions saving potential of additive manufacturing: the case of lightweight aircraft components. *Journal of Cleaner Production*, *135*, pp.1559–1570.
- Huang, S.H., Liu, P., Mokasdar, A. and Hou, L., 2013. Additive manufacturing and its societal impact: a literature review. *The International Journal of Advanced Manufacturing Technology*, *67*(5–8), pp.1191–1203.
- Huang, Y., Leu, M.C., Mazumder, J. and Donmez, A., 2015. Additive manufacturing: current state, future potential, gaps and needs, and recommendations. *Journal of Manufacturing Science and Engineering*, *137*(1).
- Hull, C.W., 1984. Apparatus for production of three-dimensional objects by stereolithography. *United States Patent, Appl., No. 638905, Filed*.
- Imperatives, S. 1987, Report of the World Commission on Environment and Development: Our common future. Accessed on August 5, 2020, <https:// sustainabledevelopment.un.org/content/documents/5987our-common-future.pdf>
- Indeed, n.d.(a), Salary of an injection mold operator, Accessed on December 23, 2019, <https://www.indeed.co.in/salaries/Injection-Mold-Operator-Salaries>
- Indeed, n.d.(b), Salary of a worker in factory, Accessed on December 23, 2019, <https://www.indeed.co.in/salaries/Factory-Worker-Salaries >
- Indeed, n.d., Machine Operator Salaries in India, Accessed on March 2, 2019, <https://in.indeed.com/salaries/machine-operator-Salaries>
- Indiamart, n.d.(a), Plastic Injection Machines, Accessed on December 23, 2019, <https://dir.indiamart.com/impcat/plastic-injection-machine.html >
- Indiamart, n.d.(b), PP Granules, Accessed on December 17, 2019, <https://dir.indiamart.com/impcat/pp-granules.html >
- IndiaMart, n.d., SLS 3D printer, Accessed on March 2, 2019, <https://dir.indiamart.com/impcat/sls-3d-printer.html>
- Inflation tool, n.d., Value of 1989 Indian Rupees today, Accessed on December 15, 2019, <https://www.inflationtool.com/indian-rupee/1989-to-present-value >
- Ingole, S.D., Madhusudan Kuthe, A., Thakare, S.B. and Talankar, A.S., 2009. Rapid prototyping–a technology transfer approach for development of rapid tooling. *Rapid Prototyping Journal*, *15*(4), pp.280–290.

- Injection Moulding, n.d., Useful life of injection molding machine, Accessed on December 16, 2019, <http://www.injectionmoldingplastic.com/useful-life-of-injection-molding machine.html>
- ISO/ASTM, ISO/ASTM 52900 (2015) Additive manufacturing-general principles-terminology
- Kechagias, J., Anagnostopoulos, V., Zervos, S. and Chryssolouris, G., 1997, July. Estimation of build times in rapid prototyping processes. In *6th European Conference on Rapid Prototyping & Manufacturing, Nottingham* (pp. 137–148).
- Kellens, K., Renaldi, R., Dewulf, W., Kruth, J.P. and Duflou, J.R., 2014. Environmental impact modeling of selective laser sintering processes. *Rapid Prototyping Journal*, *20*(6), pp.459–470.
- Komineas, G., Foteinopoulos, P., Papacharalampopoulos, A. and Stavropoulos, P., 2018. Build time estimation models in thermal extrusion additive manufacturing processes. *Procedia Manufacturing*, *21*, pp.647–654.
- Kumar, J. and Soni, V.K., 2015. An exploratory study of OEE implementation in Indian manufacturing companies. *Journal of The Institution of Engineers (India): Series C*, *96*(2), pp.205–214.
- Kwon, J., Kim, N. and Ma, J., 2020. Environmental sustainability evaluation of additive manufacturing using the NIST test artifact. *Journal of Mechanical Science and Technology*, *34*(3), pp.1265–1274.
- Laureijs, R.E., Roca, J.B., Narra, S.P., Montgomery, C., Beuth, J.L. and Fuchs, E.R., 2017. Metal additive manufacturing: Cost competitive beyond low volumes. *Journal of Manufacturing Science and Engineering*, *139*(8), 081010.
- Le Bourhis, F., Kerbrat, O., Hascoet, J.Y. and Mognol, P., 2013. Sustainable manufacturing: evaluation and modeling of environmental impacts in additive manufacturing. *The International Journal of Advanced Manufacturing Technology*, *69*(9-12), pp.1927–1939.
- Li, Y., Linke, B.S., Voet, H., Falk, B., Schmitt, R. and Lam, M., 2017. Cost, sustainability and surface roughness quality–A comprehensive analysis of products made with personal 3D printers. *CIRP Journal of Manufacturing Science and Technology*, *16*, pp.1–11.
- Liu, Z., Jiang, Q., Cong, W., Li, T. and Zhang, H.C., 2018. Comparative study for environmental performances of traditional manufacturing and directed energy deposition processes. *International Journal of Environmental Science and Technology*, *15*(11), pp.2273–2282.
- Locker A 2019, Best 3D Printer Slicer Software, Accessed on March 2, 2019, <https://all3dp.com/1/best-3d-slicer-software-3d-printer/>

- Luo, Y., Ji, Z., Leu, M.C. and Caudill, R., 1999, May. Environmental performance analysis of solid freedom fabrication processes. In *Proceedings of the 1999 IEEE international symposium on electronics and the environment (Cat. No. 99CH36357)* (pp. 1–6). IEEE.
- Ma, H., Zhang, Y., Jiao, Z., Yang, W., He, X., Xie, G. and Li, H., 2021. Comprehensive Assessment of the Environmental Impact of Fused Filament Fabrication Products Produced Under Various Performance Requirements. *Journal of The Institution of Engineers (India): Series C*, *102*, pp. 59–73.
- Ma, J., Harstvedt, J.D., Dunaway, D., Bian, L. and Jaradat, R., 2018. An exploratory investigation of Additively Manufactured Product life cycle sustainability assessment. *Journal of Cleaner Production*, *192*, pp.55–70.
- Ma, Z., Gao, M., Wang, Q., Wang, N., Li, L., Liu, C. and Liu, Z., 2021. Energy consumption distribution and optimization of additive manufacturing. *The International Journal of Advanced Manufacturing Technology*, *116*, pp.3377–3390.
- Masood, S.H. and Soo, A., 2002. A rule based expert system for rapid prototyping system selection. *Robotics and Computer-Integrated Manufacturing*, *18*(3–4), pp.267–274.
- Masood, S.H., 1996. Intelligent rapid prototyping with fused deposition modelling. *Rapid Prototyping Journal*, 2(1), pp.24–33.
- Matos, F. and Jacinto, C., 2019. Additive manufacturing technology: mapping social impacts. *Journal of Manufacturing Technology Management*. 30 (1), pp. 70–97.
- Matos, F., Godina, R., Jacinto, C., Carvalho, H., Ribeiro, I. and Peças, P., 2019. Additive manufacturing: Exploring the social changes and impacts. *Sustainability*, *11*(14), p.3757.
- Mellor, S., Hao, L. and Zhang, D., 2014. Additive manufacturing: A framework for implementation. *International Journal of Production Economics*, *149*, pp.194–201.
- Messimer, S.L., Rocha Pereira, T., Patterson, A.E., Lubna, M. and Drozda, F.O., 2019. Full-density fused deposition modeling dimensional error as a function of raster angle and build orientation: Large dataset for eleven materials. *Journal of Manufacturing and Materials Processing*, *3*(1), p.6.
- Meteyer, S., Xu, X., Perry, N. and Zhao, Y.F., 2014. Energy and material flow analysis of binder-jetting additive manufacturing processes. *Procedia CIRP*, *15*, pp.19–25.
- Michelsen, G., Adomßent, M., Martens, P. and von Hauff, M., 2016. Sustainable development–background and context. In *Sustainability Science* (pp. 5–29). Springer, Dordrecht.
- Mognol, P., Lepicart, D. and Perry, N., 2006. Rapid prototyping: energy and environment in the spotlight. *Rapid Prototyping Journal*, *12*(1), pp.26–34.

- Morrow, W.R., Qi, H., Kim, I., Mazumder, J. and Skerlos, S.J., 2007. Environmental aspects of laser-based and conventional tool and die manufacturing. *Journal of Cleaner Production*, *15*(10), pp.932–943.
- Munguía, J., Ciurana, J. and Riba, C., 2009. Neural-network-based model for build-time estimation in selective laser sintering. *Proceedings of the Institution of Mechanical Engineers, Part B: Journal of Engineering Manufacture*, *223*(8), pp.995–1003.
- Myriwell®, n.d., Myriwell 3D printing, Accessed on September 11, 2020, <http://www.myriwell.com/en/>
- Naghshineh, B., Lourenço, F., Godina, R., Jacinto, C. and Carvalho, H., 2020. A Social Life Cycle Assessment Framework for Additive Manufacturing Products. *Applied Sciences*, *10*(13), p.4459.
- Nan, W., Pasha, M. and Ghadiri, M., 2020. Numerical simulation of particle flow and segregation during roller spreading process in additive manufacturing. *Powder Technology*, *364*, pp.811–821.
- Ngo, T.D., Kashani, A., Imbalzano, G., Nguyen, K.T. and Hui, D., 2018. Additive manufacturing (3D printing): A review of materials, methods, applications and challenges. *Composites Part B: Engineering*, *143*, pp.172–196.
- Niaki, M.K., Torabi, S.A. and Nonino, F., 2019. Why manufacturers adopt additive manufacturing technologies: The role of sustainability. *Journal of Cleaner Production*, *222*, pp.381–392.
- Niazi, A., Dai, J.S., Balabani, S. and Seneviratne, L., 2006. Product cost estimation: Technique classification and methodology review. ASME. *Journal of Manufacturing Science and Engineering*, *128*(2): pp.563–575.
- Osswald, T. A., and Hernández-Ortiz, J. P., 2006, Polymer Processing, Accessed on September10,2020 <https://www.hanserpublications.com/SampleChapters/9781569903988_9781569903988_Polymer%20Processing_Osswald_Hernandez-Ortiz.pdf >
- Paul, R. and Anand, S., 2012. Process energy analysis and optimization in selective laser sintering. *Journal of Manufacturing Systems*, *31*(4), pp.429–437.
- PayScale, n.d., Average Computer Aided Design (CAD) Designer Salary in India, Accessed on March 4, 2019, <https:// www.payscale.com/ research/IN/Job=Computer_Aided_Design_ (CAD)_Designer/Salary>
- Peng, T., 2016. Analysis of energy utilization in 3d printing processes. *Procedia CIRP*, *40*, pp.62–67.
- Pham, D.T. and Wang, X., 2000. Prediction and reduction of build times for the selective laser sintering process. *Proceedings of the Institution of Mechanical Engineers, Part B: Journal of Engineering Manufacture*, *214*(6), pp.425–430.

- Plastic Ranger, 2020, Melting Point of Plastics, Accessed on September 11, 2020 < https://plasticranger.com/melting-point-of-plastics/>
- Precision, n.d., RL200A 3D Printer, Accessed on September 12, 2020 <http://thepeco.in/show-product.php?id=2>
- Priarone, P.C. and Ingarao, G., 2017. Towards criteria for sustainable process selection: On the modelling of pure subtractive versus additive/subtractive integrated manufacturing approaches. *Journal of Cleaner Production*, *144*, pp.57–68.
- Qaiser, A.A., Qayyum, A. and Rafiq, R., 2009. Rheological properties of ABS at low shear rates: effects of phase heterogeneity. *Malaysian Polymer Journal*, *4*(2), pp.29–36.
- Qattawi, A., Alrawi, B. and Guzman, A., 2017. Experimental optimization of fused deposition modelling processing parameters: a design-for-manufacturing approach. *Procedia Manufacturing*, *10*, pp.791–803.
- Rahman, H., John, T.D., Sivadasan, M. and Singh, N.K., 2018. Investigation on the Scale Factor applicable to ABS based FDM Additive Manufacturing. *Materials Today: Proceedings*, *5*(1), pp.1640–1648.
- Raigar, J., Sharma, V.S., Srivastava, S., Chand, R. and Singh, J., 2020. A decision support system for the selection of an additive manufacturing process using a new hybrid MCDM technique. *Sādhanā*, *45*(101).
- Rathee, S., Srivastava, M., Maheshwari, S. and Siddiquee, A.N., 2017. Effect of varying spatial orientations on build time requirements for FDM process: A case study. *Defence Technology*, *13*(2), pp.92–100.
- Rivera, F.J.M. and Arciniegas, A.J.R., 2020. Additive manufacturing methods: techniques, materials, and closed-loop control applications. *The International Journal of Advanced Manufacturing Technology*, *109*(1), pp.17–31.
- Roberson, D.A., Espalin, D. and Wicker, R.B., 2013. 3D printer selection: A decision-making evaluation and ranking model. *Virtual and Physical Prototyping*, *8*(3), pp.201–212.
- Ruffo, M. and Hague, R., 2007. Cost estimation for rapid manufacturing' simultaneous production of mixed components using laser sintering. *Proceedings of the Institution of Mechanical Engineers, Part B: Journal of Engineering Manufacture, 221(11),* pp.1585–1591.
- Ruffo, M., Tuck, C. and Hague, R., 2006a. Cost estimation for rapid manufacturing-laser sintering production for low to medium volumes. *Proceedings of the Institution of Mechanical Engineers, Part B: Journal of Engineering Manufacture*, *220*(9), pp.1417–1427.
- Ruffo, M., Tuck, C. and Hague, R., 2006b. Empirical laser sintering time estimator for Duraform PA. *International Journal of Production Research*, *44*(23), pp.5131–5146.

- Sachs, E., Cima, M., Williams, P., Brancazio, D. and Cornie, J., 1992. Three dimensional printing: rapid tooling and prototypes directly from a CAD model. *CIRP Annals*, *39*(1), pp.201–204.
- Schniederjans, D.G., 2017. Adoption of 3D-printing technologies in manufacturing: A survey analysis. *International Journal of Production Economics*, *183*, pp.287–298.
- Schröder, M., Falk, B. and Schmitt, R., 2015. Evaluation of cost structures of additive manufacturing processes using a new business model. *Procedia CIRP*, *30*, pp.311–316.
- Shadvar, N., Foroozmehr, E., Badrossamay, M., Amouhadi, I. and Dindarloo, A.S., 2021. Computational analysis of the extrusion process of fused deposition modeling of acrylonitrile-butadiene-styrene. *International Journal of Material Forming*, *14*, pp.121–131.
- Shahrubudin, N., Koshy, P., Alipal, J., Kadir, M.H.A. and Lee, T.C., 2020. Challenges of 3D printing technology for manufacturing biomedical products: A case study of Malaysian manufacturing firms. *Heliyon*, *6*(4), p.03734.
- Shing, O.N., 1999. Design for manufacture of a cost-based system for molded parts. *Advances in Polymer Technology: Journal of the Polymer Processing Institute*, *18*(1), pp.33–42.
- SLS SPEC 2017, MfgPro230 xS Specification, Accessed on March 4, 2019, < https://xyzwebsite.blob.core.windows.net/wwwportal/MfgPro230%20xS%20_SPEC _171006-2.pdf >
- Sonar, H.C., Khanzode, V.V. and Akarte, M.M., 2021. Ranking of Additive Manufacturing Implementation Factors using Analytic Hierarchy Process (AHP). *Journal of The Institution of Engineers (India): Series C*, *102*, pp.421–426.
- Song, R. and Telenko, C., 2017. Material and energy loss due to human and machine error in commercial FDM printers. *Journal of Cleaner Production*, *148*, pp.895–904.
- Šoškić, Z., Monti, G.L., Montanari, S., Monti, M. and Cardu, M., 2019. Production cost model of the multi-jet-fusion technology. *Proceedings of the Institution of Mechanical Engineers, Part C: Journal of Mechanical Engineering Science*, p.0954406219837300.
- Sreenivasan, R. and Bourell, D., 2010. Sustainability Study in Selective Laser Sintering- An Energy Perspective. In *2009 International Solid Freeform Fabrication Symposium*. University of Texas at Austin.
- Steenhuis, H.J. and Pretorius, L., 2017. The additive manufacturing innovation: a range of implications. *Journal of Manufacturing Technology Management*, 28(1), pp. 122–143.

- Stelson, K.A., 2003. Calculating cooling times for polymer injection moulding. *Proceedings of the Institution of Mechanical Engineers, Part B: Journal of Engineering Manufacture*, *217*(5), pp.709–713.
- Sukindar, N.A., Ariffin, M.K.A., Baharudin, B.H.T., Jaafar, C.N.A. and Ismail, M.I.S., 2016. Analyzing the effect of nozzle diameter in fused deposition modeling for extruding polylactic acid using open source 3D printing. *Jurnal Teknologi*, *78*(10).
- Tang, Y., Mak, K. and Zhao, Y.F., 2016. A framework to reduce product environmental impact through design optimization for additive manufacturing. *Journal of Cleaner Production*, *137*, pp.1560–1572.
- Telang S 2011, Carbon Footprint Calculation, Accessed on October 13, 2020, < https://greencleanguide.com/calculate-your-carbon-footprint/>
- Telenko, C. and Seepersad, C.C., 2012. A comparison of the energy efficiency of selective laser sintering and injection molding of nylon parts. *Rapid Prototyping Journal*, *18*(6), pp.472–481.
- Thomas cook, n.d., 1 USD to INR from 1947 to 2020, Accessed on December 15, 2019, < https://blog.thomascook.in/1-usd-to-inr-from-1947-to-2020/>
- Thomas, D., 2016. Costs, benefits, and adoption of additive manufacturing: a supply chain perspective. *The International Journal of Advanced Manufacturing Technology*, *85*(5–8), pp.1857–1876.
- Thrimurthulu, K.P.P.M., Pandey, P.M. and Reddy, N.V., 2004. Optimum part deposition orientation in fused deposition modeling. *International Journal of Machine Tools and Manufacture*, *44*(6), pp.585–594.
- Turner, B.N., Strong, R. and Gold, S.A., 2014. A review of melt extrusion additive manufacturing processes: I. Process design and modeling. *Rapid Prototyping Journal*, *20*(3), pp.192–204.
- Ullah, A.S., Hashimoto, H., Kubo, A. and Tamaki, J.I., 2013. Sustainability analysis of rapid prototyping: material/resource and process perspectives. *International Journal of Sustainable Manufacturing*, *3*(1), pp.20–36.
- Watson, J.K. and Taminger, K.M.B., 2018. A decision-support model for selecting additive manufacturing versus subtractive manufacturing based on energy consumption. *Journal of Cleaner Production*, *176*, pp.1316–1322.
- Weller, C., Kleer, R. and Piller, F.T., 2015. Economic implications of 3D printing: Market structure models in light of additive manufacturing revisited. *International Journal of Production Economics*, 164, pp.43–56.
- Westkämper, E., 2000. Life cycle management and assessment: approaches and visions towards sustainable manufacturing (keynote paper). *CIRP Annals*, *49*(2), pp.501–526.

- Xe 2020, XE Currency Converter: 1 USD to INR, Accessed on March 19, 2019, <https://www.xe.com/currencyconverter/convert/?Amount=1&From=USD&To=INR >
- Xu, X., Meteyer, S., Perry, N. and Zhao, Y.F., 2015. Energy consumption model of Binder-jetting additive manufacturing processes. *International Journal of Production Research*, *53*(23), pp.7005–7015.
- Yang, L., Hsu, K., Baughman, B., Godfrey, D., Medina, F., Menon, M. and Wiener, S., 2017. *Additive manufacturing of metals: the technology, materials, design and production* (pp. 65-70). Schwitzerland: Springer.
- Yang, Y. and Li, L., 2018. Cost modeling and analysis for Mask Image Projection Stereolithography additive manufacturing: Simultaneous production with mixed geometries. *International Journal of Production Economics*, *206*, pp.146–158.
- Yang, Y., Li, L., Pan, Y. and Sun, Z., 2017. Energy consumption modeling of stereolithography-based additive manufacturing toward environmental sustainability. *Journal of Industrial Ecology*, *21*(S1), pp.S168–S178.
- Yeh, C.C. and Chen, Y.F., 2018. Critical success factors for adoption of 3D printing. *Technological Forecasting and Social Change*, *132*, pp.209–216.
- Yi, L., Gläßner, C. and Aurich, J.C., 2019. How to integrate additive manufacturing technologies into manufacturing systems successfully: A perspective from the commercial vehicle industry. *Journal of Manufacturing Systems*, *53*, pp.195–211.
- Yoon, H.S., Lee, J.Y., Kim, H.S., Kim, M.S., Kim, E.S., Shin, Y.J., Chu, W.S. and Ahn, S.H., 2014. A comparison of energy consumption in bulk forming, subtractive, and additive processes: Review and case study. *International Journal of Precision Engineering and Manufacturing-Green Technology*, *1*(3), pp.261–279.
- Yosofi, M., Kerbrat, O. and Mognol, P., 2018. Energy and material flow modelling of additive manufacturing processes. *Virtual and Physical Prototyping*, *13*(2), pp.83–96.
- Zhang, Y. and Bernard, A., 2013, September. Generic build time estimation model for parts produced by SLS. In *High value manufacturing: Advanced research in virtual and rapid prototyping. Proceedings of the 6th International Conference on Advanced Research in Virtual and Rapid Prototyping* (pp. 43-48).
- Zhu, Z., Dhokia, V. and Newman, S.T., 2016. A new algorithm for build time estimation for fused filament fabrication technologies. *Proceedings of the Institution of Mechanical Engineers, Part B: Journal of Engineering Manufacture*, *230*(12), pp.2214–2228.

Appendix A

Important specifications of Riwell RL 200A

RP process	:	Fused deposition modelling
Weight	:	11 kg
Machine size	:	570 mm × 515 mm × 470 mm
Model size	:	225 mm × 145 mm × 150 mm
Layer thickness	:	0.15–0.4 mm
Modelling speed	:	10–60 mm/s
Nozzle diameter	:	0.4 mm
Working temperature of extruder	:	180–260 °C
Working temperature of baseplate	:	60–110 °C
Maximum power consumption	:	250W
Raw material	:	ABS/PLA
Filament diameter	:	1.75 mm
File format	:	STL

Appendix B

Estimation of standard deviation, grand mean and confidence interval for evaluating build time in FDM

	(*)	Sample number (replicate)					Standard deviation (s_m)	Grand mean $(\bar{\bar{l}})$	Confidence interval (C_I)	
		1	2	3	4	5			Lower limit	Upper limit
Part 1	l_1	30	30	30	30	30	2.19	19.6	16.88	22.32
	l_2	30	30	30	30	30				
	l_3	10	30	10	30	10				
	l_4	10	10	10	10	10				
	l_5	10	10	10	10	10				
Part 2	l_1	5	4	9	3	6	1.24	14.68	13.14	16.22
	l_2	11	12	19	21	20				
	l_3	26	27	28	26	26				
	l_4	12	22	12	12	11				
	l_5	10	14	11	10	10				
Part 3	l_1	3	11	4	16	2	1.56	15.2	13.27	17.13
	l_2	6	6	15	29	8				
	l_3	17	1	10	3	15				
	l_4	27	28	30	26	20				
	l_5	21	19	25	9	29				
Part 4	l_1	10	24	26	25	27	1.07	12.44	11.11	13.77
	l_2	25	26	26	23	21				
	l_3	7	6	7	4	5				
	l_4	7	6	3	4	5				
	l_5	4	2	5	7	6				
Part 5	l_1	3	2	9	8	5	1.71	17.48	15.35	19.61
	l_2	20	17	22	23	28				
	l_3	29	36	30	37	35				
	l_4	34	11	11	13	13				
	l_5	9	8	12	10	12				

* Measurements of length traversed by the nozzle (l_n)

Appendix C

Estimation of mould manufacturing cost (Based on Boothroyd 2010)

Manufacturing time (M_e) in hr for the ejector system (ejector pins + plate):

$$M_e = t_e A_p^{0.5}, \tag{B.1}$$

where A_p is the projected area of the part in cm^2 and t_e is a coefficient (suggested as 2.5 by Boothroyd et al. (2010) but taken as fuzzy in the present work).

Manufacturing time (in hr) associated with the geometrical complexities of the part (M_x):

$$M_x = 5.83 (X_i + X_o)^{1.27}, \tag{B.2}$$

where X_i and X_o are the inner and outer complexities of the part. The measure of complexities for both the inner or outer surface is given by

$$X_{i/o} = 0.1 N_{sp}, \tag{B.3}$$

where N_{sp} is the number of surface patches. If multiple identical numbers of features are present in the part, N_{sp} is modified by incorporating a power index:

$$N_{sp} = N_{id}^{0.7}, \tag{B.4}$$

where N_{id} is the number of identical features in the part.

Total time (in hr) for manufacturing one cavity and one core (M_{po}):

$$M_{po} = 5 + 0.085 A_p^{1.2}, \tag{B.5}$$

where A_p is the projected area in cm^2 of the part. The summation of Eqs. (B.1), (B.2) and (B.5) gives an approximate estimate of time to convert a mould base into a working mould. Depending on the surface finish requirement, time components evaluated by Eqs. (B.2) and (B.5) are multiplied by a factor in the range of 1.1–1.4. The mould manufacturing cost is obtained by multiplying the total time required for mould manufacturing with an hourly average rate for mould manufacturing.

Appendix D

Estimation of injection and cooling times (Based on Boothroyd 2010, Stelson 2003)

Injection time or fill time (t_f) to fill the molten plastic material into the cavity via the sprue, runners and gates:

$$t_f = 2V_p \frac{p_j}{P_j}, \tag{C.1}$$

where V_p is the part volume, p_j is the injection pressure of the polymer at the nozzle of the injector and P_j is the injection power of the machine. Injection power (P_j) in Eq. (C.1) is based on the machine clamp force. The clamping force (F_{clamp}) is given by

$$F_{clamp} = c_1 c_2 A_p p_j, \tag{C.2}$$

where A_p is the projected area of the part, c_1 is a coefficient to account for increase in the area due to runner system (1.15 in the present work) and c_2 is a coefficient to account for the pressure loss (0.5 in the present work).

The cooling time (t_c) based on the ejection criterion of the mid-plane temperature of the part (the temperature at the centre of the part):

$$t_c = \frac{b^2}{\pi^2 \alpha} \ln \frac{4(T_i - T_m)}{\pi (T_e - T_m)}, \tag{C.3}$$

where b is the maximum thickness of the part, α is the thermal diffusivity coefficient, T_i is the material injection temperature, T_m is the mould temperature and T_e is the part ejection temperature. Cooling time based on the ejection criterion of the average temperature of the part:

$$t_c = \frac{b^2}{\pi^2 \alpha} \ln \frac{8(T_i - T_m)}{\pi^2 (T_e - T_m)}. \tag{C.4}$$

Eq. (C.3) can be used for determining the upper bound estimate of t_c whereas Eq. (C.4) can be used for determining the lower bound estimate of t_c.

Appendix E

MATLAB code for evaluating the reliability of fuzzy cost that lies between most likely and high estimate

```
% mu = degree of membership
% m = intermediate value, h = higher value
% Cstar = Value of cost
%---------- Entering starting and end values of cost ----------
a = input ('Enter the starting value of Cstar ');
b = input ('Enter the end value of Cstar ');
z = input ('enter the number of intermediate points ');
Cstar = linspace(a,b,z)
%---------- Evaluating the intermediate limits of "mu" ----------
for i = 1:z;
if Cstar(i) == m;
   mu = 1
elseif Cstar(i) > m & Cstar(i) <= h;
mu = (((0.5 * (Cstar(i) - m))/(m - h)) + 1)
elseif Cstar(i) >= l & Cstar(i) < m;
mu = (((0.5 * (Cstar(i) - m))/(m - l)) + 1)
else
    disp ('Invalid Input !!')
end
%---------- Rounding off "mu" up to 4 decimal places ----------
p = round (mu,4)
% N1i = Reliability index at different values of cost from lower limit to intermediate limit
% N2i = Reliability index at different values of cost from intermediate limit to upper limit
```

```
% --------------Evaluating the integral(N1i) from 0.5 to intermediate limit----------

syms mu

N1i = int ((((Cstar(i) - (2.*(m-l).*(mu-1)+m))./(2.*(mu-1).*(l-h))).*(1 + mu.*log2(mu) +
(1-mu).*log2(1-mu))), 0.5, p);

%---------- Conversion of N1i to a double precision number ----------

N1 = double (N1i)

 %---------- Evaluating the integral(N2i) from intermediate limit to 1----------

syms mu

N2i = int ((1 + (mu.*log2(mu)) + ((1-mu).*log2(1-mu))), p, 1);

%---------- Conversion of N2i to a double precision number ----------

N2 = double (N2i)

%N = Overall reliability index

%--------------Summation of both N1 and N2----------

N = N1+ N2

%---------- Evaluating the integral "1 - mu" from 0.5 to 1 ----------

D1 = int ((1 + (mu.* log2(mu)) + ((1 - mu).* log2(1-mu))), 0.5, 1);

D = double (D1)

%---------- Calculation of Reliability----------

Re(i) = N/D

disp ([' Value of Re is ' num2str(Re)]);

end
```

Publications

Journal papers

- Sharma, F. and Dixit, U.S., 2019. Fuzzy set based cost model of additive manufacturing with specific example of selective laser sintering. *Journal of Mechanical Science and Technology*, 33(9), pp. 4439–4449. DOI: https://doi.org/10.1007/s12206-019-0840-x
- Sharma, F. and Dixit, U.S., 2021. Cost Comparison of Selective Laser Sintering with Injection Molding in the Presence of Uncertainties. *Journal of Advanced Manufacturing Systems*, *20*(2), pp. 401–422. DOI: https://doi.org/10.1142/S0219686721500190
- Sharma, F. and Dixit, U.S., 2021. An Analytical Method for Assessing the Utility of Additive Manufacturing in an Organization. *Journal of The Institution of Engineers (India): Series C*, *102*(1), pp. 41–50. DOI: https://doi.org/10.1007/s40032-020-00624-0

Book chapters

- Sharma, F. and Dixit, U.S., 2021. Sustainability Analysis of Fused Deposition Modelling Process. In *Fused Deposition Modeling Based 3D Printing* (pp. 227–254), Springer, Switzerland. DOI: https://doi.org/10.1007/978-3-030-68024-4_13
- Sharma, F. and Dixit, U.S., 2021. A Fuzzy Set-Based Energy Consumption Model of Selective Laser Sintering. In *Next Generation Materials and Processing Technologies* (pp. 535–551), Springer, Singapore. DOI: https://doi.org/10.1007/978-981-16-0182-8_40
- Sharma, F. and Dixit, U.S., 2022. An analytical model for estimation of build time in fused deposition modelling. In *Optimization of Industrial Systems* (pp. 423–437), Wiley, USA. ISBN: 978-1-119-75505-0

Conferences

- Sharma, F. and Dixit, U.S., 2019. Cost comparison of additive manufacturing with traditional manufacturing in the presence of uncertainties. *7th International Conference on Advancements and Futuristic Trends in Mechanical and Materials Engineering (AFTMME) 2019, Indian Institute of Technology Ropar, India, December 05–07, 2019*
- Sharma, F. and Dixit, U.S., 2020. An analytical model for the estimation of build time in fused deposition modelling. *International Conference on Industrial and Manufacturing Systems (CIMS) 2020*, *Dr. B.R. Ambedkar National Institute of Technology Jalandhar, India, October 09–11, 2020* (Online mode)
- Sharma, F. and Dixit, U.S., 2020. A fuzzy set based energy consumption model of selective laser sintering. *National Online Conference on Research and Developments in Material Processing, Modelling and Characterization (RDMPMC) 2020, National Institute of Technology Jamshedpur, India, August 26–27, 2020* (Online mode)